The role of brassinosteroids and salicylic acid in plant defense response to Potato spindle tuber viroid infection

Milanović, Jasna

Sveučilište u Zagrebu

FACULTY OF SCIENCE

DEPARTMENT OF BIOLOGY

Jasna Milanović

THE ROLE OF BRASSINOSTEROIDS AND SALICYLIC ACID IN PLANT DEFENSE RESPONSE TO *POTATO SPINDLE TUBER* VIROID INFECTION

DOCTORAL THESIS

Zagreb, 2017

Sveučilište u Zagrebu

PRIRODOSLOVNO-MATEMATIČKI FAKULTET

BIOLOŠKI ODSJEK

Jasna Milanović

ULOGA BRASINOSTEROIDA I SALICILNE KISELINE U OBRAMBENOM ODGOVORU BILJAKA NA ZARAZU VIROIDOM VRETENASTOGA GOMOLJA KRUMPIRA

DOKTORSKI RAD

Zagreb, 2017.

Ovaj je doktorski rad izrađen u Zavodu za zaštitu bilja i Institutu Ruđer Bošković, pod vodstvom dr. sc. Snježane Mihaljević i dr. sc. Césara Llavea Correasa, u sklopu Sveučilišnog poslijediplomskog doktorskog studija Biologije pri Biološkom odsjeku Prirodoslovno–matematičkog fakulteta Sveučilišta u Zagrebu.

This dissertation could not have been completed without the great support that I have received from so many people over the years.

I would like to express my sincere gratitude to my mentors, Snježana Mihaljević from the Ruđer Bošković Institute, Zagreb and César Llave Correas from the Centro de Investigaciones Biológicas, Madrid who have accepted me to their research groups and whose invaluable contributions have helped accomplishing this work. The knowledge I gained from them is something that will stay with me for a lifetime and benefit me greatly in my future career.

Further, I would like to thank the Croatian Ministry of Agriculture and the CCAFRA – Institute for Plant Protection, Zagreb for financial support with a project funding.

I also wish to express my appreciation to my former colleagues and coordinators, Vesna Kajić under whose guidance I had commenced this project and Irena Gregurec–Tomiša for leading phytosanitary field surveys.

Many thanks to Mario Santor and Darko Jelković for providing solanaceous plants.

My acknowledgments would not be complete without an earnest thanks to my family and friends. Although they haven't a clue of what I'm actually doing, they have supported me through these years. Without their love and encouragement I would not have been able to finish this work.

Jasna Milanović

The study of biology is partly an exercise in natural esthetics. A virologist is among the luckiest of biologists because he can see into his chosen pet down to the details of all of its molecules. The virologist sees how an extreme parasite functions using just the most fundamental aspects of biological behavior.

DAVID BALTIMORE

Nobel Lecture

December 12, 1975

BASIC DOCUMENTATION CARD

University of Zagreb
Faculty of Science
Department of Biology

Doctoral thesis

THE ROLE OF BRASSINOSTEROIDS AND SALICYLIC ACID IN PLANT DEFENSE RESPONSE TO *POTATO SPINDLE TUBER VIROID* INFECTION

JASNA MILANOVIĆ
Institute for Plant Protection, Gorice 68b, 10 000 Zagreb; Ruđer Bošković Institute, Bijenička cesta 54, 10 000 Zagreb

Viroids are plant–pathogenic molecules characterized by a single–stranded circular non–coding RNA genome. Despite their genomic simplicity, these plant pathogens are able to induce disease in a wide range of host plants with significant economic impact. The surveillance activities described in this study, revealed the presence of *Potato spindle tuber viroid* (PSTVd) in Croatia in two ornamental species, while no PSTVd infection was found in tomato or potato. This study was also aimed to evaluate the effects of PSTVd infection on endogenous plant growth regulator (PGR) content, and to identify common, but also specific, features of systemic hormonal response in solanaceous plant species in which PSTVd causes different degrees of symptoms. Endogenous brassinosteroide castasterone, salicylic acid, abscisic acid, indole–3–acetic acid, jasmonic acid and its precursor *cis*–12–oxophytodienoic acid were quantified using UHPLC–MS/MS. The study provides new evidences about the involvement of different PGRs and antioxidant enzymes in plant defense response against PSTVd infection, in both symptomatic and asymptomatic solanaceous species.

(119 pages, 30 figures, 8 tables, 243 references, original in: English)

Keywords: PSTVd, Solanaceae, plant growth regulators, antioxidant response, latent infection

Supervisors: Snježana Mihaljević, PhD, Senior Research Associate
César Llave Correas, PhD, Tenured Scientist

Reviewers: Željka Vidaković–Cifrek, PhD, Associate Professor
Edyta Đermić, PhD, Associate Professor
Mojca Virščeк Marn, PhD, Tenured Scientist

Substitution: Sandra Radić Brkanac, PhD, Associate Professor

TEMELJNA DOKUMENTACIJSKA KARTICA

Sveučilište u Zagrebu
Prirodoslovno–matematički fakultet
Biološki odsjek

Doktorski rad

ULOGA BRASINOSTEROIDA I SALICILNE KISELINE U OBRAMBENOM ODGOVORU BILJAKA NA ZARAZU VIROIDOM VRETENASTOGA GOMOLJA KRUMPIRA

JASNA MILANOVIĆ
Zavodu za zaštitu bilja, Gorice 68b, 10 000 Zagreb; Institut Ruđer Bošković,
Bijenička cesta 54, 10 000 Zagreb

Viroidi su najmanji poznati uzročnici bolesti biljaka čiji genom karakterizira nekodirajuća jednolančana kružna molekula RNA. Unatoč njihovoj jednostavnosti, ovi biljni patogeni uzrokuju bolesti mnogih kultiviranih biljaka širom svijeta, kao i značajne ekonomske gubitke. Bolest uzrokovana viroidom vretenastoga gomolja krumpira (*Potato spindle tuber viroid*, PSTVd), otkrivena je u okviru redovitih nadzornih aktivnosti u dvije ukrasne vrste u Hrvatskoj, dok zaraza u rajčici i krumpiru nije potvrđena. Cilj ovog istraživanja ujedno je bio ispitati utjecaj zaraze viroidom vretenastoga gomolja krumpira na biljne regulatore rasta te odrediti zajedničke, kao i vrsno specifične značajke hormonskog odgovora u vrstama iz porodice Solanaceae koje pokazuju različite simptome bolesti. Izmjeren je sadržaj endogenog brasinosteroida kastasterona, salicilne kiseline, apscizinske kiseline, indol–3–octene kiseline, jasmonske kiseline i *cis*–12–oksofitodienoične kiseline, primjenom UHPLC–MS/MS metode. Ova studija daje nove dokaze o ulozi biljnih regulatora rasta i antioksidacijskih enzima uslijed staničnog odgovora biljke na zarazu viroidom PSTVd.

(119 stranica, 30 slika, 8 tablica, 243 literaturna navoda, jezik izvornika: engleski)

Ključne riječi: PSTVd, Solanaceae, biljni regulatori rasta, antioksidacijski odgovor, latentna zaraza

Mentori: dr. sc. Snježana Mihaljević, viša znanstvena suradnica
dr. sc. César Llave Correas, znanstveni savjetnik

Ocjenjivači: dr. sc. Željka Vidaković–Cifrek, izv. prof.
dr. sc. Edyta Đermić, izv. prof.
dr. sc. Mojca Virščeк Marn, znanstvena savjetnica

Zamjena: dr. sc. Sandra Radić Brkanac, izv. prof.

TABLE OF CONTENTS

1.1. INTRODUCTION

Viroids are single–stranded, covalently closed RNA molecules that range in size from 246 to 401 nucleotides (Diener, 1987). These RNA molecules belong to a group of non–coding RNAs that are able to regulate the host gene expression through mean others than encoding proteins of specific functions (Qi and Ding, 2003). Viroids have a worldwide distribution and are the causal agents of a number of agriculturally important plant diseases. In host plants *Potato spindle tuber viroid* (PSTVd) induces symptoms range from necrosis to developmental disorders including leaf chlorosis, stunting, changes in flowering, and fruit and seed deformations (Hadidi et al., 2003). Also, in certain plant species there is a lack of symptoms like in ornamental species of the family Solanaceae. The existence of such a latent infection is one of the most efficient dissemination routes and the major risk for transmission of viroid infection among commercially important species (Flores et al., 2011). Since there is no curative options, viroids are the targets of active detection and eradication.

Viroid pathogenicity is a complex phenomenon influenced by virulence modulating regions within viroid RNA genome, but also by numerous specific components of the host response system (Owens and Hammond, 2009). Viroids are shown to affect the transcription level of genes involved in various functions including plant defense response, protein metabolism, structure and function of the cell wall and chloroplasts (Itaya et al., 2007). Many of the macroscopic symptoms associated with PSTVd infection, as well as recent global expression profiling studies (Owens et al., 2012; Katsarou et al., 2016; Zheng et al., 2017), strongly suggest the ability of viroids to perturbate plant hormone metabolism and signaling, and by that affect host growth and development. Moreover, plant hormone signaling pathways are not isolated but rather interconnected with a complex regulatory network involving various defense signaling pathways, including reactive oxygen species and antioxidative metabolism (Bari and Jones, 2009).

Despite increasing evidence of significant differential expression of genes involved in the control of hormone biosynthesis and signaling due to PSTVd infection, studies reporting changes in endogenous hormone content and antioxidant enzymes activity in PSTVd infected plants are limited. To the best of our knowledge, there is no data on changes in endogenous hormone content and antioxidant enzymes activity in plant species that do not develop visible symptoms after PSTVd infection.

1.2. AIMS AND OBJECTIVES

The first objective of this thesis was to investigate the occurrence of *Potato spindle tuber viroid* in ornamental solanaceous species and crops grown in Croatia. Therefore, a survey was conducted from 2009 to 2014 in the framework of the Plant Pest Quarantine Program funded by the Croatian Ministry of Agriculture, according to the EU Commission Decision 2007/410/EC and Croatian legislation (Plant Health Act Official Gazette 75/05, 25/09 and 55/11). All samples collected were tested by reverse transcription–polymerase chain reaction (RT–PCR) using universal primers for pospiviroids and specific primers for PSTVd. Subsequently, molecular characterization and phylogenetic analysis of detected isolates were carried out.

The second objective of this study was to evaluate effects of PSTVd infection on endogenous PGRs content, and to identify common, but also specific, features of systemic hormonal response in host plant species in which PSTVd causes different degrees of symptoms: from severe in *Solanum lycopersicum* cv. Rutgers, mild *S. tuberosum* cv. Désirée, to no visible symptoms in *Solanum laxum*, *Lycianthes rantonnetii* and *Petunia hybrida*. Endogenous brassinosteroide castasterone (CS), salicylic acid (SA), abscisic acid (ABA), indole–3–acetic acid (IAA), jasmonic acid (JA) and its precursor *cis*–12–oxophytodienoic acid (*cis*–OPDA) were simultaneously quantified using ultra–high performance liquid chromatography–tandem mass spectrometry (UHPLC–MS/MS).

The third objective of this thesis was to estimate the activity of antioxidant enzymes: guaiacol peroxidase (GPX), ascorbate peroxidase (APX), catalase (CAT) and superoxide dismutase (SOD), in order to get an insight into changes in ROS–scavenging metabolism during plant defense response to PSTVd infection. The antioxidant enzymes are known to be involved in plant defense response against viruses (Hernández et al., 2006), and thus the status of antioxidant metabolism can provide insight into the physiological response of plants to PSTVd and the dynamic of symptom development. New evidence can contribute to better understanding of mechanisms associated with symptom expression in various plant species upon PSTVd infection, as well as improve control of latent infections and the development of defense strategies.

2.1. *POTATO SPINDLE TUBER VIROID*

2.1.1. Potato spindle tuber viroid disease

Viroids are the smallest known agents of infectious disease characterized by a 246–401 nucleotide long single–stranded, circular, highly structured, unencapsidated non–coding RNA genome. Despite their lack of mRNA polypeptide–coding capacity, they are still able to replicate autonomously in natural hosts using host enzymes and cause diseases in susceptible plant species (Diener, 1971). Visible symptoms of the infection resemble those associated with many plant virus diseases and can affect either the entire plant or specific organs such as leaves, flowers, fruits, roots and storage organs (Flores et al., 2011). Symptom expression is strongly influenced by the viroid genomic RNA sequence, the host and the environment, as well as the developmental stage of the plant at the time of infection, and may vary from severe symptoms to extremely mild and symptomless infections.

The first viroid to be identified and characterized was *Potato spindle tuber viroid* (PSTVd), diagnosed in Irish Cobbler potato (*Solanum tuberosum* L.) in North America, and described by Martin (1922) who suggested that the disease might be caused by an infectious virus. Symptoms of the disease were characterized by stunting of the plants and elongated tubers, hence the disease was named ‘spindle tuber’ (Schultz and Folsom, 1923). Although the causal agent was initially described as the potato spindle tuber ‘virus’, it was later found not to be a conventional virus with a nucleic acid encapsidated by a viral protein, but a small, naked RNA molecule for which the name viroid was proposed (Diener, 1971).

Viroids have a worldwide distribution and are the etiologic agents of diverse diseases affecting numerous crop and ornamental plants (Gómez et al., 2009). The direct effects of PSTVd infection mainly concern members of the family Solanaceae. Due to the presence of serious symptoms and large scale outbreaks, potato is considered the main host of PSTVd (Singh, 1973). Other symptomatic hosts include tomato (*Solanum lycopersicum* L.) (Singh, 1973) and pepper (*Capsicum annuum* L.) (Lebas et al., 2005). Pepino (*Solanum muricatum* Ait.) (Puchta et al., 1990), avocado (*Persea americana* Mill.) (Querci et al., 1995) and solanaceous ornamentals (e.g. *Lycianthes rantonnetii* (Carrière ex Lesc.) Bitter (Di Serio, 2007), *Solanum laxum* Spreng. (Verhoeven et al., 2008a), *Streptosolen jamesonii* (Benth.) Miers (Verhoeven et al., 2008b), *Brugmansia* Pers. spp. (Verhoeven et al., 2008a), *Petunia* spp. (Mertelik et al., 2010), *Physalis*

peruviana L. (Verhoeven et al., 2009), *Cestrum* spp. (Luigi et al., 2011)) have also been found to be naturally infected with PSTVd, but without visible symptom expression. In addition, the experimental host range of PSTVd includes about 160 species among 10 families, suggesting a broad potential of this viroid to spread within various species (Singh, 1973).

Although their origins are often unknown, many viroid diseases appear to be an unintended consequence of modern agricultural practices. The idea that viroids have emerged in the last century probably reflects the significant horticultural changes that occurred during the last 150 to 200 years. These included improved access to remote geographical areas and the development of means that enabled the rapid transport of large volumes of vegetatively propagated plant specimens to great distances. Small plantings of locally adapted varieties have been replaced by large–scale monoculture of genetically identical plants that are often mass produced in a central location. PSTVd has never been isolated from any of the wild potato species from the Andes, the center of origin for the cultivated potato. This observation, and the absence of any known source of genetic resistance to PSTVd in cultivated potatoes, has been taken as an indication that this viroid and its potato host did not coevolve (Diener, 1987). Viroid infections are assumed to have been introduced by chance in crops from wild plants, with further spread by propagation and breeding activities (Diener, 1995). How and when PSTVd was introduced into cultivated potatoes is unclear, but it appears to have been a comparatively recent event. Namely, several wild *Solanum cardiophyllum* Lindl. plants growing in Mexico were latently infected with *Mexican papita viroid* (Martínez–Soriano et al., 1996; Verhoeven et al., 2011) suggesting that wild solanaceous species introduced into the United States from Mexico in the late 19th century may have acted as the initial sources of pospiviroid infection of potatoes or other solanaceous crops. Moreover, PSTVd has been recently identified in ornamentals originating from South America (e.g. *Brugmansia* Pers. spp., *Solanum laxum* Paxton, *Physalis peruviana* L.) selected from wild plants that may already have been infected (EFSA, 2011).

Field and greenhouse studies have demonstrated that PSTVd is easily transmitted mechanically through contact with contaminated pruning tools and farming implements, by human hands and by contact between plants (Owens and Hammond, 2009). PSTVd can also be spread vegetatively by graft inoculation, cuttings, micro–plants and tuber propagation (Gos, 1926). Vegetative propagation has been the major pathway for PSTVd transmission in ornamental species such as *Brugmansia* spp. and *Solanum laxum* where the absence of symptoms

increases the risk that infected plants will be used for propagation (Verhoeven et al., 2010b). PSTVd is also transmitted through both infected botanical seed and pollen (Singh et al., 1992). Although not usually considered insect–transmissible, the green peach aphid (*Myzus persicae*) can efficiently transmit PSTVd if potato plants are coinfected with *Potato leafroll virus* (PLRV) (Querci et al., 1997). No transmission of PSTVd was shown with *Apis mellifera*, *Bombus terrestris*, *Frankliniella occidentalis* or *Thrips tabaci* (Nielsen et al., 2012). Recently, Mehle et al. (2014) revealed the potential of water as a transmission route for PSTVd during hydroponic growth.

The most effective means of viroid disease control are the prevention of the introduction of infected plant material into the field or greenhouse, strict hygiene procedures, eradication and monitoring of crops for unusual symptoms. Seed certification programs and quarantine enforcement by the European and Mediterranean Plant Protection Organization (EPPO, www.eppo.int) and the North American Plant Protection Organization (NAPPO, www.nappo.org) have resulted in effective control of several diseases caused by viroids (Barba et al., 2003). The starting point for the control of PSTVd is the use of a rapid and reliable detection method to identify the pathogen. Since viroid RNA does not code for any proteins, diagnostic approaches based upon serology are not applicable. As well, diagnostic discrimination between viroids is challenging because of the relatively short PSTVd nucleotide sequence (356–361 nucleotides) and the high level of homology between different pospiviroids. Nowadays, a combined RT and real–time PCR single–tube test, that provides high sensitivity and specificity (Boonham et al., 2004; Lenarcic et al., 2012) is widely used for routine detection of PSTVd. DNA microarrays and next–generation sequencing technologies may also have applications for detection of viroid infections (Zhang et al., 2013; Visser et al., 2016). In addition to the use of healthy planting material, different chemical substances (1–5% sodium hypochlorite, 6% hydrogen peroxide, 2% sodium hydroxide with 2% formaldehyde) are used for disinfection of cutting surfaces of agricultural tools such as knives, pruning, grafting and other appliances to eliminate viroid spread through contaminated equipment (Singh et al., 1989). Control measures based on biotechnology, including creation of viroid–resistant plants using transgenic technology, are currently being developed but are not yet employed in field (Kovalskaya and Hammond, 2014).

2.1.2. Organization and expression of the viroid RNA genome

Based on comparative analyses of the primary and highly conserved secondary structures, thirty–two viroid species have been classified into two families, the *Avsunviroidae* (type member *Avocado sunblotch viroid*, ASBVd) and the *Pospiviroidae* (type member *Potato spindle tuber viroid*, PSTVd). These families have significant differences in their predicted structures, replication mechanisms and location of subcellular accumulation. The *Pospiviroidae* family consists of the 28 members classified into five genera, while the less numerous members of the *Avsunviroidae* family are grouped into three genera (Table 1). An arbitrary level of less than 90% sequence similarity and distinct differences in biological properties, particularly host range and disease symptoms, distinguish most species within the different genera. The later criterion is now mandatory for the classification and nomenclature of new viroid species (Verhoeven et al., 2011).

The 359 nucleotide genome of PSTVd was predicted to form a thermodynamically favorable rod–like secondary structure in its native *in vitro* state (Gross et al., 1978). This rod–like structural model was well supported by microscopic and biophysical studies (Sänger et al., 1976; Riesner et al., 1979), chemical/enzymatic mapping (Gast et al., 1996), and nuclear magnetic resonance spectroscopic studies (Dingley et al., 2003). Based on sequence and structural comparisons among members of the family *Pospiviroidae*, Keese and Symons (1985) proposed that PSTVd and related viroids contain five structural and functional domains. These include: (1) a central domain that contains a central conserved region (CCR) capable of forming alternative structures that regulate the replication cycle, (2) a domain associated with pathogenicity, (3) a domain exhibiting high sequence variability, and (4 and 5) two terminal domains important for duplication and movement of the viroid. Figure 1, shows the location of these five domains as well as several other important structural features of PSTVd. Functional analysis of specific RNA sequences and structural motifs residing in the viroid genome have revealed specific elements such as the virulence modulating region (VM) and RY motifs (Gozmanova et al., 2003; Maniataki et al., 2003). Moreover, several regions of low thermostability in the native structure of PSTVd were identified and subsequent refolding led to the formation of metastable hairpin structures (e.g. secondary hairpins I and II) and loops (e.g. loop E) via pairing of distant complementary nucleotide sequences (Flores et al., 2012). Site–directed mutagenesis has revealed that sequence motifs within one or more of domains play

Table 1. Current taxonomy of viroids (modified from Di Serio et al., 2014).

FAMILY	GENUS	SPECIES NAME
Pospiviroidae	***Pospiviroid***	**PSTVd (*Potato spindle tuber viroid*)** TCDVd (*Tomato chlorotic dwarf viroid*) TPMVd (*Tomato planta macho viroid*)* CSVd (*Chrysanthemum stunt viroid*) CEVd (*Citrus exocortis viroid*) TASVd (*Tomato apical stunt viroid*) IrVd–1 (*Iresine viroid 1*) CLVd (*Columnea latent viroid*) PCFVd (*Pepper chat fruit viroid*)
	Hostuviroid	**HSVd (*Hop stunt viroid*)** DLVd (*Dahlia latent viroid*)
	Cocadviroid	**CCCVd (*Coconut cadang-cadang viroid*)** CTiVd (*Coconut tinangaja viroid*) HLVd (*Hop latent viroid*) CBCVd (*Citrus bark cracking viroid*)
	Apscaviroid	**ASSVd (*Apple scar skin viroid*)** CDVd (*Citrus dwarfing viroid*) ADFVd (*Apple dimple fruit viroid*) GYSVd–1 (*Grapevine Yellow speckle viroid 1*) GYSVd–2 (*Grapevine Yellow speckle viroid 2*) CBLVd (*Citrus bent leaf viroid*) PBCVd (*Pear blister canker viroid*) AGVd (*Australian grapevine viroid*) CVd–V (*Citrus viroid V*) CVd–VI (*Citrus viroid VI*)
	Coleviroid	**CbVd–1 (*Coleus blumei viroid 1*)** CbVd–2 (*Coleus blumei viroid 2*) CbVd–3 (*Coleus blumei viroid 3*)
Avsunviroidae	***Avsunviroid***	**ASBVd (*Avocado sunblotch viroid*)**
	Pelamoviroid	**PLMVd (*Peach latent mosaic viroid*)** CChMVd (*Chrysanthemun chlorotic mottle viroid*)
	Elaviroid	**ELVd (*Eggplant latent viroid*)**

Bold species name indicates the type species for the genus.

* Mexican papita viroid isolates are recently assigned to the species *Tomato planta macho viroid* (Verhoeven et al., 2011).

essential roles in viroid replication, intracellular and cell–to–cell movement, induction of disease, and entry/exit of the viroid molecule from the vascular system (Kovalskaya and Hammond, 2014).

Because viroids are non–protein coding RNAs they need to usurp the transcription and processing machinery of their hosts to replicate, thus can be regarded as essentially transcriptional parasites. Viroids of the family *Pospiviroidae*, including PSTVd, replicate via an asymmetric rolling–circle mechanism in the nucleus (Flores et al., 2009). The most abundant form of monomeric circular RNA *in vivo*, which is arbitrarily assigned as (+) RNA, is transcribed into oligomeric linear (–) RNA. This short–lived concatemer serves as an intermediate for the synthesis of linear concatemeric (+) RNA, which is then cleaved to monomeric linear (+) RNA molecules and ligated to form the mature circular viroid RNA (Fig. 2). Early evidence demonstrated that viroids replicating in the nucleus use DNA–dependent RNA polymerase II (Pol II) in this process (Schindler and Muhlbach, 1992). In PSTVd, transcription of (–) strand RNA initiation has been mapped to the left terminal loop and specifically at position 1 (Kolonko et al., 2006). However, the site of initiation for (+) strand RNA transcription and possible cofactors that may allow DNA–dependent RNA–polymerase II employment in the viroid replication process remain to be identified. It is known that cleavage of the transient concatemeric (+)RNA replication is mediated by a class III RNase enzyme (Gas et al., 2007), while the circularization is

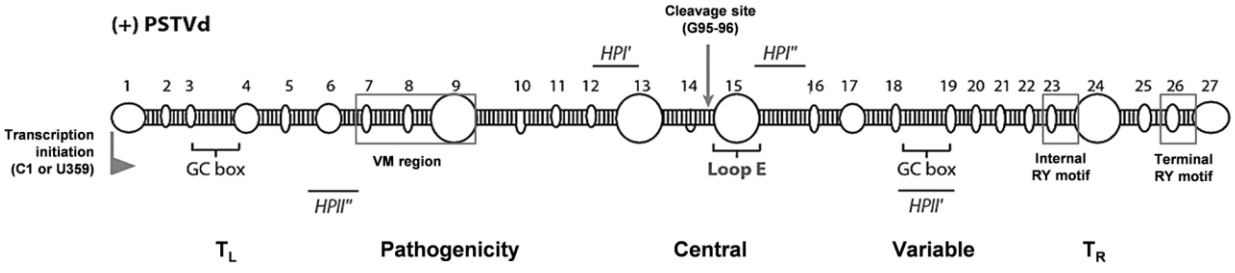

Figure 1. Scheme of the rod–like secondary structure and functional domains proposed for PSTVd intermediate strain. Flags and arrows indicate transcription initiation and cleavage sites, whereas numbers indicate the loops. *HPI'*, *HPI''*, *HPII'*, and *HPII''* indicate positions of nucleotide sequences proposed to form the metastable hairpins I and II, respectively. T_L, left–terminal domain; T_R, right–terminal domain. Adapted from Ding (2009).

achieved through the activity of nuclear DNA ligase I redirected to circularize RNA substrates (Nohales et al., 2012). Furthermore, it has been shown that loop E has an essential role in the stabilization of RNA structure, allowing the circularization of viroids (Baumstark et al., 1997; Gas et al., 2007). Manifesting their extraordinary parasitic abilities, pospiviroids reprogram the template specificity of a DNA–dependent RNA polymerase to function as an RNA–dependent RNA polymerase, and the substrate specificity of a DNA ligase to operate as an RNA ligase. The evolutionary reasons behind this preference are not clear. To complete their infectious cycle, viroids also need to move to invade distal plant parts. Recent data indicate that specific loops/bulges in the rod–like structure of PSTVd and related pospiviroids are stabilized by arrays of non–canonical pairs, with some of these elements functioning in replication and others in systemic trafficking (Zhong et al., 2008).

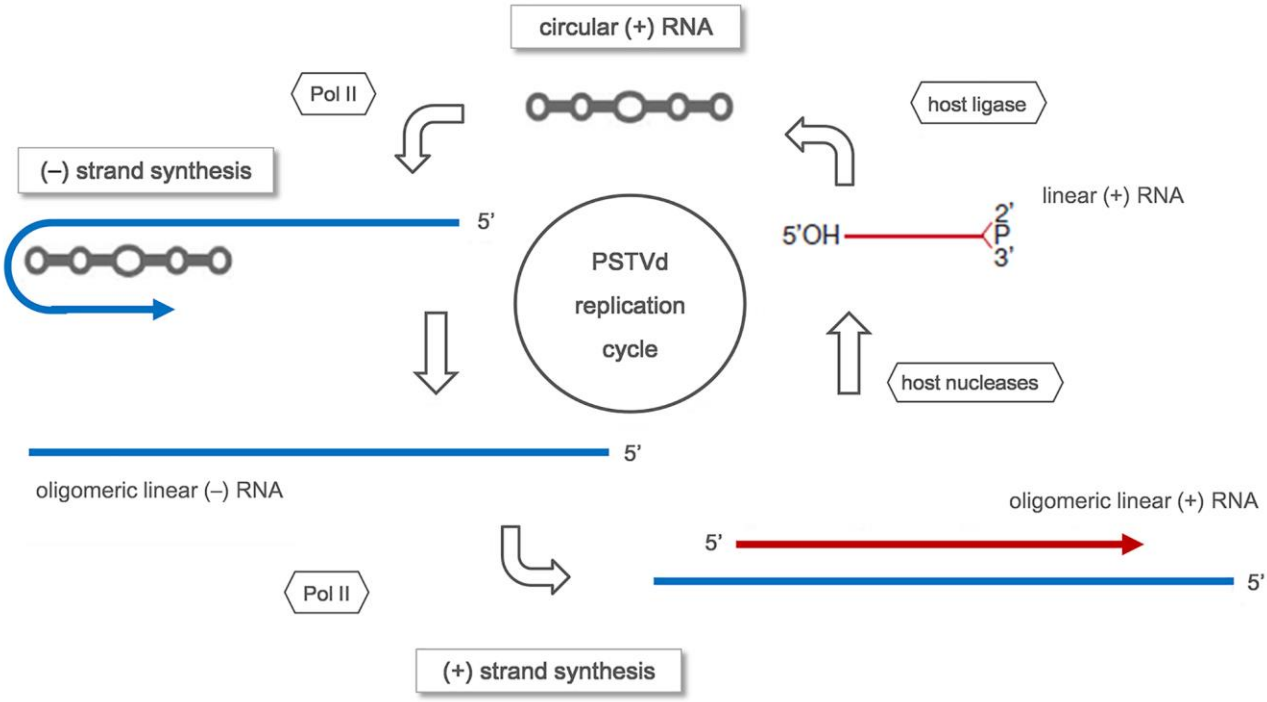

Figure 2. Replication of PSTVd follows an asymmetric rolling–circle mechanism. Red and blue lines refer to (+) and (–) strands, respectively. Modified from Hammann and Steger (2012).

In infected plants, PSTVd propagates as a population of closely related but not identical sequence variants, fitting the quasi–species concept defined by Eigen (1993). One genotype usually dominates the population and is termed the predominant genotype or master sequence (Verhoeven and Roenhorst, 2010). The variants appear due to the high rate of replication, disabled error prone activity of RNA polymerase II and selective pressure of the host (Góra–Sochacka et al., 1997). The effect of sequence variations on disease expression was studied in a pool of single–point mutants (Wassenegger et al., 1996; Gozmanova et al., 2003), 'thermomutants' (Matoušek et al., 2004) and in libraries of mutants with genomes partially or fully randomized at certain positions. It was found that the mutations affected either replication or movement of the PSTVd (Wiesyk et al., 2011). Thus, many mutations were identified as stably maintained and preserved in the progeny (Wassenegger et al., 1996), while others were identified as intolerated in a given host and were substituted by changes in different positions of the genome or by reversion to the wild–type sequence (Owens et al., 1996; Góra–Sochacka et al., 1997; Owens and Thompson, 2005). Characterization of new PSTVd variants emerging as a result of adaptation to alternative hosts might help for further determination of specific nucleotide changes that contribute to the systemic infectivity of PSTVd (Matoušek et al., 2012).

2.1.3. Movement of potato spindle tuber viroid RNA in plants

RNA trafficking has broad implications in the systemic spread of infectious agents, plant defense and the regulation of gene expression. Plasmodesmata and the vascular tissue phloem form a symplasmic network of channels for cell–to–cell and long–distance transport of RNA molecules and/or proteins, as well as photoassimilates from source where they are generated to various sink organs. Unlike viruses, which encode their own movement proteins, viroids must interact directly with host factors to accomplish all of the functions necessary for infection. Systemic infection by PSTVd involves the following processes: (i) import into the nucleus for replication to begin; (ii) export of progeny RNA out of the nucleus; (iii) trafficking from cell to cell; and (iv) long–distance trafficking to distant sink organs (the upper parts of shoots and the roots) to establish new sites of infection (Takeda and Ding, 2009).

In order for replication to take place, viroid RNAs must be localized to the correct subcellular sites to gain access to the cellular machineries that recognize, transcribe and process these RNAs. Recent data suggest that nuclear import of PSTVd may derive from interaction of a

viroid sequence or structural motif with cellular factors and lead to the formation of a ribonucleoprotein complex which would shuttle the viroid to the nucleus (Flores et al., 2005). Pertinent to this point was the identification of a bromodomain–containing VIROID RNA–BINDING PROTEIN 1 (VIRP1) from tomato that binds specifically PSTVd *in vitro* and *in vivo* (Martínez de Alba et al., 2003). To establish a systemic infection, viroid RNAs must traffic from initially infected cells into neighboring cells and further into distant organs (Fig. 3). Cell–to–cell

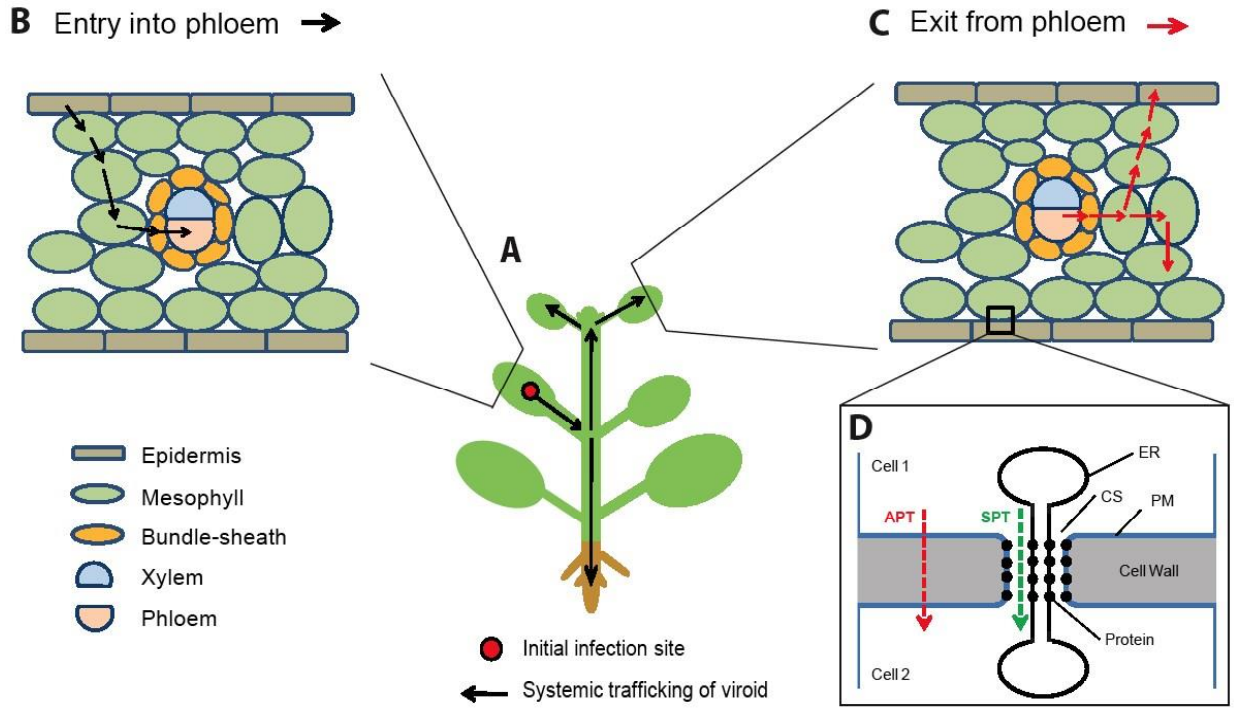

Figure 3. Pathways for systemic trafficking of PSTVd in an infected plant. (A) Schematic drawing illustrating the movement of viroid progeny from the inoculated leaf (photosynthetic source) to the upper leaves and roots (metabolic sinks). (B) Cross section of an inoculated leaf showing cell–to–cell trafficking from an initially infected epidermal cell to the phloem prior to long–distance transport to other organs. For simplicity, not all cell types in the mesophyll, xylem, and phloem tissues are illustrated. (C) In a systemically infected leaf, the viroid exits the phloem and traffics into the surrounding nonvascular cells. (D) Intercellular movement of viroids occurs via plasmodesmata and allow direct cell–to–cell symplasmic transport (SPT). The plasma membrane (PM) also permits exchange of certain molecules across the cell wall via apoplastic transport (APT). ER, endoplasmic reticulum; CS, cytoplasmic sleeve. Adapted from Takeda and Ding (2009).

movement of PSTVd occurs through plasmodesmata and appears to be an active process mediated by specific sequence or by structural motifs (Ding et al., 1997). The first evidence on viroid systemic trafficking within an infected plant was provided by Palukaitis (1987). The data showed that PSTVd accumulated in the root and leaves above the inoculated leaf, but not in leaves below the initial infection site. This pattern is similar to the distribution of photoassimilates from source to sink organs, thereby implicating the phloem as the pathway for long–distance trafficking of PSTVd. Direct visualization of PSTVd in the phloem came later from *in situ* hybridization by Zhu et al. (2001). Moreover, Zhu et al. (2001) and Qi and Ding (2003) showed that PSTVd was absent from the region of the shoot apical meristem (SAM) in infected tomato and *Nicotiana benthamiana* plants. The mechanistic basis for these differences remains to be elucidated. It is possible that PSTVd does not have structural motifs recognizable by plant factors that are required for entry into the SAM of tomato and *N. benthamiana*. Alternatively, RNA silencing may play a role to prevent the entry of PSTVd RNA in the SAM (Di Serio and Flores, 2008), but other possible mechanisms such as selective degradation of viroid RNA by nucleases, absence of critical cellular factors to support replication, or the presence of factors that repress replication, cannot be excluded. Zhu et al. (2002) revealed that two PSTVd mutants are able to enter and replicate in the phloem of *N. tabacum* but unable to leave the vascular tissue. Most likely, these viroid motifs mimic endogenous plant RNA motifs such that they may be recognized by cell factors for trafficking (Zhu et al., 2002). How viroids traffic into roots of an infected plant has not been explored (Wang and Ding, 2010).

2.2. MOLECULAR MECHANISMS OF VIROID PATHOGENESIS

The non–translatable nature of their genomic RNA has made viroids a very attractive model system for analyzing different aspects of RNA biology (Gómez et al., 2009). Since their discovery, much has been learned about their biochemical nature, while their mechanism of pathogenicity remains elusive. Sequence analysis of viroid variants and reverse genetics on infectious cDNA copies with the introduction of mutations has revealed that there are complex relationships between viroid sequence/structure and function (Owens and Hammond, 2009; Flores et al., 2012). In light of recent discoveries of the many regulatory roles of non–coding RNAs in gene expression, development, and pathogen–host interactions, elucidating the mechanisms of viroid pathogenicity should contribute to a broad understanding of the mechanisms of RNA–based regulation of gene expression. It has been proposed that the mechanism of viroid pathogenesis is mediated directly by the viroid genome itself, or by viroid genome–derived ss– or dsRNAs, and that expression of symptoms as a result of systemic infection may be an outcome of direct interactions of viroid–derived small RNAs with so far unknown host plant factors, either in the organelle where the viroid replicates or in the cytoplasm where they accumulate during its movement (Flores et al., 2005). Three general pathways account for this mechanism, influencing host gene expression: (A) mature viroid RNA–host factor interactions via induction, activation or blocking protein functions; (B) viroid dsRNAs processed by specific Dicer–like (DCL) enzymes into small RNAs which guide the RNA–induced silencing complex (RISC) (host mRNA cleavage/host DNA methylation and transcriptional silencing); and (C) hormone–mediated responses (trough altered plant gene expression and endogenous miRNA) (Avina–Padilla et al., 2015).

2.2.1. Effects of viroid RNA on host plant proteins and gene expression

Structural changes in host cells (cytopathic effects) induced by nuclear–replicating viroids consist in irregular proliferation of membranous structures in the cytoplasm known as paramural bodies or plasmalemmasomes, cell wall distortions and chloroplast malformations (Hari, 1980; Diener, 1987). Di Serio et al. (2013) summarized the evidence linking viroid–induced cytopathic effects with macroscopic symptoms and the potential biochemical pathways underlying the observed effects and concluded that, although a tentative model of modified gene expression and

its role in cytopathic effects has been put forward, additional multidisciplinary studies are needed to integrate molecular data with ultrastructural studies (Kovalskaya and Hammond, 2014).

Over the years, several viroid–binding proteins have been defined, however, with the exception of tomato protein VIRP1 whose binding site in the right terminal domain has been well characterized (Gozmanova et al., 2003), very little is known about PSTVd interaction with plant cellular proteins. Several reports (Camacho Henriquez and Sänger, 1984; Gadea et al., 1996) have described the effect of viroid infection on the transcription levels of stress–induced and defense–related genes, including those encoding pathogenesis–related (PR) proteins, PR1a and PR1b, and β–1, 3–glucanases. As well, PSTVd infection of tomato plants has been shown to selectively alter the phosphorylation state of the plant–encoded 68–70 kDa analog of PKR, the mammalian double–stranded RNA–dependent protein kinase implicated in the regulation of animal RNA virus replication (Hiddinga et al., 1988). Diener et al. (1993) demonstrated the differential *in vitro* activation of the mammalian PKR by intermediate and mild strains of PSTVd and suggested that activation of a plant enzyme homologous to mammalian P68 protein kinase may represent the triggering event in viroid pathogenesis. Unfortunately, all efforts to clone the gene encoding this kinase have been unsuccessful. More recently, Hammond and Zhao (2000) have characterized a second 55 kDa protein kinase, known as PKV (i.e. protein kinase viroid–induced), whose expression was upregulated by infection of tomato seedlings with either the intermediate or a severe strain of PSTVd. Sequence analysis of the gene encoding PKV (*pkv*) revealed that it is a novel member of the AGC VIIIa group of signal–transducing protein kinases that appear to play a key role in regulating gibberellic acid (GA) metabolism and signaling (Owens and Hammond, 2009). Further gene expression analyses suggested that gibberellic acid biosynthetic and/or signaling pathways are regulated by PKV, resulting in lower levels of active GAs and a dwarf phenotype (Hammond and Zhao, 2009).

Several studies have examined the effects of viroid infection on the pattern of gene expression in their hosts. These include PSTVd infection in tomato (Wang et al., 2011b; Owens et al., 2012), CEVd infection in Etrog citron (Rizza et al., 2012), and PLMVd infection in peach (Herranz et al., 2013). Viroid infection obviously perturbed the gene expression of its tested hosts, with numerous genes upregulated or downregulated in expression, although very few genes were found altered in expression of PLMVd infection of peach (16 of 4,261), compared with the numbers found altered for CEVd in Etrog citron (132 of 21,081), or especially PSTVd in tomato

(5,354 of 10,000). The genes altered in expression in Etrog citron and tomato encoded protein of various functional classes, but also included genes encoding miRNAs in tomato (Diermann et al., 2010; Owens et al., 2012). Recently, Zheng et al. (2017) employed RNA–Seq analysis to achieve a higher resolution in dynamic changes of gene expression profiles in response to PSTVd infection in the Heinz 1706 tomato cultivar. They identified 830 and 766 genes that were significantly up– and downregulated upon PSTVd infection, respectively. The affected genes were dominantly metabolic genes and genes responsive to stimuli, which is in line with previous reports. Gene ontology analysis showed significant expression changes of 93 genes involved in cell wall biogenesis, 221 genes involved in ion transport, 90 genes involved in ROS (reactive oxygen species) metabolism and 107 genes involved in ROS responses upon PSTVd infection in tomato (Zheng et al., 2017).

Although it is generally accepted that viroid diseases are induced by specific interference with regulation of host gene expression, the host factors that serve at the primary targets of any viroid sequences or structures for symptom expression still remain elusive.

2.2.2. Small viroid RNAs and RNA silencing

Discovery of RNA silencing has revealed that apart from mediating protein translation, RNA plays additional roles in defense against invading agents, regulation of gene expression and maintenance of genome stability (Carthew and Sontheimer, 2009). The primary trigger of transcriptional and post–transcriptional gene silencing (TGS and PTGS, respectively) are double–stranded (ds)RNAs or single–stranded (ss)RNAs with compact secondary structure that are cleaved into small RNAs (sRNAs) by RNases of class III termed Dicer (or Dicer–like, DCL, in plants) (Qi et al., 2005). After unwinding, these perfect or partial sRNA duplexes release microRNAs (miRNAs, 21–22 nt) of endogenous origin, or small interfering RNAs (siRNAs, 21, 22 and 24 nt) of either endogenous or foreign origin (Axtell, 2013). Both, miRNAs and siRNAs bind to Argonaute (AGO) proteins, which together with an RNase H–like domain are the core constituents of the RNA inducing silencing complex (RISC), and guide this complex to inactivate the complementary RNA and DNA, resulting in PTGS and TGS, respectively (Mallory and Vaucheret, 2010; Flores et al., 2016).

During plant–microbial pathogen interaction, host miRNAs and siRNAs play a role in modulating host immunity while some small RNAs (sRNAs) derived from pathogens can

decrease host defense or increase pathogen virulence (Huang et al., 2016). Identification (Itaya et al., 2001; Papaefthimiou et al., 2001; Martínez de Alba et al., 2002) and characterization (Itaya et al., 2007) of viroid–derived small RNAs (vd–sRNAs) of 21–24 nt in plants infected by viroids of both families strongly indicates that these agents are also inducers and targets of RNA silencing (Flores et al., 2016). Sequence–specific effects associated with vd–sRNAs, including attenuation of the expression of a reporter gene (Itaya et al., 2007) and of the viroid titer RNA in infected plants (Carbonell et al., 2008), suggest that certain AGOs recruit vd–sRNAs according to their size and 5‘–terminal nucleotide, and that over–expression of these proteins reduce PSTVd accumulation (Minoia et al., 2014). One specific RNA–directed RNA polymerase (RDR6) is also involved in reducing the titer of PSTVd and in blocking its entry into meristems (Di Serio et al., 2010). Since viroids are non–protein coding RNAs, they cannot incite disease via RNA silencing suppressors (RSSs) but vd–sRNAs might do so by targeting and inactivating specific host mRNAs (Papaefthimiou et al., 2001; Wang et al., 2004; Gómez et al., 2009). Studies on PLMVd showed that vd–sRNAs could target a complementary 21–nt fragment of the peach mRNA encoding the chloroplastic heat–shock protein 90 (cHSP90) and direct its cleavage by the RNA silencing machinery (Navarro et al., 2012). Using different approaches, three independent studies showed the implication of vd–sRNAs harboring pathogenic determinants from TPMVd in symptom induction in tomato and PSTVd in tomato and two *Nicotiana* species (Eamens et al., 2014; Adkar–Purushothama et al., 2015; Avina–Padilla et al., 2015). Surprisingly, three different mRNA targets (a soluble inorganic pyrophosphatase, a callose–like synthase and a WD40–repeat protein) have been identified, thus leaving the identity of the primary target somewhat open (Flores et al., 2016).

Matoušek et al. (2012) reported the suppression of mRNA levels of several regulatory factors influencing the leaf morphogenesis of tomato infected with pathogenic viroid variants PSTVd–AS1. They also found strong genotype–dependent suppression of tomato morphogenesis–regulating transcription factor SANT/HTHMyb (SlMyb) due to PSTVd pathogenesis. Its relative mRNA level was found to be significantly decreased in PSTVd–sensitive tomato (cvs. Rutgers and Heinz 1706) due to degradation processes, but increased in PSTVd–tolerant cv. Harzfeuer (Matoušek et al., 2015).

A microarray and deep sequencing analysis of small RNA from PSTVd–infected tomato plants showed that pathogenicity was related to alterations in the biosynthesis of GA and

brassinosteroids (Owens et al., 2012). Moreover, some genes involved in GA and jasmonic acid biosynthesis that were downregulated in PSTVd–infected tomato, were shown to contain binding sites for PSTVd small RNAs (Wang et al., 2011b). On the other hand, studies using transgenic tomato lines expressing non–infectious PSTVd hairpin RNA (Wang et al., 2004; Schwind et al., 2009) gave contradictory results about possible relation between the accumulations of PSTVd hairpin–derived short interfering RNAs and disease symptoms development. Whether vd–sRNAs indeed results in viroid disease symptoms requires further investigation (Huang et al., 2016).

2.3. MAJOR ELEMENTS OF PLANT INNATE IMMUNE RESPONSE

Plants in their natural environment are continuously exposed to a variety of stress factors, both abiotic and biotic, and thus have evolved a multitude of defense mechanisms in order to maintain their fitness (Mickelbart et al., 2015). Under natural conditions, both the timing and the intensity of the stressors can vary; thus, appropriate fine–tuning of the defense responses is required to minimize detrimental effects on plant fitness (Kissoudis et al., 2016). After recognition, the plants' constitutive basal defense mechanisms lead to an activation of complex signaling cascades of defense varying from one stress to another (Abouqamar et al., 2009). Following exposure to abiotic and/or biotic stress, specific ion channels and kinase cascades are activated, reactive oxygen species (ROS), and plant growth regulators (PGRs) accumulate, and a reprogramming of the genetic machinery results in adequate defense reactions in order to minimize the biological damage caused by the stress (Fujita et al., 2006; Ben Rejeb et al., 2014).

2.3.1. Roles of plant growth regulators in the regulation of host–viroid interactions

Plant growth regulators (PGRs) are chemical substances that profoundly influence the growth and differentiation of plant cells, tissues and organs, and also function as chemical messengers for intercellular communication to confer tolerance to a variety of stress factors, both abiotic and biotic. Four PGRs hormones primarily regulate plant defense to pathogens: salicylic acid (SA), jasmonic acid (JA), ethylene (ET) and abscisic acid (ABA). Others, which are mostly known for their roles in plant growth and development, have recently been found to play a role in plant–pathogen interactions, such as auxins (AUXs), brassinosteroids (BRs) and cytokinins (CKs). Hormones have antagonistic or synergistic inter–relations (often referred to as signaling crosstalk), through which certain hormones can prevail over others under specific circumstances.

In susceptible plants, viral infections result in hormonal disruption, which manifests as the simultaneous induction of several antagonistic hormones. However, these antagonistic hormones may exhibit some sequential accumulation in resistant lines (Alazem and Lin, 2015).

Salicylic acid (SA) is a phenolic compound synthesized by plants in response to a wide range of pathogens, including viruses, and is essential for the establishment of local and systemic resistance (Raskin, 1992; Klessig and Malamy, 1994; Vlot et al., 2009). SA has been known to be present in some plant tissues for quite some time, but has only recently been recognized as a potential plant growth regulator. SA has been found to promote flowering, enhances longevity of flowers, inhibits ethylene biosynthesis, and reverse the effects of ABA. The biosynthesis of SA in plants occurs via the shikimate–phenylpropanoid pathway (Zenk and Müller, 1964), where phenyl alanine is first converted to trans–cinnamic acid (t–CA) by phenylalanine ammonia lyase (PAL). This enzyme is induced by a range of biotic and abiotic stresses and is a key regulator of the phenylpropanoid pathway, which yields a variety of phenolics with structural and defense related functions (Yalpani et al., 1993). The role of SA in the defense mechanisms against biotic and abiotic stresses has been well documented (Yalpani et al., 1994; Szalai et al., 2000). Normally, plants responding to pathogen attack exhibit significantly higher levels of SA than uninfected plants. Activation of the incompatible interaction results in several responses to limit viral propagation at the infection site, including the accumulation of ROS and pathogenesis–related proteins, induction of the hypersensitive response, callose deposition, tissue disorganization, changes in the size and shape of chloroplasts, nuclear and nucleolar degradation, and programmed cell death (Baebler et al., 2014). SA is also responsible for the activation of systemic acquired resistance (SAR) in distal tissues, which lessens the effects of secondary attacks (Alazem and Lin, 2015). The role of SA in virus resistance was first established for the interaction between *Tobacco mosaic virus* (TMV) and the tobacco *N* resistance gene (Gaffney et al., 1993). Tobacco (NN) transgenic lines, in which the level of endogenous SA is reduced due to the expression of the *salicylate hydroxylase* (*NahG*) gene, inefficiently restrict TMV movement, and establishment of SAR is inhibited (Gaffney et al., 1993). Biosynthesis of SA is also induced (although at lower levels) during some compatible interactions, suggesting that SA–dependent pathways may be involved in basal defense responses (Carr et al., 2010). The exogenous application of SA to susceptible plants improves their resistance to different viruses (Alazem and Lin, 2015). For example, SA treatment has been reported to reduce the coat protein levels of

TMV and *Potato virus X* (PVX) during their compatible interactions with *N. benthamiana* plants (Lee et al., 2011). The effects of SA on plant defense seem to be diverse, and depend on both the host and infecting virus (Alazem and Lin, 2015). Finally, virus resistance is influenced by the age of the plant in both compatible and incompatible interactions (Yalpani et al., 1993). In the case of the tobacco–TMV interaction, this age–dependent resistance was correlated with elevated levels of SA in older leaves (Yalpani et al., 1993; Jovel et al., 2011). SA repression of viral replication has been suggested to be partially mediated through the siRNA pathway, and evidence for positive cross–talk between SA and siRNA antiviral defenses is accumulating (Jovel et al., 2011; Alazem and Lin, 2015).

Jasmonic acid (JA) is a key signaling phytohormone in numerous plant responses to stresses, such as wounding (León et al., 2001), ultraviolet light and ozone exposure (Rao et al., 2000), drought (Sugano et al., 2003), defenses against insects (McConn et al., 1997) and necrotic pathogens (Kloek et al., 2001). Wasternack (2007) reported that JA alters gene expression positively or negatively in a regulatory network with synergistic and antagonistic effects in relation to other plant hormones such as salicylic acid, auxin, ethylene and abscisic acid. Together with ethylene, JA regulates induced systemic resistance, which is invoked by non–pathogenic microbes. Several studies supported the positive roles of JA in compatible interactions, but in a phase–specific mode. For example, co–infection with *Potato virus Y* (PVY) and PVX, or infection with PVY carrying helper component–proteinase (HC–Pro) from a *Potyvirus*, induced oxylipin biosynthesis genes at early stages of infection and programmed cell death (Pacheco et al., 2012). JA treatment at early stages of PVY–PVX double infection enhanced resistance, but later application increased susceptibility, probably as a result of the antagonistic effect of JA on SA (Garcia–Marcos et al., 2013). Similar studies have shown that JA–responsive genes are modulated at early stages of infection, e.g. in *Cauliflower mosaic virus* (CaMV) in *A. thaliana* (Love et al., 2005). It has also been reported that silencing of *AOS* (*ALLENE OXIDE SYNTHASE*), a JA biosynthesis gene, enhanced resistance, and exogenous application of methyljasmonate (MeJA) reduced local resistance to TMV and permitted systemic movement, implying that such treatment abolished the tobacco mosaic virus *N* resistance gene. Unravelling the effects of JA on compatible and incompatible interactions requires further kinetic analyses involving other antagonistic/synergistic defense hormones, which may be involved in such regulation at the initial phase of infection (Alazem and Lin, 2015). Crosstalk between

salicylic acid/jasmonic acid plant defense signaling pathways and hormone signaling pathways (Grant and Jones, 2009) likely plays a role in viroid pathogenesis and presents challenges in unraveling the complex interactions leading to symptom formation (Owens and Hammond, 2009).

Abscisic acid (ABA) belongs to a class of metabolites known as isoprenoids, it regulates diverse plant growth and developmental processes such as germination, lateral root development, seedling growth, seed development, seed dormancy, transition from vegetative to reproductive phase and abiotic stress tolerance (Wasilewskaa et al., 2008). Although ABA signaling pathways in plants are not thoroughly understood, it is established that most of the ABA responses are regulated by ABA–mediated transcriptional regulation, which have been reviewed extensively (Nambara and Marion–Poll, 2005; Wasilewska et al., 2008). Several groups have reported that ABA plays important roles in plant defense responses (Adie et al., 2007). However, the role of ABA in plant defense appears to be more complex, and vary among different types of plant–pathogen interactions. In general, ABA is shown to be involved in the negative regulation of plant defense against various biotrophic and necrotrophic pathogens and in addition to its antagonistic roles in defense hormone pathways, such as SA and JA/ET, ABA appears to have multifaceted roles in defense against the same pathogen, depending on the stage of infection. It can positively regulate plant defense at the early stages of infection by the mediation of stomatal closure against invaders, or induction of callose deposition if the pathogen evades the first line of defense. However, if activated at later stages, ABA can suppress ROS induction and SA or JA signaling transduction, thereby negating defenses controlled by these two pathways (Ton et al., 2009). Although the involvement of ABA in biotic stress has been studied extensively, the roles of ABA in virus replication and movement are not well characterized (Alazem and Lin, 2015). ABA–virus interaction was first reported in the context of the effect of TMV on ABA accumulation in tobacco and tomato, which revealed that ABA increases callose deposition and limits virus movement (Whenham et al., 1986; Fraser and Whenham, 1989). A recent study has proposed a role for ABA in incompatible interactions, by controlling the localization of temperature–sensitive resistance genes (*R* genes) (Mang et al., 2012). ABA also affects plant defenses at the level of the RNA silencing machinery, which is considered to be a broader defense system against viruses when compared with *R*–gene–specific resistance. RNA silencing affects both the local accumulation and systemic movement of a wide range of viruses, and is

considered to be the cause of non–host resistance for some viruses, such as PVX (Ruiz–Ferrer and Voinnet, 2009). In summary, ABA appears to influence viral defense at several levels, including mRNA processing, siRNA and miRNA biogenesis, and hormone–regulated defense pathways, such as SA. Therefore, modulation of disease resistance by ABA is a complex process, and earlier reports of diverse regulatory effects of ABA on defense responses are insufficient to provide us with clear–cut models of how ABA affects disease resistance (Alazem and Lin, 2015).

Auxins are important plant hormones essential for many aspects of plant growth and development. They stimulate cell elongation and influence host developmental responses such as root initiation, vascular differentiation, tropic responses, apical dominance and the development of auxiliary buds, flowers and fruits. Though auxins have long been considered as the phytohormone responsible for plant growth and phototropism, recent evidences indicate that it may have a direct/indirect role in plant stress management as well (Tuteja et al., 2010). Many viral infections result in aberrant phenotypes, such as stunting, leaf curl and loss of apical dominance, which resemble those of mutants with compromised auxin biosynthesis and/or signaling (Fig. 4) (Kazan and Manners, 2009). A variety of different pathogens, including TMV (Culver and Padmanabhan, 2007), have been shown to manipulate AUX signaling to promote virulence and cause disease. In contrast to *Cabbage leaf curl virus* (CaLCuV), in which an extensive series of effects on various components of the AUX signaling pathway, including the F–box protein TIR1 (TRANSPORT INHIBITOR RESPONSE 1), were apparent (Ascencio–Ibáñez et al., 2008), the effects of PSTVd infection were much more limited. One of the main initial symptoms of viroid infection in both susceptible Rutgers and tolerant Moneymaker tomato cultivars is losses of apical dominance (Bagherian et al., 2016), which may be associated at least in part with change in indole–3–acetic acid (IAA) levels (Ludwig–Müller, 2014). Owens et al. (2012) showed that the expression of three genes involved in the auxin signaling pathway (*ASK2* (*APOPTOSIS SIGNAL–REGULATING KINASE 2*), involved in ubiquitin–mediated proteolysis; *IAA3/SHY2* (*INDOLE–3–ACETIC ACID INDUCIBLE 3/SHORT HYPOCOTYL 2*), transcription factor and *IAR1* (*IAA–ALANINE RESISTANT 1*), auxin homeostasis) were upregulated in PSTVd–infected Rutgers plants (Bagherian et al., 2016). Auxin activation appeared to be induced by upregulation of indole–3–acetate activation II pathway. Induction of auxin activity was proposed following indole–3–acetate II pathway activation in viroid infected leaves of both Rutgers and Moneymaker tomato cultivars (Bagherian et al., 2016). Moreover, their results

showed that glucose was over–produced in viroid infected leaves of both Moneymaker and Rutgers (Bagherian et al., 2014) and may have caused outgrowing of lateral buds through affecting indole–3–acetate components.

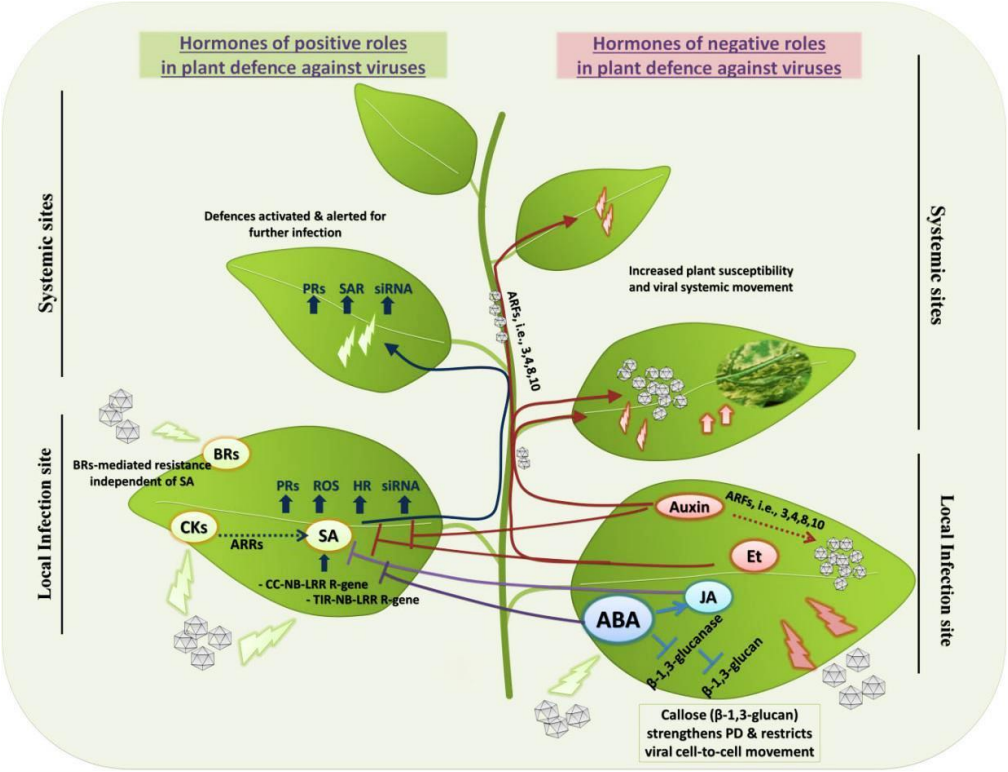

Figure 4. General effects of hormones on plant defense against viruses. Hormones in light green circles have positive effects on defense against viruses. The recognition of viral effectors by R proteins initiates defensive pathways, including the activation of salicylic acid (SA) and small interfering RNA (siRNA) pathways, induction of reactive oxygen species (ROS) and the hypersensitive response (HR). These responses limit viral spread in necrotic lesions, and activate siRNA antiviral mechanisms. SA activates systemic acquired resistance (SAR) and siRNA machinery at distal sites. Hormones in red circles have primarily negative effects on plant defenses to viruses. Jasmonic acid (JA) and abscisic acid (ABA) have both positive and negative effects on defense against viruses; JA seems to support plant defense at early stages of infection, but, if it is induced or applied at later stages, it decreases plant resistance. ABA has multifaceted roles in plant defense; on the one hand, it increases callose deposition on plasmodesmata (PD) and restricts cell–to–cell movement of viruses, whereas, on the other, it antagonizes the SA pathway and reduces resistance at local sites of infection by repressing HR induction, decreasing the production of ROS and SA, and weakening distal SAR and siRNA systems (Alazem and Lin, 2015).

Brassinosteroids (BRs) are a unique class of plant polyhydroxysteroids that are structurally related to the animal steroid hormones and involved in the regulation of growth, development and various physiological responses in plants (Bajguz, 2007). Although, BRs are known to influence various developmental processes including seed germination, cell division, cell elongation, flowering, reproductive development, senescence, and abiotic stress responses in plants, very little is known about their role in plant responses to biotic stresses (Bari and Jones, 2009). When applied exogenously to plants, BRs induce resistance against a broad range of diseases, notably against fungal and bacterial pathogens in tobacco and rice (Nakashita et al., 2003; Vriet et al., 2012). Another important aspect of the plant protective action of BRs is their capacity to improve virus resistance. Treatment of tobacco plants with brassinolide (BL) reduced infection by the TMV (Nakashita et al., 2003). Similarly, potato cuttings cultured in a medium containing BL, epi–brassinolide (EBL) or 28–homobrassinolide were more resistant to viral infection through all developmental stages (Khripach et al., 2000; Vriet et al., 2012). The increased resistance to sprouting and diseases in BR–treated potato tubers were found to be associated with enhancement of the synthesis of ABA as well as phenolic and terpenoid substances (Khripach et al., 2000). BR–induced resistance in tobacco was not associated with an increase in SA level or induction in pathogenesis–related gene expression, suggesting that the mechanism of BR–induced resistance is distinct from SAR and wound–inducible resistance (Nakashita et al., 2003).

2.3.1.1. Viroids and PGRs

The viroid infection process culminates in systemic spread of the viroid, concomitant with the appearance of a developmental syndrome in the plant. Infected tomatoes show growth reduction which may develop into permanent stunting (internode shortening), epinasty, and rugosity of the leaves, and abnormal development of roots and vascular tissues (Semancik and Conejero, 1987). In potato PSTVd–infected plants, tubers may be reduced in size, misshapen, spindle– or dumbbell–shaped, with conspicuous and prominent eyes that are evenly distributed (Owens, 2007). Although many of the visible symptoms associated with viroid infection are indicative of altered hormone metabolism, relatively little information is available regarding changes of endogenous hormone levels in plants infected with PSTVd. Microarray analysis and other transcript profiling techniques have been widely used to study host–pathogen interaction in

the context of entire biochemical or developmental pathways (Hammond and Zhao, 2000, 2009), and over the past several years, it is has become increasingly clear that RNA silencing plays a key role in modulating many of these interactions (Owens et al., 2012).

Changes in mRNA levels for the PSTVd–infected tomato cultivar Rutgers were extensive, involving more than half of the approximately 10,000 genes present on the array. Among analyzed transcripts, Owens et al. (2012) detected decreased levels of *JASMONATE RESISTANT1* (*JAR1*) mRNA in PSTVd infected tomato cultivar Moneymaker. Pathway analysis using MapMan indicated while jasmonic acid biosynthesis pathway was upregulated in both tolerant and susceptible cultivars, the number of genes involved in the upregulation JA biosynthesis was higher in Rutgers than that observed in Moneymaker plants (Bagherian et al., 2016). Owens et al. (2012) also showed that in PSTVd–infected Rutgers, two components of a mitogen–activated protein (MAP) kinase cascade were strongly upregulated. One of these components, MAP kinase 4 (MPK4), acts as both a positive regulator of JA signaling and a downregulator of salicylic acid (SA) signaling. Evidence on the change of endogenous levels of JA and SA in PSTVd–infected plants is still missing.

One of the main initial symptoms of viroid infection in both susceptible Rutgers and tolerant Moneymaker tomato cultivars is losses of apical dominance (Bagherian et al., 2016), which may be associated at least in part with change in IAA levels (Ludwig–Müller, 2014). Auxin activation appeared to be induced by upregulation of indole–3–acetate activation II pathway. Induction of auxin activity was proposed following indole–3–acetate II pathway activation in viroid infected leaves of both Rutgers and Moneymaker tomato cultivars (Bagherian et al., 2016). Moreover, their results showed that glucose was over–produced in viroid infected leaves of both Moneymaker and Rutgers (Bagherian et al., 2014) and may have caused outgrowing of lateral buds through affecting indole–3–acetate components. A variety of plant pathogens such as TMV modify auxin signaling to promote virulence and cause disease (Culver and Padmanabhan, 2007). CaLCuV infection also was shown to cause induction of the auxin pathway components (Ascencio–Ibáñez et al., 2008). Owens et al. (2012) showed that the expression of three genes involved in the auxin signaling pathway (*ASK2*, involved in ubiquitin–mediated proteolysis; *IAA3/SHY2*, transcription factor and *IAR1*, auxin homeostasis) were upregulated in PSTVd–infected Rutgers plants (Bagherian et al., 2016). To our best knowledge, there is no direct evidence related to changes in the hormonal status of AUX in infected plants.

Furthermore, symptoms of PSTVd–infected tomatoes such as stunting, reduction in flowering and leaf epinasty, strongly suggest that viroid infection leads to downregulation of gibberellin biosynthesis pathway (Bagherian et al., 2016). A significant decrease in endogenous gibberellins (GA3 and/or GA1) was first observed in CEVd–infected plants (Rodriguez et al., 1978). Joint gene expression and pathway analyses of GA biosynthesis in PSTVd–infected tomato leaves (Owens et al., 2012) showed downregulation of the gibberellin biosynthesis genes in both the susceptible (Rutgers) and tolerant (Moneymaker) cultivars, however the pathway is further downregulated in PSTVd infected tolerant tomato cultivar Moneymaker (Bagherian et al., 2016). While both positive and negative signaling components in GA signal transduction pathways have been characterized, and include the plant growth–repressing DELLA proteins (DELLAs) and bZIP (basic leucine–zipper) transcriptional activators/repressors (Sun and Gubler 2004; Fleet and Sun, 2005), their role in biochemical pathways responsible for the dwarfing phenotype in viroid–infected plants is not yet understood.

In addition, the brassinosteroide–mediated signaling in viroid disease induction was shown in tomato upon viroid infection (Owens et al., 2012). Results by Katsarou et al. (2016), finding BR pathway genes (e.g. *DWARF1/DIMINUTO*) showing differential expression in viroid infected potato plants support the idea that the reason of altered plant development and tuber formation might be the misregulation of BR pathway genes and a direct or indirect effect on GA signaling. These findings become even more interesting when considered in light of data from Unterholzner et al. (2015) suggesting that BRs are master regulators of GA biosynthesis in *Arabidopsis*. So far, no experimental data analyses on the hormonal status of BRs in PSTVd–infected plants are provided.

Altogether, these data suggest that the visible symptoms of viroid infection could be strongly influenced by various hormone signaling pathways affected. As host plant responses to viroid infection are complex, simultaneous profiling of transcriptome, proteome and metabolome will improve our knowledge about viroid strategies for successful infection and host strategies to resist the viroid attack Bagherian et al. (2014). Advances made in the precise analysis of PGR employing powerful and reliable physiochemical techniques (Flokova et al., 2014) will contribute to this progress.

2.3.2. Involvement of plant microRNA–mediated gene expression regulation in the development of potato spindle tuber disease

The coordination of plant growth and development in response to environmental changes involves complex hormonal regulatory networks, and plant miRNAs are clearly involved in this crosstalk (Curaba et al., 2014). Plant miRNAs are produced from precursors with unique stem–loop structures which are sequentially processed by the RNase III DICER–like 1 (DCL1) to give rise to a miRNA–miRNA* duplex. Alternative pathways for miRNA biogenesis involving DCL4 or DCL3 have also been described (Rajagopalan et al., 2006; Vazquez et al., 2008). The miRNA–miRNA* duplex intermediates are translocated to the cytoplasm, where the miRNA guide strand is selectively incorporated into an ARGONAUTE1 (AGO1)–containing RNA–induced silencing complex (RISC) (Baumberger and Baulcombe, 2005; Xie et al., 2005). miRNAs direct post–transcriptional gene silencing by triggering the cleavage or translational repression of the target transcripts (Llave et al., 2002).

The control of hormonal responses by miRNAs occurs mostly downstream of the phytohormone transduction signal by regulating the expression of early phytohormone–responsive genes. Only four miRNA families (miR167, miR393, miR319, and miR396) have been found to act upstream by regulating genes involved in phytohormone biosynthesis, transport, or perception, and consequently may play a more crucial role in controlling the hormonal response (Curaba et al., 2014). With the growing number of studies using small RNAs and mRNA degradome libraries from different plant species, the number of hormone–regulated miRNAs and miRNA targets involved in hormone signaling continues to increase.

Several studies have demonstrated miRNA–mediated changes in gene expression associated with PSTVd infection and symptom development in tomato plants (Diermann et al., 2010; Owens et al., 2012; Palukaitis, 2014; Zheng et al., 2017). Moreover, reduced levels of some miRNAs in PSTVd infected plants were related to changes in expression levels of certain plant regulatory factors involved in disease development. PSTVd infection of tomato cv. Rutgers showed decrease in the accumulation levels of miR159, miR396, miR319 and miR403, whereas miR162 was slightly raised (Diermann et al., 2010). Decreased level of miR319 was followed by increase of one of its possible targets – tomato TEOSINTE BRANCHED/CYCLOIDEA/PCF (TCP) gene, which might be responsible for leave blade malformations and morphogenic changes (Diermann et al., 2010). In contrast, Owens et al. (2012) detected dramatically decrease in

miR156 levels in PSTVd–infected Rutgers plants, while miR159 was increased in infected Rutgers and Moneymaker plants as well as in transgenic sRNA producing line of Moneymaker. The increased levels of miR159 in both PSTVd–infected and transgenic Moneymaker plants were suggested to be associated with downregulated expression of GAMYB, a transcription factor involved in GA signaling (Owens et al., 2012). In addition, microarray experiment revealed differential expression of 43 miRNA genes in parasitic weed *Phelipanche ramose* (L.) Pomel. upon PSTVd infection (Ivanova et al., 2014). Several members of miRNA390, miRNA396, miRNA319, miRNA166, miRNA167 and miRNA159 were strongly downregulated in infected *P. ramosa* and only two members of miRNA395 family were significantly accumulated (Ivanova et al., 2014).

In their analyses, Zheng et al. (2017) found that the activity of miR167–guided cleavage of *ARF8* (*AUXIN RESPONSE FACTOR 8*) was enhanced upon PSTVd infection, leading to the suppression of ARF8 expression. This likely impacts the auxin signaling pathways. It is noteworthy that miR167 regulation over *ARF8* was also affected during plant defense against bacterium and fungus (Li et al., 2010) representing a common strategy in plant defense against a broad spectrum of pathogens. It appears that miRNA–based regulation of genes involved in auxin signaling is a general activity during plant–pathogen interactions (Zheng et al., 2017).

To date, only a limited number of solanaceous miRNAs have been deposited in the miRNA database. Comparing with the current number of identified miRNAs for model plants such as *Arabidopsis*, a large number of potential miRNAs still remains to be identified in potato and petunia. Some potato miRNAs were described in prediction studies, using previously available sequence data (Zhang et al., 2009; Xie et al., 2010; Yang et al., 2010; Kim et al., 2011). Other studies, using large scale analysis focused only on finding conserved miRNAs in potato (The Tomato Genome Consortium, 2012). Few miRNAs were studied in depth as having a role in tuberization or regulation of defense genes in potato (Martin et al., 2009; Li et al., 2012). Despite relatively extensive genetic information, the first small RNA libraries from *Petunia hybrida* have been created recently (Tedder et al., 2009). Information on the miRNA expression in potato and petunia in relation to PSTVd infection are rather rare. To our best knowledge, there is no data on the profiling of miRNAs PSTVd–infected petunia plants.

2.3.3. Beyond genes and pathways: antioxidative stress response

Recent progress in dissecting the mechanisms through which virus–host interactions affect host physiology (Culver and Padmanabhan, 2007), suggest that it may be time to take a fresh look at the metabolic changes associated with viroid infection (Owens and Hammond, 2009). For example, the same phenylpropanoid–derived isoflavonoids that serve as primary defense compounds and key signaling molecules mediating plant–microbe interactions (Farag et al., 2009) also act as antioxidants that buffer plant cells against changes in redox status. Redox potential appears to have been used for signal transduction from very early evolutionary times. Plants regulate their redox status by continuous and balanced production of reactive oxygen species (ROS). Under favorable conditions, ROS are constantly being generated at basal levels and implicated as second messengers that mediate several key physiological mechanisms (Das and Roychoudhury, 2014). However, the delicate balance between production and quenching of ROS may be disturbed by various environmental perturbations like drought, heat, chilling, high light intensity, salinity, herbicides, heavy metals, wounding and attack of pathogens (Kapoor et al., 2015).

In biological systems, oxidative stress results from the presence of elevated levels of oxidizing agents that are able to abstract electrons from essential organic molecules and disturb cellular function (Tripathy and Oelmüller, 2012). The most common ROS include free radicals like superoxide ($O_2^{\bullet -}$), hydroxyl radical ($OH^{\bullet}$), non–radicals like hydrogen peroxide (H_2O_2), and singlet oxygen ($^1O_2$) (Fig. 5). To avoid potential damage of cellular components caused by ROS as well as to maintain growth, metabolism and development, the balance between production and elimination of ROS at the intracellular level must be tightly regulated and/or efficiently metabolized. This equilibrium between the production and detoxification of ROS is sustained by non–enzymatic and enzymatic antioxidants (Mittler et al., 2004). Table 2 shows various antioxidant enzymes that play important role in scavenging stress–induced ROS generated in plants. Non–enzymatic components include the major cellular redox buffers ascorbate (AsA) and glutathione (GSH) as well as tocopherol, carotenoids and phenolic compounds (Caverzan et al., 2016). The enzymatic components comprise several antioxidant enzymes, such as superoxide dismutase (SOD), catalase (CAT), guaiacol peroxidase (GPX), and enzymes of the ascorbate–glutathione (AsAGSH) cycle, such as ascorbate peroxidase (APX), monodehydroascorbate reductase (MDHAR), dehydroascorbate reductase (DHAR), glutathione peroxidase and

glutathione reductase (GR). SODs are considered the first line of defense against ROS–induced damage (De Gara et al., 2003), it catalyzes the removal of $O_2^{\bullet -}$ by dismutating it into O_2 and H_2O_2. The H_2O_2 produced is then scavenged by catalase and several classes of peroxidases (Fig. 5). While CAT predominantly scavenges H_2O_2 in the peroxisomes, APX performs the same function in the cytosol and the chloroplast. Enhanced peroxidase activity has been correlated with resistance in different plants inoculated with phytopathogens. Many isoenzymes of guaiacol peroxidase exist in plant tissues localized in vacuoles, the cell wall, and the cytosol, thus GPX is associated with many important biosynthetic processes, including lignification of cell wall, degradation of indole acetic acid, biosynthesis of ethylene, wound healing, and defense against abiotic and biotic stresses (Sharma et al., 2012).

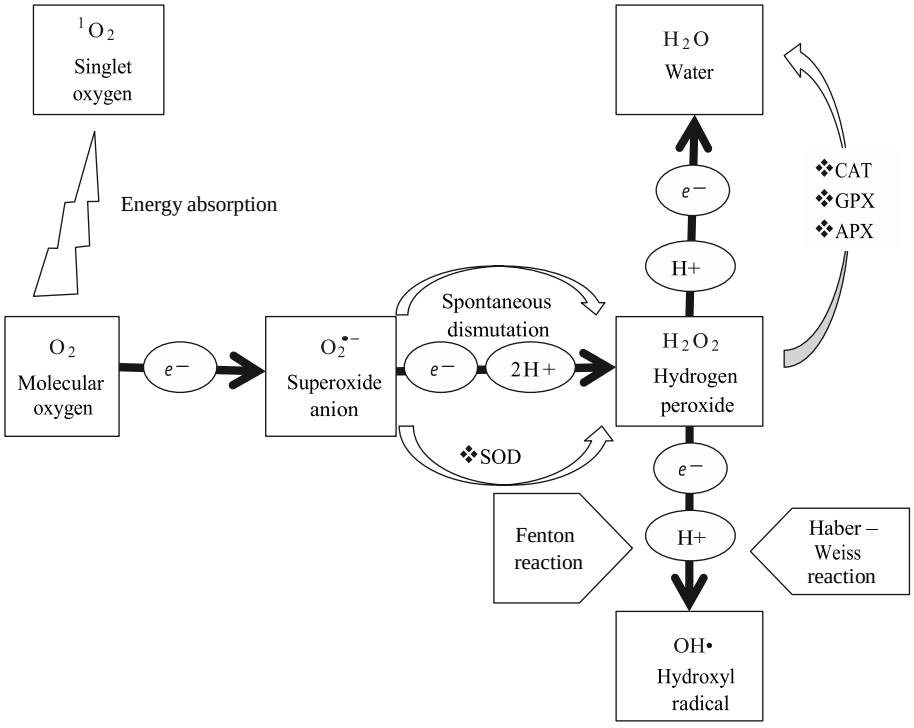

Figure 5. Schematic representation of generation of reactive oxygen species (ROS) in plants. Activation of O_2 occurs by two different mechanisms. Stepwise monovalent reduction of O_2 leads to formation of $O_2^{\bullet -}$, H_2O_2, and $OH^{\bullet}$, whereas energy transfer to O_2 leads to formation of $^1O_2$. $O_2^{\bullet -}$ is easily dismutated to H_2O_2 either non–enzymatically or by superoxide dismutase (SOD) catalyzed reaction to H_2O_2. H_2O_2 is converted to H_2O by catalase (CAT), guaiacol peroxidase (GPX), and ascorbate peroxidase (APX), (modified from Sharma et al., 2012).

Table 2. Major enzymatic and non–enzymatic antioxidants along with their functions and cellular localization (modified from Das and Roychoudhury, 2014).

Enzymatic antioxidants	**Reaction catalyzed**	**Subcellular location**
Superoxide dismutase (SOD)	$O_2^{\bullet -} + O_2^{\bullet -} + 2H^+ \rightarrow 2H_2O_2 + O_2$	per, mit, cyt, chl
Catalase (CAT)	$2H_2O_2 \rightarrow O_2 + 2H_2O$	per, mit, gly
Ascorbate peroxidase (APX)	$H_2O_2 + AA \rightarrow 2H_2O + DHA$	per, mit, cyt, chl
Monodehydroascorbate reductase (MDHAR)	$2MDHA + NADH \rightarrow 2AA + NAD$	mit, cyt, chl
Dehydroascorbate reductase (DHAR)	$DHA + 2GSH \rightarrow AA + GSSG$	mit, cyt, chl
Glutathione reductase (GR)	$GSSG + NADPH \rightarrow 2GSH + NADP^+$	mit, cyt, chl
Guaiacol peroxidase (GPX)	$H_2O_2 + DHA \rightarrow 2H_2O + GSSG$	mit, cyt, chl, er
Glutation *S*–transferase (GST)	$RX + GSH \rightarrow HX + R–S–GSH$	mit, cyt, chl, nuc, apo
Non–enzymatic antioxidants	**Function**	**Subcellular location**
Ascorbic acid (AA)	Substrate for APX. Detoxifies H_2O_2.	cyt, chl, mit, per,vac, apo
Reduced glutathione (GSH)	Substrate for various peroxidases, GST and GR. Detoxifies H_2O_2, other hydroperoxides and toxic compounds.	cyt, chl, mit, per, vac, apo
α–Tocopherol	Protects membrane lipids from peroxidation, detoxifies lipid peroxides and quenches $^1O_2$.	membranes
Carotenoids	Quench $^1O_2$. Photosystem assembly, key components of the light harvesting complex, precursors of ABA.	chl and other non–green plastids
Flavonoids	Direct scavengers of H_2O_2 and $^1O_2$ and $OH^{\bullet}$.	vac
Proline	Efficient scavenger of $OH^{\bullet}$ and $^1O_2$ and prevent damages due to lipid peroxidation.	mit, cyt, chl

Abbreviations: per, peroxisomes; mit, mitochondria; cyt, cytosol; chl, chloroplasts; er, endoplasmatic reticulum; nuc, nucleus; apo, apoplast; vac, vacuole; gly, glyoxysomes.

In their natural environment, plants encounter a vast array of pathogenic microorganisms such as bacteria, fungi, viruses, invertebrates and even other plants. However, only a small number of pathogens are able to provoke disease in a certain species or cultivar (compatible response), whereas most potential aggressors are recognized and blocked in their penetration by plant defenses (incompatible response). The production of ROS is a common feature of incompatible and compatible plant–pathogen interactions (De Gara et al., 2003; Torres et al., 2006). In an incompatible reaction, development of the receptor–ligand complex triggers a cascade of transduction signals that ultimately leads to the hypersensitive response (HR)

response, characterized by local cell death at the infection site (Heath, 2000). The oxidative burst, which occurs in cells in the immediate vicinity of the infection site, is due predominantly to the activation of NADPH oxidase associated with the plasma membrane. In the gene–for–gene interaction, the burst is biphasic, with a rapid but weak transient accumulation (phase I) and a second, massive, and prolonged accumulation (phase II; Lamb and Dixon, 1997). The first phase of ROS accumulation is associated with infection of plants by either virulent or avirulent pathogens and is likely independent of *de novo* synthesis of ROS–generating enzymes. The second phase of ROS accumulation, however, is associated only with infection by avirulent pathogens and is an induced response dependent on the increased transcription of mRNA encoding ROS–generating enzymes (Palukaitis and Carr, 2008). Plants undergoing an HR also induce a state of resistance called systemic acquired resistance (SAR). Unlike HR, SAR is a long–lasting immune response primed to provide distant tissue resistance against subsequent infections (Mandadi and Scholthof, 2013). Although ROS are important for the initial plant–pathogen interactions, healthy uninfected plant cells must avoid collateral damage from locally released ROS if the plant is to survive and systemic resistance is to develop (Clarke et al., 2002). An example of SAR that was mediated by a burst of ROS was described in tobacco plants inoculated with TMV (Lamb and Dixon, 1997).

Several groups have reported the effects of virus infection on plant antioxidant systems. CAT activity has been shown to decline following TMV infection of tobacco plants and this is believed to lead to increased H_2O_2 levels, which might in turn lead to the induction of SAR (Neuenschwander et al., 1995). SOD activity declines following the infection of resistant soybean with *Soybean mosaic virus* (SMV) (Zhuang et al., 1993), while glutathione reductase activity increases in tobacco plants reacting hypersensitivity to TMV and displaying SAR (Fodor et al., 1997). Virus infection has also been shown to increase peroxidase activity, which can utilize H_2O_2 as a substrate for cell wall crosslinking (Montalbini et al., 1995; Clarke et al., 2002). Riedle–Bauer (2000) studied oxidative stress in *Cucumis sativus* L. and *Cucurbita pepo* L. plants infected with *Zucchini yellow mosaic virus* (ZYMV) and *Cucumber mosaic virus* (CMV), and concluded that virus–enhanced peroxidation via formation of ROS is involved in the development of both mosaic and yellowing symptoms in virus–infected tissues. Clarke et al. (2002) proposed that a decline in antioxidant enzymes with a consequent increase in ROS may be necessary for the establishment of infection, replication and spread of *White clover mosaic*

potexvirus (WCIMV) in *Phaseolus vulgaris* L. De Gara et al. (2003) suggested that alterations in the activities of ROS–scavenging enzymes could be a key step in the activation of the phytopathogenic response. Furthermore, the findings of Love et al. (2005), implicate reactive oxygen species and ethylene in signaling in response to CaMV infection. After a detailed study of resistant and susceptible cultivars of *Prunus armeniaca* L. inoculated with *Plum pox virus* (PPV), Hernández et al. (2006) suggested that ROS could activate defense genes, thus regulation of antioxidant enzymes could be of importance in determining susceptibility or resistance to the plant viruses (Hakmaoui et al., 2012).

Peroxidase activity and/or peroxidase gene expression can also be induced by viroids (Vera et al., 1993), but little research has been performed to address these issues. An increase in the expression level of peroxidase was observed in Troyer citrange and sour orange infected with CDVd (Tessitori et al., 2007) whereas alemow showed a significant reduction of the peroxidase expression. Furthermore, Rizza et al. (2012) investigated changes in the gene expression profile during the early (pre–symptomatic) and late (post–symptomatic) stages of Etrog citron infected with CEVd. Their results indicate an increase in peroxidase activity at the pre–symptomatic stage, whereas the activity decreases at the post–symptomatic stage. Although CEVd and CDVd induce quite different phenotypic reactions in Etrog citron, the results of these studies reveal certain potential similarities in the pathogenic effect mediated by peroxidases, such as changes in auxin metabolism, lignifications, suberization and amino acid transport. These changes might allow the plants to survive the infection and delay its disease–associated decline (Rizza et al., 2012). Therefore, a better understanding of the molecular mechanisms underlying the localized activation of the oxidative burst following perception of pathogen, avirulence signals and key downstream responses including gene activation, cell death, and long–distance signaling, allows development of new strategies for engineering enhanced protection against pathogens by manipulation of the oxidative burst and oxidant–mediated signal pathways in the future (Bastas, 2014).

3.1. MATERIALS

3.1.1. Plant material

A total of five plant species were used in experiments: *Solanum lycopersicum* L. cv. Rutgers (Miagra, Zagreb, Croatia) and cv. BELLE F1 (Enza Zaden, Enkhuizen, Nizozemska), *Solanum tuberosum* L. cv. Désirée (kindly provided by PPK Velebit, Gospić, Croatia), *Petunia hybrida* Vilm. (Semenarna Ljubljana, Ljubljana, Slovenia), *Solanum laxum* Spreng. and *Lycianthes rantonnetii* (Carrière) Bitter (kindly provided by Ciklama, Koprivnički Ivanec, Croatia).

3.1.2. Viroid isolates

The isolates of PSTVd (GeneBank, accession number KF418768 and KF418770) from *Solanum laxum* Spreng. characterized and reported previously (Milanović et al., 2014) were used for assessing pathogenicity by bioassays on symptomatic tomato plants (*Solanum lycopersicum* L. cvs. Rutgers and BELLE F1). To evaluate effects of PSTVd infection on the status of endogenous PGRs, the isolate KF418768 from tomato cv. Rutgers was used. PSTVd strain PV–0064, purchased from DSMZ GmbH (Braunschweig, Germany), was used as a positive control for reverse transcription–polymerase chain reaction (RT–PCR) assays.

3.1.3. Bacterial strain

Escherichia coli strain DH5α (genotype: F^- φ80d*lac*ZΔM15 Δ(*lac*ZYA–*arg*F)U169 *rec*A1 *end*A1 *hsd*R17(r_k^-, m_k^+) *pho*A *sup*E44 *thi*–1 *gyr*A96 *rel*A1 λ^-) was used for plasmid cloning and multiplication.

3.1.4. Plasmid vector

The pGEM®–T Easy Vector (Promega, Germany) was used as convenient system for cloning of PCR products. The pGEM®–T Easy is 3015 bp long, linearized vector with a single 3´–thymidine (T) overhangs at the insertion site which greatly improve the efficiency of ligation of PCR products into the plasmid (Fig. 6). The vector also contains an ampicillin resistance gene as selective marker. Blue/white colony screening can be used to directly identify recombinant clones as T7 and SP6 RNA polymerase promoters flank a multiple cloning region within the α–peptide coding region for β–galactosidase permitting insertional inactivation of the α–peptide.

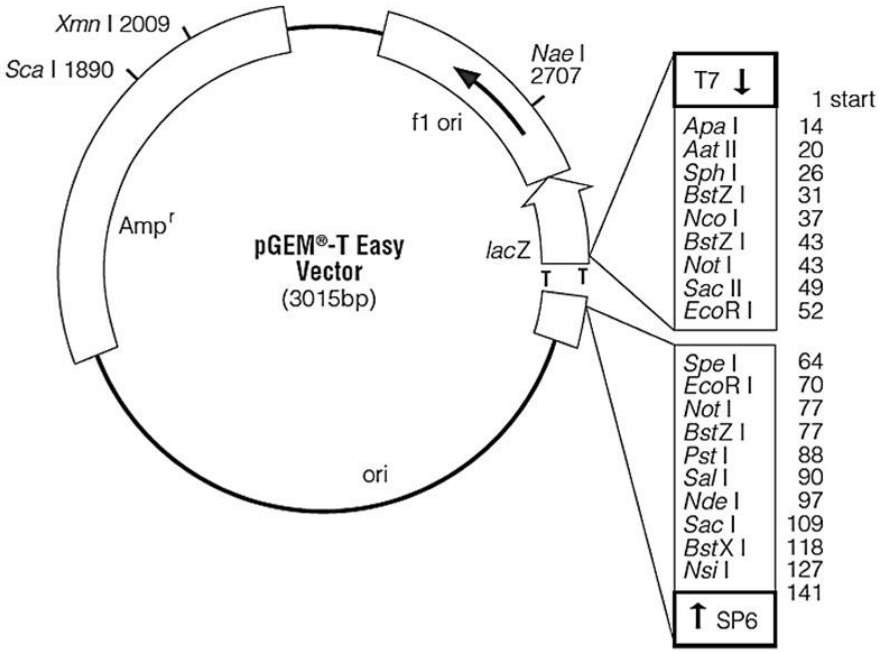

Figure 6. Map of the pGEM®–T Easy Vector (reproduced from the pGEM®–T Easy Vector's technical manual, Promega, http://www.promega.com).

3.1.5. Media, buffers and solutions

3.1.5.1. Media

LB solid medium: 40 g/L of dehydrated culture media Difco™ Luria–Bertani (LB) Agar, Miller, with the following composition: 1% tryptone, 0.5% yeast extract, 1% NaCl and 1.5% agar was dissolved in mqH_2O and autoclaved at 121ºC for 15 minutes.

Selective LB media were prepared by adding ampicillin to a final concentration of 100 µg/ml. Stock aqueous solution of ampicillin (100 mg/ml) was filter sterilized through a sterile 0.22 µm Millex® GS filter unit (Millipore, Bedford, USA) and added to the autoclaved medium after it has cooled to approx. 55 ºC.

In order to prepare X–gal and IPTG selective LB agar plates for the blue–white colony screening, 100 µl of 100 mM isopropyl β–D–thiogalactopyranoside (IPTG) and 20 µl of 50 mg/ml 5–bromo–4–chloro–3–indol–β–D–galactoside (X–gal) were spread over the surface of a LB–ampicillin agar plates and allowed to absorb for 30 minutes at 37 ºC prior to use.

LB liquid medium: 25 g/L of dehydrated culture media Difco™ Luria–Bertani (LB) Broth, Miller with the following composition: 1% tryptone, 0.5% yeast extract and 1% NaCl was dissolved in mqH_2O (pH 7.0) and autoclaved at 121 ºC for 15 minutes.

SOC medium: Liquid super optimal broth with catabolite repression (S.O.C. medium) was purchased from Thermo Fisher Scientific (Waltham, USA), with the following composition: 2% tryptone, 0.5% yeast extract, 10 mM NaCl, 2.5 mM KCl, 10 mM $MgCl_2$, 10 mM $MgSO_4$ and 20 mM glucose.

3.1.5.2. Buffers and solutions

Ascorbate peroxidase assay solution (pH 7.0): 50 mM potassium phosphate buffer (pH 7.0) containing 0.1 mM ethylene diamine tetra–acetic acid (EDTA), 0.5 mM ascorbic acid and 0.12 mM H_2O_2. The volume was completed to 50 ml by adding 500 µl of 10 mM EDTA, 1.538 ml of 1 M K_2HPO_4 and 0.963 ml of 1 M KH_2PO_4 to mqH_2O. Solution was stored at 4 ºC until used. Ascorbic acid and hydrogen peroxide was added before the use of the reaction mixture.

Ascorbic acid (50 mM): 88 g of L–ascorbic acid was dissolved in 10 ml of 50 mM potassium phosphate buffer (pH 7.0) containing 0.1 mM ethylene diamine tetra–acetic acid (EDTA). Solution was prepared fresh daily.

Bradford reagent: 100 mg of Coomassie Brilliant Blue G–250 was dissolved in 50 mL 95% (v/v) ethanol, and 100 mL 85% (v/v) phosphoric acid was added. The Bradford reagent was diluted five–fold in water, filtered through Whatman no. 1 paper (Sigma–Aldrich, Germany) to remove the precipitates and stored in a dark bottle for later use.

Catalase assay solution: 50 mM potassium phosphate buffer (pH 7.0) supplemented with 10 mM H_2O_2. The volume was completed to 50 ml by adding 66.3 µl of 30% (w/w) H_2O_2 to 50 mM potassium phosphate buffer (pH 7.0). Solution was prepared fresh daily and stored at 4 ºC until used.

DNA loading buffer (10x): BlueJuice™ Gel Loading Buffer (10x) with the following composition: 65% (w/v) sucrose, 10 mM Tris–HCl (pH 7.5), 10 mM EDTA and 0.3% (w/v) bromophenol blue was purchased from Thermo Fisher Scientific (Waltham, USA).

Extraction buffer: 50 mM potassium phosphate buffer (pH 7.0) containing 10 mM ethylene diamine tetra–acetic acid (EDTA) and 2% (w/v) insoluble polyvinylpolypyrrolidone (PVPP). Solution was stored at 4 ºC until used.

Guaiacol peroxidase assay solution: 50 mM potassium phosphate buffer (pH 7.0) containing 18 mM guaiacol and 5 mM H_2O_2. The volume was completed to 50 ml by adding 100.65 µl of 18 mM guaiacol and 25.5 µl of 30% (v/v) H_2O_2 to 50 mM potassium phosphate buffer (pH 7.0). Solution was prepared fresh daily and stored at 4 ºC until used.

H_2O_2 (12 mM): 13.6 µl of 30% (v/v) H_2O_2 was added to 10 ml of sterile mqH_2O. Solution was prepared immediately before use.

Potassium phosphate buffer (50 mM, pH 7.0): The volume was completed to 50 ml by adding 1.538 ml of 1 M K_2HPO_4 and 0.963 ml of 1 M KH_2PO_4 to sterile mqH_2O. Solution was stored at 4 ºC until used.

Riboflavin (250 µM): 0.00941 g of riboflavin was dissolved in 50 ml of mqH_2O. The solution (500 µM) was filtered through Whatman no. 1 paper (Sigma–Aldrich, Germany), diluted in water (1:1) and stored in a dark bottle at 4 ºC.

Sodium phosphate buffer (20 mM, pH 7.4): 1.9 ml 0.2 M NaH_2PO_4, 8.1 ml 0.2 M Na_2HPO_4, 90 ml sterile mqH_2O.

Superoxide dismutase assay solution (pH 7.8): 50 mM potassium phosphate buffer (pH 7.0) containing 0.1 mM ethylene diamine tetra–acetic acid (EDTA), 13 mM L–methionine, 75 µM nitroblue tetrazolium salt (NBT) and 2 µM riboflavine. The volume was completed to 200 ml by adding 9.08 ml of 1 M K_2HPO_4 and 0.92 ml of 1 M KH_2PO_4, 2 ml of 10 mM EDTA, 0.388 g of L–methionine, and 127 mg of nitroblue tetrazolium salt (NBT) to sterile mqH_2O. Solution was stored in a dark bottle at 4 ºC. Riboflavine was added before the use of the reaction mixture.

TBE buffer (10x, pH 8.3): AccuGENE™ 10x TBE electrophoresis buffer with the following composition: 0.89 M Tris–borate, and 0.02 M EDTA (pH 8.3), was purchased from Lonza (Basel, Switzerland).

3.1.6. Chemicals, reagents and enzymes

All used chemicals were analytically pure according to the manufacturers and were obtained from Becton, Dickinson and Company (New Jersey, USA, www.bd.com), Biotium (Fremont, USA, www.biotium.com), Kemika (Zagreb, Croatia, www.kemika.hr), Lonza (Basel, Switzerland, www.lonza.com), Promega (Mannheim, Germany, www.promega.com), Qiagen (Hilden, Germany, www.qiagen.com), Roche (Basel, Switzerland, www.roche.com), Sigma–Aldrich (München, Germany, www.sigmaaldrich.com) and Thermo Fisher Scientific (Waltham, USA, www.thermofisher.com): 2–propanol (Sigma–Aldrich), amonium molybdate (Sigma–Aldrich), ampicillin sodium salt (Sigma–Aldrich), AMV Reverse Transcriptase (Promega), bovine serum albumin (Sigma–Aldrich), Coomassie Brilliant Blue G-250 (Thermo Fisher Scientific), D(+)glucose (Sigma–Aldrich), Difco™ Luria–Bertani (LB) agar, DNA Loading Dye (Thermo Fisher Scientific), Miller (Becton, Dickinson and Company), Difco™ Luria–Bertani (LB) Broth, Miller (Becton, Dickinson and Company), EDTA (Kemika), ethanol (Kemika), ethidium bromide (Sigma–Aldrich), GelRed™ (Biotium), GeneRuler™ 100 bp Plus DNA Ladder (Thermo Fisher Scientific), glycerol (Sigma–Aldrich), GoTaq® DNA Polymerase (Promega), GoTaq® Green Master Mix (Promega), guaiacol (Sigma–Aldrich), High Pure Plasmid Isolation Kit (Roche), hydrogen peroxide (Sigma–Aldrich), IPTG (Promega), L–ascorbic acid (Sigma–Aldrich), L–methionine (Sigma–Aldrich), NaCl (Thermo Fisher Scientific), NBT (Thermo Fisher Scientific), **N,N–dimethylformamide** (Sigma–Aldrich), One–Step RT–PCR Kit (Qiagen), PCR Nucleotide Mix (Promega), phosphoric acid (Kemika), potassium phosphate monobasic (Sigma–Aldrich), potassium phosphate dibasic (Sigma–Aldrich), PVPP (Sigma–Aldrich), PVP (Sigma–Aldrich), QIAquick® Gel Extraction Kit (Qiagen), riboflavin (Sigma–Aldrich), RNase AWAY™ (Thermo Fisher Scientific), RNaseOUT™ Recombinant Ribonuclease Inhibitor (Thermo Fisher Scientific), RNeasy Plant Mini Kit (Qiagen), RT–PCR Grade Water (Thermo Fisher Scientific), sodium hypochlorite solution (Sigma–Aldrich), TBE buffer (Lonza), UltraPure™ Agarose (Thermo Fisher Scientific), X–gal (Promega).

3.1.7. Primers

All primers were purchased from Metabion (Steinkirchen, Germany, www.metabion.com). The primers were delivered as lyophylisates and were solved in sterile mqH_2O to prepare a 100 µM stock solution.

Cloning primers used for plasmid construction:

T7 promoter 5'–TAATACGACTCACTATAGGG–3'

SP6 promoter 5'–ATTTAGGTGACACTATAG–3'

Primer sequences used for cDNA amplification:

Primers for pospiviroid generic detection (Verhoeven et al., 2004)

Pospi1–FW 5´–GGG ATC CCC GGG GAA AC–3´

Pospi1–RE 5´–AGC TTC AGT TGT (T/A)TC CAC CGG GT–3´

Vid–FW 5´–TTC CTC GGA ACT AAA CTC GTG–3´

Vid–RE 5´–CCA ACT GCG GTT CCA AGG G–3´

Primers for species–specific (PSTVd) detection (Di Serio, 2007)

PSTVd–32 5'–AAACCCTGTTTCGGCGGGAATTAC–3'

PSTVd–33 5'–TCACCCTTCCTTTCTTCGGGTGTC–3'

3.2. METHODS

3.2.1. Field surveys and sample collection

In order to investigate the presence of PSTVd in solanaceous ornamentals and crops in Croatia, a survey was conducted from 2009 to 2014 in the framework of the Plant Pest Quarantine Program (project. no. PPN 11/PSTVd) funded by the Croatian Ministry of Agriculture. Ornamental plants such as *Solanum laxum* Spreng., *Lycianthes rantonnetii* (Carrière) Bitter, *Brugmansia* sp. and *Petunia* sp. were sampled in places of retail trade, commercial nurseries and consignments of imported seedlings, whereas potato plants and tomato seedlings were taken from domestic field production and greenhouses, respectively. Each sample consisted of one shoot or five upper leaves taken from individual plants, one to four samples per stock. Samples were stored at –80 ºC until further analysis.

3.2.2. Biological detection

3.2.2.1. Propagation of test plants

A total of five plant species were propagated for the experiments. Tomato (*Solanum lycopersicum* L., cv. Rutgers) and petunia (*Petunia hybrida* Vilm.) commercial seeds were surface sterilized with 0.5% NaOCl and rinsed with tap water. The seeds were sown in greenhouse seedling

trays filled with commercial substrate TS 1 fine (Klasmann–Deilmann, Geeste, Germany), covered with paper to minimize evaporation losses and germinated at room temperature within 10–14 days. The young seedlings (5 ± 2 cm high) were planted into 15–cm diameter pots and maintained in a growth chamber (Kambič Laboratory Equipment d.o.o., Semič, Slovenia) at 16–h day (20 ± 2 ºC)/8–h night (18 ± 2 ºC) temperature regime, with a relative humidity of 70% ± 2%.

Plants of *Solanum laxum* Spreng. and *Lycianthes rantonnetii* (Carrière) Bitter, were kindly provided by a commercial nursery and propagated by stem cuttings. Semi–hardwood cuttings from healthy plants were taken. Using a sharp sterile knife, a clean cut at a 45º angle just below the leaf node was made to maximize the rooting area. The cuttings were no more than 15 cm long. To reduce water loss, the leaves from the lower one–third to one–half of the cutting were removed. The cuttings were rooted in plain tap water at room temperature out of direct light. After roots were formed (approximately 2 weeks), plants were carefully potted into 25–cm diameter pots containing a mixture of soil and perlite (3:1) and placed in a growth chamber under the same growing conditions as tomato plantlets. The young plants were grown up to 5 weeks, until the stem has rooted.

About a week before planting, the seed potatoes (*Solanum tuberosum* L., cv. Désirée) were placed in a warm spot (18 ± 2 ºC) until the eyes of the potato developed sprouts (0.6 – 1.2 cm long). Prior to planting, healthy seed–tubers were cut into several pieces (3 cm), each with one potato eye. The seed pieces were air–dried for 24 hours and planted into 25–cm diameter pots (1 per pot) with the cut side down and the eyes (sprouts) facing up. The plantlets were grown in a growth chamber at 70% ± 2% humidity, under a regime of 16 h light at 20 ± 2 ºC and 8 h darkness at 18 ± 2 ºC up to 3 weeks, until at least two true leaves had developed on each plant.

3.2.2.2. Mechanical inoculation

Test plants were mechanically inoculated at a young stage. Before being mechanically inoculated, all vegetatively propagated plants were found to be free from pospiviroids (as described in chapter 3.2.3.2.). Two to three series of bioassays were independently carried out for each plant species. Within each bioassay, a set of mock– and PSTVd–inoculated plants was arranged. For inoculum preparation, approximately 4 mg of frozen plant material infected with PSTVd (isolate KF418768) was ground with a mortar and pestle in 1 mL of 20 mM sodium phosphate buffer (pH 7.4) containing 2% polyvinylpyrrolidone (MW 10 000). Three fully developed lower leaves of selected test plants (3–4–week–old tomato, petunia and potato seedlings; 9–month–old *S. laxum* and

L. rantonnetii seedlings) were dusted with carborundum powder (silicon carbide, 400 mesh) and inoculated mechanically with the PSTVd–containing buffer suspension (at least 5 plants per experiment). Residual inoculum was washed off with tap water after 5 minutes of infection. Plants that were mock–inoculated only with buffer, served as healthy controls (2–3 per experiment). Bioassays were performed in separate growth chambers (both mock– and PSTVd–inoculated plants, respectively) with a 16 h photoperiod, a temperature cycle of 28 ± 2 ºC/24 ± 2 ºC (day/night) and a relative humidity of 70 ± 2%. Watering and visual inspections were done once per week.

3.2.2.3. Sampling for plant tissue analysis

A total of five plant species, both mock– and PSTVd–infected, were used as test plants for measuring the activities of the antioxidant enzymes, soluble protein determination and endogenous hormone content. Samples from systematically infected leaves placed above those used for the inoculation (except for the top two leaves) were harvested from each biological replicate. Infected and healthy samples (at least three per plant for each type of analyses) were collected at comparable time points, respectively. The harvested material was immediately frozen in liquid nitrogen, and stored at –80 ºC prior to analysis.

3.2.3. Molecular detection

3.2.3.1. Total RNA extraction

Total RNA was extracted from 0.1 g of fresh leaf tissue (collected from field surveys or bioassays, respectively) using the RNeasy Plant Mini Kit, according to the manufacturer's recommendations with minor modifications. Namely, ß–mercaptoethanol was omitted from the procedure, and RNase–free water at 65 ºC was added to the Qiagen column where it was incubated for 5 min before final elution (50 µl). Quantification and quality control of RNA samples were checked by gel electrophoresis and spectrophotometrically. Crude extracts were stored at –80 ºC until used for further analysis.

3.2.3.2. One–step RT–PCR

One–step reverse transcription–polymerase chain reaction (RT–PCR) was performed for the pospiviroid generic detection using the Qiagen One–Step RT–PCR Kit and Pospi1–FW/RE and Vid–FW/RE primers (Verhoeven et al., 2004). Two microliters of template is added to 23 µl master

mix comprising 1.0 µl each of forward and reverse primer (10 µM), 5 µl of 5x One–Step RT–PCR buffer, 1.0 µl One–Step RT–PCR enzyme mix, 1.0 µl dNTPs (10 mM each dNTP) and 14 µl water. The thermocyling programme was as follows: 50 °C for 30 min; 95 °C for 15 min; 35 cycles of 94 °C for 30 s, 62 °C for 60 s and 72 °C for 60 s and a final extension step of 72 °C for 7 min. Positive (PSTVd strain PV–0064; DSMZ, Germany) and negative (water) controls were used to assess test validity. After ending the thermocycler program, the amplified products were immediately separated by agarose gel electrophoresis.

One–step RT–PCR was performed as described by Faggioli et al. (2005) using the specific primers PSTVd–32 and PSTVd–33 complementary and identical, respectively, to positions 156–179 and 180–203 of the PSTVd reference variant (NCBI GenBank acc. no. NC002030) (Di Serio, 2007). For each reaction, 2 µl template RNA was added to 23 µl master mix comprising: 0,16 µM each of forward and reverse primer, 100 µM dNTPs, 1x Colorless GoTaq® Reaction Buffer, 1.25 U GoTaq® DNA Polymerase, 2.5 U AMV Reverse Transcriptase, 20 U RNaseOUT™ and nuclease–free water. The reaction was performed in an Applied Biosystems 2720 Thermal Cycler (Thermo Fisher Scientific, Waltham, USA) with the following thermal profile: 30 min at 46 ºC for reverse transcription, 5 min for initial PCR activation at 94 ºC, followed by 35 cycles of 15 sec at 94 ºC for denaturation, 30 sec at 64 ºC for annealing, 1 min at 72 ºC for primer extension and 7 min at 72 ºC for final extension. Positive (PSTVd strain PV–0064; DSMZ, Germany) and negative (water) controls were used to assess test validity. After ending the thermocycler program, the amplified products were immediately separated by agarose gel electrophoresis.

3.2.3.3. Agarose gel electrophoresis

The PCR amplified products were analyzed by 2% agarose gel electrophoresis in 1x TBE buffer using a RunOne™ (Embi Tec, San Diego, USA) horizontal electrophoresis unit. Each amplification reaction containing 1x DNA Loading Dye was loaded into the gel along with the GeneRuler™ 100 bp Plus DNA Ladder as the size marker. For visualization of bands, gel was stained with ethidium bromide (0.5 µg/ ml) for 10 min and destained in water for 5 min. The target fragments were imaged under UV light using an UVIdoc HD2 (Uvitec, Cambridge, UK).

3.2.3.4. Gel extraction and purification of DNA fragments

In addition, gel electrophoresis was used as a preparative technique to separate PCR amplified cDNA molecules prior to use of other methods such as cloning or DNA sequencing. The amplicons of the expected size were excised from the agarose gel and purified using the QIAquick® Gel Extraction Kit according to manufacturer's instructions. The concentration of each DNA sample was measured using a Jenway Genova Nano micro–volume spectrophotometer (Cole–Parmer, Staffordshire, UK).

3.2.3.5. Molecular cloning

DNA ligation

The pGEM®–T Easy Vector System was used for the cloning of PCR products at a molar ratio of 3:1 (insert:vector) according to manufacturer's instructions. In a 0.5 ml nuclease–free centrifuge tube, 5 µl of 2x Rapid Ligation Buffer, 1 µl of pGEM®–T Easy Vector (50 ng), 1 µl of T4 DNA Ligase enzyme and 3 µl of PCR product were mixed to the final volume of 10 µl. The ligation reaction was gently mixed and incubated at 4 ºC for overnight (~16 h).

Preparation of electrocompetent Escherichia coli cells

In this work, *E.coli* strain DH5α were used for transformation via electroporation due to high transformation efficiency and stable replication of a high number of plasmids. The following protocol describes a method for preparing electrocompetent *E.coli* strain DH5α:

1. One bacterial colony from a freshly grown plate was directly inoculated into LB media (5 ml) and grown overnight (O/N) at 37 ºC with moderate shaking (200 rpm);
2. An overnight culture of bacteria (1 ml) was inoculated into a sterile Erlenmeyer flask containing 100 ml of LB media and incubated at 37 ºC in an orbital shaker (200 rpm). The growth rate of the culture was determined by reading the optical density at 600 nm wavelength using a spectrophotometer (Jenway Genova Nano, Cole–Parmer, Staffordshire, UK). As soon as the bacteria reached mid–logarithmic phase of growth (OD_{600} = 0.4 to 0.5), the flask was put on ice for 15 minutes. In addition, 10% (v/v) sterile glycerol and all corresponding centrifuge tubes (50 ml or 1.5 ml) were prechilled to 4 ºC and kept on ice The bacteria were then harvested by centrifugation (Sigma 2–16KL refrigerated bench–top centrifuge, Sartorius AG, Gottingen, Germany) for 10 minutes at 2,400 x g (4 ºC). After discarding the supernatant, the bacterial pellet was resuspended in 50 ml of ice cold 10% glycerol and centrifuged once more for 10 minutes

at 2,400 x g (4 ºC). Over again, the supernatant was discarded and the pellet was resuspended in 25 ml of ice cold 10% glycerol. This centrifugation and washing step were repeated successively for volume reduction from 10 to 0.2 ml. In the end, small volumes (40 µl) of cell aliquots were snap–frozen with liquid nitrogen and stored at –80 ºC.

Transformation of Escherichia coli by electroporation

1. Electrocompetent cells *E. coli* strain DH5α were thawed on ice for 5 minutes;
2. For a single transformation, 3–5 µl of the ligation reaction was added to one aliquot (40 µl) of bacterial suspension and stirred gently with the pipette tip;
3. All samples were electroporated in a pre-chilled, 0.2 cm gap sterile electroporation cuvette placed into the electroporation chamber of the Gene Pulser Xcell™ Electroporation System (Bio–Rad, Hercules, CA) at 2.5 kV (field strength), 200 Ω (resistor) and 25 µF (capacitor) during 5.0 milliseconds;
4. Immediately after the pulse, the cells were resuspended with 1 ml of prewarmed (37 ºC) SOC medium and transferred to a 15 ml conical tube followed by incubation at 37 ºC in an orbital shaking incubator (GFL, Burgwedel, Germany) at 200 rpm for 1 hour;
5. 200 µl from each transformation culture was spread on LB–ampicillin agar plate with X–gal/IPTG coating;
6. Inverted plates were incubated overnight at 37 ºC (Binder BD 400 Series Incubator, Tuttlingen, Germany).

Selection of recombinants and protocol for screening bacterial colonies by PCR

1. Transformed bacterial colonies were blue–white selected using the X–gal/IPTG system. For each colony PCR screening reaction, five white colonies were picked from a single transformation plate;
2. A sterile micropipette tip was used to transfer a few cells from each colony to a corresponding microcentrifuge tube (0.2 ml), where cells were resuspended in 10 µl of sterile water. In addition, a few cells of the colony were transferred into a 15 ml centrifuge tube containing 4 ml of liquid LB–ampicillin media (100 µg/mL) and left for overnight culture in a shaking incubator (37 ºC, 200 rpm) prior to plasmid DNA isolation;
3. After short incubation at 95 ºC for 10 min in a thermal cycler, microcentrifuge tubes (0.2 ml) with denatured bacterial suspension were snap–cooled on ice and centrifuged at 11,200 x g for 5 min (Eppendorf Centrifuge 5415 R, Hamburg, Germany);

4. The supernatant (1 µl) was used as template for colony PCR. A 10 µl PCR reaction was set up on ice using 5 µl of 2x GoTaq® Green Master Mix, 0.4 µl of each insert–specific primer at 10 µM (Di Serio, 2007) and nuclease–free water to a final volume. The mixture was incubated in an Applied Biosystems 2720 Thermal Cycler (Thermo Fisher Scientific, Waltham, USA) with the following cycling conditions: initial denaturation at 94 ºC for 2 min and further 30 cycles at 94 ºC for 30 sec, 52 ºC for 30 sec and 72 ºC for 45 sec and 72 ºC for 7 min. Positive (PSTVd PV–0064) and negative (nuclease–free water) controls were used for all tests;
5. The size range of the PCR products was determined by analytical agarose gel electrophoresis;
6. Colonies exhibiting proper response to the screening assay were selected for further plasmid isolation. For each sample, 3.5 ml of overnight bacterial culture from a single colony pick (step 2 above) was harvested by centrifugation (9,200 x g, 8 min, 4 ºC). The supernatant was discarded and the pellet was used in minipreparation method (minipreps) for plasmid DNA isolation. The remaining cells were frozen in bacterial glycerol stock format for longer–term access, i.e. 187 µl of each overnight culture was transferred into a labeled cryovial (1.5 ml), gently mixed with 63 µl of 80% sterile glycerol (v/v) and stored at –20 ºC.

Plasmid isolation from E. coli

Plasmid DNA was isolated from bacterial cultures using the High Pure Plasmid Isolation Kit according to the manufacturer's instructions. The kit was used to prepare purified plasmid DNA from *E. coli* in small quantities (minipreps) relying on an alkaline lysis method. Plasmids were eluted in 50 µl of nuclease–free water and stored at –80 ºC. Plasmid DNA was quantified using a nanodrop spectrophotometer (Jenway Genova Nano, Cole–Parmer, Staffordshire, UK).

3.2.3.6. DNA sequencing and bioinformatic analysis of Croatian PSTVd isolates

Plasmids were subjected for bidirectional sequencing at the Macrogen Inc. (Amsterdam, the Netherlands) using universal T7 and SP6 promoter primers, provided by the sequencing service. Single pass sequencing was performed using 10 µl of 100 ng/µl plasmid DNA preparation (at least three clones per transformation). The sequence data obtained for each isolate were combined and edited using the BioEdit software package (www.mbio.ncsu.edu/bioedit/bioedit.html). Consensus sequences were trimmed to the correct length and identified by comparison with the sequences available in the GenBank database of NCBI (www.ncbi.nih.gov) (Altschul et al., 1997). Multiple alignments of the obtained sequences were performed using the MAFFT software version 7 (Katoh

and Standley, 2013). The nucleotide sequences of PSTVd have been deposited in the NCBI GenBank.

3.2.3.7. Phylogenetic analysis of *Solanum*, *Lycianthes* and *Petunia* species based on *ndhF* chloroplast gene sequences

A phylogenetic analysis of several solanaceous species was conducted using sequence data for the chloroplast NADH dehydrogenase F (*ndhF*) gene (Bohs and Olmstaed, 1997). The following *ndhF* gene sequences were compared from *Solanum tuberosum* (GenBank Accession No. L76287.1), *Solanum lycopersicum* (U08921.1), *Solanum muricatum* (AF500846.1), *Solanum laxum* (AF500836.1), *Lycianthes rantonnetii* (AF500840.1), *Capiscum* spp. (DQ667528.1), *Physalis peruviana* (FJ914034.1), *Brugmansia* spp. (KP756872.1), *Petunia* (U08926.1), *Cestrum* spp. (KU376250.1) and *Persea americana* (JQ437545.1). Multiple sequence alignment was created using the ClustalW algorithm with default parameters as implemented in MEGA version 7.0 computer software (Kumar et al., 2016). A phylogenetic tree was inferred with the maximum–likelihood (ML) algorithm in MEGA version 7.0 using the closest neighbor interchange as the ML heuristic search method with 1000 bootstrap replicates.

3.2.4. Determination of chlorophyll and carotenoid content

Total chlorophylls and carotenoids were extracted from lyophilized leaf tissues in 80% acetone, followed by centrifugation at 20,000 x g for 15 minutes. The pellet was rewashed with acetone until it became colorless. The absorbance of acetone extract was measured at 647, 664 and 453 nm against an acetone blank, using a BioSpec–1601 spectrophotometer (Shimadzu, Kyoto, Japan). The concentration of chlorophyll *a* and *b*, and carotenoids (mg g^{-1} dry weight) was calculated using formulae given by Lichenthaler (1987).

3.2.5. Quantitative analysis of the major stress–related plant growth regulators in crude plant extracts by ultra–performance liquid chromatography–tandem mass spectrometry (UPLC–MS/MS)

The freeze–dried plant samples were subjected to plant hormones analysis service (Laboratory of Growth Regulators, Centre of the Region Haná for Biotechnological and Agricultural Research, Institute of Experimental Botany ASCR & Palacký University, Olomouc, Czech

Republic). Endogenous contents of SA, JA, *cis*–OPDA, ABA, and IAA were simultaneously quantified in MeOH extracts pre–cleaned by microscale solid–phase extraction on silica–based aminopropyl matrix (Varian, Darmstadt, Germany) using UHPLC–MS/MS as previously described (Floková et al., 2014). In a separate set of samples, the endogenous BR–castasterone was quantified with the addition of isotope–containing internal standards for several different BRs according to Oklestkova et al. (2017). The isolation and identification of CS was performed according to a modified protocol described by Oklestkova et al. (2017). Briefly, the plant material (100 mg of fresh weight) was homogenized in 2 ml ice–cold 80% methanol. After centrifugation (15 min, 2,000 x g, 4 ºC), the supernatants were collected, an internal standard solution was added to all samples that contained deuterium labeled BRs, and the resulting solutions were passed through Discovery columns (Supelco, Bellefonte, USA). The extracts were evaporated under vacuum on Rotavapor R–215 (BÜCHI, Switzerland). Samples were resuspended in 1 ml of 7.5% MeOH in phosphate–buffered saline (50 mM NaH_2PO_4, 15 mM NaCl, pH 7.2), and passed through an immunoaffinity column (manufactured by the Laboratory of Growth Regulation, Olomouc, Czech Republic). After evaporation the samples were redissolved in methanol and the CS was determined by UHPLC with tandem mass spectrometry (UHPLC–MS/MS) by using an ACQUITY UPLC® I–Class System (Waters, Milford, MA, USA) and a triple quadrupole mass spectrometer XevoTM TQ–S MS (Waters MS Technologies, Manchester, UK). The endogenous contents of PGRs (plant hormones) quoted are mean values from three extracts of at two to three independent experiments.

3.2.6. Determination of antioxidant enzyme activities

3.2.6.1. Preparation of enzyme extract

Preparation of crude enzyme extract from test plants was identical for all enzymes examined. Frozen samples of leaf and tuber tissues were ground to a fine powder and 0.2 g of such a sample was further homogenized with 1 ml of ice–cold extraction buffer. The homogenate was centrifuged at 9,200 x g for 30 min at 4 ºC and the supernatant (crude protein extract) was aliquoted (5 x 200 µl), and stored at –80 ºC. A minimum of three extractions were prepared for each sample, in order to be used for enzyme activity measurements and soluble protein determination according to Bradford (1976).

3.2.6.2. Bradford protein assay

The Bradford (1976) protein assay was used to measure the concentration of total protein in a sample using bovine serum albumin (BSA) as standard. The assay was performed in a 96–well microplate wells (Thermo Scientific™ Nunc™, USA). In each well, 200 µl of Bradford reagent and 10 µl of standard/ blank/ sample was added, and incubated for 15 minutes at room temperature. The absorbance at 595 nm was measured with an ELx800 absorbance microplate reader (BioTek Instruments, Winooski, USA). With every assay a blank was included (extraction buffer for enzyme activity assay) to set the instrument to the 100% transmittance (absorbance value zero). The standard curve was prepared with the independent variable (protein concentration–mg/mL) on the X axis and the dependent variable (absorbance–595 nm) on the Y axis. The protein concentration of the experimental samples was calculated using the standard curve equation. Results were expressed as µg of proteins per gram of fresh weight.

3.2.6.3. Analysis of ascorbate peroxidase activity

Ascorbate peroxidase (APX) activity was determined spectrophotometrically by monitoring the decrease in ascorbate at A_{290} ($\boldsymbol{\varepsilon} = 2.8\ mM^{-1}\ cm^{-1}$) as described by Nakano and Asada (1981). The assay was performed in quartz cuvettes with a 1 cm path length. The total volume (1 ml) of each reaction mixture consisted of 880–945 µl ascorbate peroxidase assay buffer (pH 7.0), 10 µl of 50 mM ascorbic acid and 25–180 µl of crude enzyme extract. The reaction was started by the addition of 10 µl of 12 mM H_2O_2 and mixed by inversion. The decrease in absorbance at 290 nm for 30 seconds was recorded using BioSpec–1601 spectrophotometer (Shimadzu, Kyoto, Japan) and the enzyme activity was expressed as unit min^{-1} mg^{-1} protein. One unit was defined as one micromole of ascorbic acid oxidized min^{-1} (mg of total protein) $^{-1}$ at 25 ºC. A blank for each sample was prepared by adding 25–180 µl of 50 mM potassium phosphate buffer instead of crude enzyme extract.

3.2.6.4. Analysis of catalase activity

Catalase activity (CAT) was determined using a colorimetric assay based on the stable yellow complex formed by ammonium molybdate with hydrogen peroxide (modified from Luhova et al. 2003). The enzyme extract (50–100 µl) was incubated in 50 mM potassium phosphate buffer (pH 7.0) supplemented with 65 mM H_2O_2 at 25 ºC for 4 min, in a total volume of 1 ml. After this period of time, the addition of 1 ml of 32.4 mM ammonium molybdate stopped the consumption of

hydrogen peroxide present in the extract. Absorbance of the yellow complex formed in a test cuvette (S) was measured at 405 nm in BioSpec–1601 spectrophotometer (Shimadzu, Kyoto, Japan). A blank for each sample was prepared by adding 1 ml of ammonium molybdate to 1 ml of 50 mM potassium phosphate buffer (pH 7.0). Also, the assay used a correction factor to exclude the interference that arises from the presence of amino acids and proteins in the sample that contains catalase enzyme. A control–test cuvette (M) contained 50–100 µl of crude enzyme extract, 900–950 µl of 50 mM potassium phosphate buffer (pH 7.0) without H_2O_2, and 1 ml ammonium molybdate. A standard cuvette (S°) contained 50–100 µl of 50 mM potassium phosphate buffer (pH 7.0), 900–950 µl of 50 mM potassium phosphate buffer (pH 7.0), supplemented with 65 mM H_2O_2 and 1 ml of ammonium molybdate. The absorbance of the test cuvette (S) in the procedure refers to two types of compounds, un–reacted hydrogen peroxide and interferences found in the extract, while the absorbance of the control–test tube (M) refers to interference compounds found in the extract only. By subtracting the absorbance of the control–test tube from the absorbance of the test tube, the interference of any compound that may be reacting with ammonium molybdate was eliminated. This means the remaining absorbance belongs to un–reacted hydrogen peroxide only (Hadwan and Abed, 2016). The rate constant of a first–order reaction equation was used to determine catalase activity, according to Hadwan and Abed (2016):

$$A\ (U/ml) = [2.303 / t] \times \log [S^{\circ} / (S - M)] \times [Vt/Vs]$$

t – time; S^{o} – absorbance of a standard cuvette; S – absorbance of a test cuvette; M – absorbance of a control–test (correction factor); Vt – total volume of reagents in test tube; Vs – volume of extract

3.2.6.5. Analysis of guaiacol peroxidase activity

Guaiacol peroxidase (GPX) activity was determined at 470 nm by its ability to convert guaiacol to tetraguaiacol ($\varepsilon = 26.6\ mM^{-1}\ cm^{-1}$) according to the method of Chance and Maehly (1955). The enzymatic reaction was initiated by addition of 10–50 µl enzyme extract to 950–990 ul guaiacol peroxidase assay solution. The initial rate of guaiacol oxidation was measured by the rate of formation of tetraguaiacol at 470 nm for 1 minute (BioSpec–1601 spectrophotometer, Shimadzu, Kyoto, Japan). The peroxidase activity was expressed as µmol min^{-1} mg^{-1} of protein. One unit is defined as the amount of enzyme required to catalyze the conversion of one micromole of hydrogen peroxide, with guaiacol as hydrogen donor, per minute under specified conditions. In a control

(blank) test cuvettes, the sample was replaced by 10–50 µl of 50 mM potassium phosphate buffer (pH 7.0) and the absorbance was measured at OD_{470}.

3.2.6.6. Analysis of superoxide dismutase activity

The assay for superoxide dismutase (SOD) activity was performed by a modified method of Giannopolitis and Reis (1977). Aliquots (780 µl) of the superoxide dismutase assay solution (50 mM potassium phosphate buffer (pH 7.0) containing 0.1 mM EDTA, 13 mM L–methionine and 75 µM NBT) were delivered into cuvettes, followed by the addition of 100–190 µl of 50 mM potassium phosphate buffer (pH 7.0), 10–100 µl of crude enzyme extract, and 20 µl of 250 µM riboflavin to a total volume of 1 ml. The content was mixed by inversion and then illuminated for 8 minutes under the fluorescent lamps (25 W). The control test cuvettes, containing 10–100 µl of 50 mM potassium phosphate buffer (pH 7.0) and 20 µl of 250 µM riboflavin, were illuminated (a positive control) or kept in the dark (blank). The reaction was stopped by switching off the light and placing the tubes in the dark. Increase in absorbance due to the photoreduction of NBT was measured at 560 nm (BioSpec–1601 spectrophotometer, Shimadzu, Kyoto, Japan). Under the described conditions, the increase in absorbance in the control was taken as 100% and the enzyme activity in the samples was calculated by determining the percentage inhibition per minute. One unit of SOD was the amount of enzyme that causes a 50% inhibition of the rate for photoreduction of NBT under the conditions of the assay.

3.2.6.7. Statistical analysis

Each experiment had at least two mock–inoculated and five PSTVd–infected plants, and was replicated two to three times. The values were presented as mean ± standard error (SE). The statistical significance between the observed mean values of mock– and PSTVd–inoculated plants was measured by Student's t–test using the Microsoft Excel "data analysis 2007" tool pack. A probability of $*P \leq 0.05$, $**P \leq 0.01$, $***P \leq 0.001$ was considered significant.

4.1. OCCURRENCE AND MOLECULAR CHARACTERIZATION OF PSTVd IN CROATIA

4.1.1. Potato spindle tuber viroid disease in Croatia

In order to identify the presence of *Potato spindle tuber viroid* in solanaceous ornamentals and crops in Croatia, a survey was conducted from 2009 to 2014 in the framework of the Plant Pest Quarantine Program, funded by the Croatian Ministry of Agriculture. A total of 235 samples were collected from 137 locations in continental west, continental east and Adriatic regions of Croatia. The survey was targeted at various members of the family Solanaceae, mainly ornamentals such as *Solanum laxum* Spreng., *Lycianthes rantonnetii* (Carrière) Bitter., *Brugmansia* sp. and *Petunia* spp., sampled in places of retail trade, commercial nurseries and consignments of imported seedlings (Fig. 7). Also, horticultural crops such as *Solanum lycopersicum* L. and *Solanum tuberosum* L. from domestic field production and greenhouses were sampled (Fig. 7). Amongst 235 samples submitted for diagnosis to the Institute for Plant Protection in Zagreb, two ornamental solanaceous species, *S. laxum* and *L. rantonnetii* were found to be infected with PSTVd (Table 3). In 2009, the presence of PSTVd was confirmed in three samples of *S. laxum* collected from different garden centres in Varaždin and Umag, and in two samples of *L. rantonnetii* collected from retail nurseries in Kutina and Ribnik (Table 4, Fig. 8). In accordance with Croatian legislation (Plant Health Act Official Gazette 75/05, 25/09, 55/11) and the EU Commission Decision 2007/410/EC, eradication measures were taken and infections were traced back to prevent any further spread of PSTVd. In general, when PSTVd was detected in ornamental species, contaminated lots were destroyed by incineration. All material in contact with the contaminated lot was disinfected and strict hygienic measures were imposed. No further findings of PSTVd were made during official surveys in 2010 and 2011. In 2012, PSTVd was detected in three samples of *S. laxum* collected from a retail nursery in Velika Ludina and a garden center in Varaždin (Table 4, Fig. 8). Repeated infection found at the same location in Varaždin as it was in 2009 was from new imported stock. In 2013, three findings were made on *S. laxum* in a garden center in Zadar, as well as retail nurseries in Koprivnički Ivanec and Lazina Čička (Table 4, Fig. 8). No further findings were made during the official survey in 2014. All samples of other ornamental species (*Brugmansia* sp. and *Petunia* spp.), as well as tomato and potato plants taken during the official controls from 2009 to 2014, were found to be negative.

Figure 7. Solanaceous species collected during the survey for PSTVd in Croatia. (A) Potato field in Lika, (B) harvested potato tubers, (C) rows of tomato plants growing hydroponically (photo by T. Rehak), (D) tomato plants growing in an open field in Istra (photo by T. Rehak), (E) *Solanum laxum*, (F) *Petunia* sp., (G) *Petunia* x *atkinsiana* 'Surfinia', (H) *Lycianthes rantonnetii*, (I) *L. rantonnetii* leaf tissue sampling and (J) potted *Brugmansia* sp. plants.

Table 3. Solanaceous species assayed for PSTVd by one–step RT–PCR and primers specific for PSTVd. The number of tested plants is followed by the number of plants tested positive for PSTVd.

Plant species	2009	2010	2011	2012	2013	2014
Solanum laxum	45/3	7/0	3/0	7/3	7/3	1/0
Lycianthes rantonnetii	12/2	3/0	2/0	3/0	3/0	3/0
Brugmansia sp.	9/0	3/0	5/0	2/0	1/0	nt
Petunia spp.	nt	11/0	18/0	19/0	20/0	3/0
Solanum lycopersicum	nt	4/0	8/0	4/0	4/0	5/0
Solanum tuberosum	nt	3/0	8/0	6/0	5/0	1/0
Total	66/5	31/0	44/0	41/3	40 /3	13/0

nt – not tested

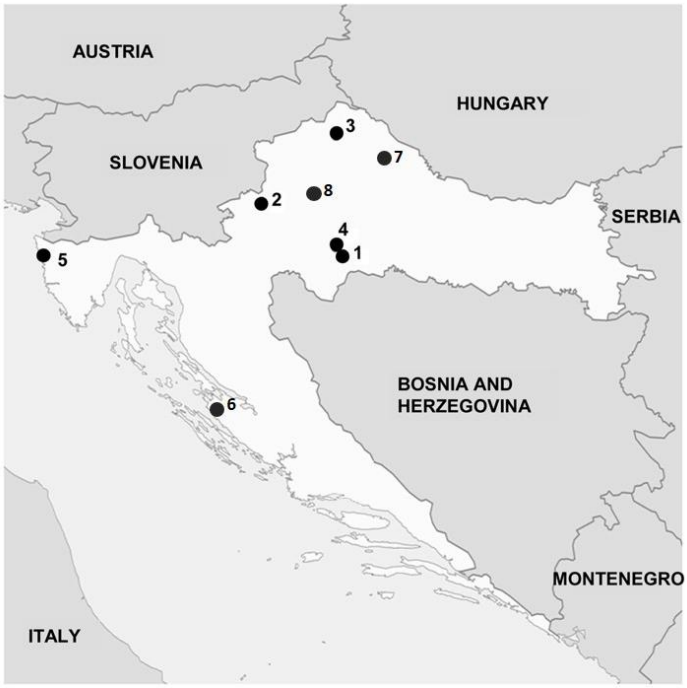

Figure 8. Map of Croatia specifying the locations where the positive samples were found: (1) Kutina, (2) Ribnik, (3) Varaždin, (4) Velika Ludina, (5) Umag, (6) Zadar, (7) Koprivnički Ivanec and (8) Lazina Čička.

Table 4. PSTVd–infected solanaceous ornamentals collected during the survey in Croatia from 2009 to 2014.

Host	Location	Year	Genome size (nt)	Accession No.
Lycianthes rantonnetii	Kutina	2009	357	KF418769
Lycianthes rantonnetii	Ribnik		357	KF418771
Solanum laxum	Varaždin		357	KF418772
Solanum laxum	Varaždin		357	KF418773
Solanum laxum	Umag		357	KF418774
Solanum laxum	Varaždin	2012	357	KF418768
Solanum laxum	Velika Ludina		357	KF418767
Solanum laxum	Velika Ludina		357	KF418770
Solanum laxum	Zadar	2013	357	KM204319
Solanum laxum	Koprivnički Ivanec		357	KM204317
Solanum laxum	Lazina Čička		357	KM204318

4.1.2. Variability of PSTVd isolates from nursery–grown ornamental plants

To characterize PSTVd isolates from ornamental plants, total RNA was extracted from leaf tissue and utilized as a template in one–step RT–PCR assay. The obtained amplicons of about 360 bp, corresponding to the full length viroid genome of PSTVd, were extracted from agarose gel, cloned into pGEM®–T Easy Vector System and sequenced in both directions. The viroid identity of obtained sequences was confirmed using the NCBI BLAST sequence analysis tool (Altschul et al., 1997) and the sequenced clones were deposited in the GeneBank under the accession numbers listed in Table 4. Sequence alignment revealed that nine isolates from *S. laxum* (KF418772, KF418773, KF418774, KF418768, KM204319, KF418767, KF418770, KM204317, KM204318) and two PSTVd isolates from *L. rantonnetii* (KF418769, KF418771) were identical to PSTVd variants previously reported from the Netherlands, Italy, Greece, Slovenia and Belgium (Table 5). The difference between discovered isolates was located in the region associated with pathogenicity (P domain) and exhibited the substitution of G to U at the sequence position 65 (Table 5), which is in accordance with Viršček Marn et al. (2013) who identified a hotspot for sequence variability at the position 65. Our results confirm for the first time the presence of PSTVd in Croatia.

Table 5. PSTVd sequence comparison between isolates from Croatia and similar sequence variants from the GeneBank, identified by multiple sequence alignment. The only nucleotide change was observed at position 65.

Accession No.	Host	Origin	Substitution at position 65	Reference
KF418772[a]	*S.laxum*	Croatia	G	Milanović et al. (2014)
EF192393	*S.laxum*	The Netherlands	G	Verhoeven et al. (2008a)
EF459700	*L. rantonnetii*	Italy	G	Navarro et al. (2009)
FJ872823	*S. lycopersicum*	Italy	G	Navarro et al. (2009)
FM998542	*S.laxum*	Belgium	G	CABI/EPPO (2014)
GU481091	*S.laxum*	Greece	G	Malandraki et al. (2010)
HQ454914	*S.laxum*	Slovenia	G	Virščček Marn et al. (2013)
HQ454915	*L. rantonnetii*	Slovenia	G	Virščček Marn et al. (2013)
HQ454916	*Petunia sp.*	Slovenia	G	Virščček Marn et al. (2013)
KF418769[b]	*L. rantonnetii*	Croatia	U	Milanović et al. (2014)
KF418767[c]	*S.laxum*	Croatia	U	Milanović et al. (2014)
FM998550	*S.laxum*	Belgium	U	CABI/EPPO (2014)
HQ454917	*S.laxum*	Slovenia	U	Virščček Marn et al. (2013)
HQ454918	*L. rantonnetii*	Slovenia	U	Virščček Marn et al. (2013)

[a] The sequence variant identical to KF418773, KF418774, KF418768 and KM204319, isolated from the same host but from different locations in Croatia (Milanović et al., 2014).

[b] The sequence variant identical to KF418771, isolated from the same host but from a different location in Croatia (Milanović et al., 2014).

[c] The sequence identical to KF418770, KM204317 and KM204318 isolated from the same host but from different locations in Croatia (Milanović et al., 2014).

4.1.3. Characterization of PSTVd isolates from *Solanum laxum* by bioassays on symptomatic tomato plants

To test the pathogenicity of potato spindle tuber viroid isolates from ornamental plants, bioassays were performed by mechanical inoculation of sap prepared from fresh plant tissue of *Solanum laxum* infected with PSTVd (isolates KF418768 and KF418770) onto three plants of each tomato cultivar, *Solanum lycopersicum* cv. Rutgers and cv. BELLE F1. Bioassays were performed in a growth chamber with a 16 h photoperiod, a temperature cycle of 28 ± 2 ºC/24 ± 2 ºC (day/night) and a relative humidity of 70 ± 2%. The results of biological assays showed that PSTVd was transmitted successfully to indicator tomato plants. The PSTVd infection was determined by observation of symptoms and RT–PCR (Fig. 9), followed by sequencing of the cloned PCR products, as described previously. The severity of symptoms in tomato differed between cultivars: cv. Rutgers showed much stronger symptoms (epinasty, leaf distortion and brittleness) of infection than cv. BELLE F1 (Fig. 9A, B). There was no difference in symptoms depending on the sequence variability of isolates. Healthy tomato mock inoculated controls were asymptomatic (Fig. 9C). Sequence analysis of progeny molecules derived after the first passage, confirmed the presence of PSTVd but no nucleotide sequence mutations compared to the predominant genotype were detected. Leaf tissue of tomato cv. Rutgers infected with isolate KF418768, the most prevalent sequence variation, was preserved at –80 ºC and used as an inoculum source in further experiments.

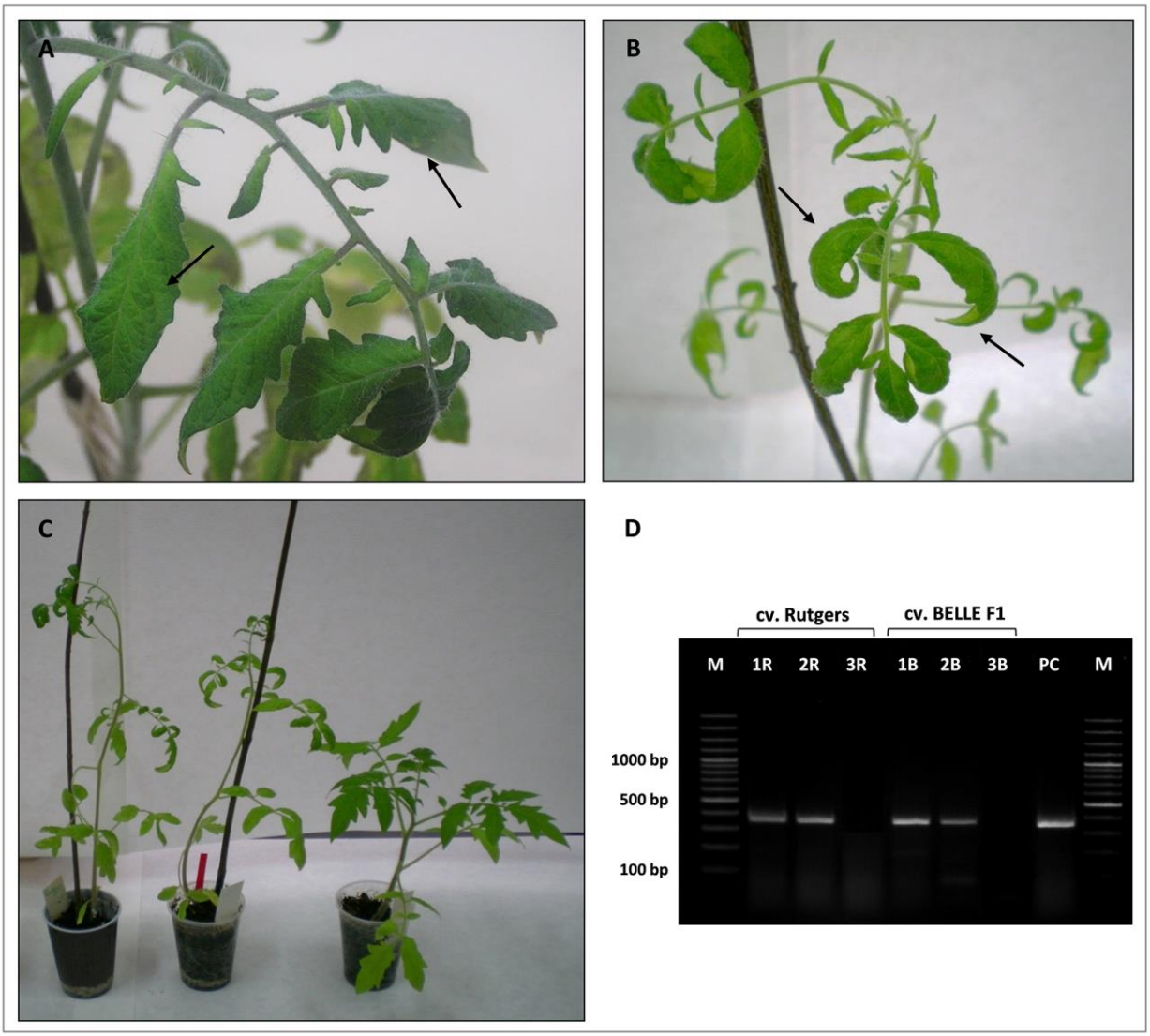

Figure 9. The pathogenicity test of PSTVd isolate KF418768 on symptomatic tomato plants. Symptom development in (A) tomato cv. BELLE F1 and (B) cv. Rutgers plants, 4 wpi. Arrows show leaf curling, lesions and rugosity. (C) Comparison of a mock–inoculated control (right) and two PSTVd–inoculated plants (center and left) of tomato cv. Rutgers. (D) RT–PCR analysis of tomato plants (6 wpi) with individual sample number: PC, positive control PV–0064 (360 bp); M, molecular weight marker (100 bp DNA ladder); 1R, 2R – infected cv. Rutgers; 1B, 2B – infected cv. BELLE F1; 3R, 3B – mock–inoculated control cv. Rutgers and cv. BELLE F1 plants, respectively.

4.2. DIFFERENCES IN THE DEFENSE RESPONSE AGAINST PSTVd AMONG SOME SOLANACEOUS SPECIES

Viroid infections are frequently accompanied by physiological and developmental disorders that ultimately result in expression of symptoms. PSTVd mainly infects species of the family Solanaceae with a potential to cause economic damage in important horticultural crops such as potato and tomato. Both potato and tomato are natural hosts of PSTVd which can cause characteristic symptoms on developing plants including stunting phenotype and distortion of leaves and tubers (Katsarou et al., 2016). In potato, growth of PSTVd infected plants may be severely reduced or even cease entirely. Tubers may be reduced in size, misshapen, spindle– or dumbbell–shaped, with conspicuous and prominent eyes that are evenly distributed (Owens, 2007). Infected tomatoes show growth reduction which may develop into permanent stunting with occasional death or recovery. However, in many solanaceous ornamentals, PSTVd progressively spreads without the appearance of visible disease symptoms and therefore, these plants represent a danger as a latent source for new infections (Flores et al., 2011). PSTVd can alter the composition and concentration of plant hormones, which may be linked to morphological changes. Nevertheless, physiological effects of hormones in ornamental species upon PSTVd infection are still unknown.

In this study, changes in endogenous hormone status and antioxidant enzymes activity in *Solanum lycopersicum* cv. Rutgers, *S. tuberosum* cv. Désirée, *S. laxum*, *Lycianthes rantonnetii* and *Petunia hybrida* upon PSTVd infection were investigated. These plant species have been chosen because they are natural and experimental hosts of PSTVd (Singh, 1973), belong to the same botanical family, and for most of them genome has been completely sequenced and annotated (apart from evergreen vines, *S. laxum* and *L. rantonnetii*). The level of endogenous hormones and antioxidant enzymes activity was measured in mock– and PSTVd–inoculated plants to access to which extent PSTVd infection causes changes in PGRs content and antioxidant response in symptomless ornamentals in comparison to symptomatic solanaceous crops.

4.2.1. Differences in symptom expression among indicator plants

4.2.1.1. Symptom development in tomato

The tomato cultivar Rutgers is known to be susceptible to PSTVd and therefore we used it to test the efficacy of the inoculum and to provide visual evidence of pathogenicity (Fig 10). In infected tomato plants, the foliar symptoms became apparent about 5 weeks post–inoculation (wpi). The first sign noted was leaf distortion with downward curling of the terminal leaves, subsequently accompanied by uneven distribution of pigments, mild interveinal chlorosis, overlapping of leaflets and/or wrinkling of the leaf surface (Fig. 10E–G). Severe chlorosis with the yellow leaf tissue and necrotic dieback along the leaf margins developed later (about 9 wpi) on the older leaves (Fig. 10H). The presence of viroid RNA in systemically infected leaves of tomato was confirmed by RT–PCR 5 wpi (Fig. 10I).

4.2.1.2. Symptom development in potato

In infected potato cv. Désirée, vague leaf symptoms were observed about 8 wpi, at the same time when viroid RNA was detected by RT–PCR. The leaflets of infected plants were smaller in size, pointed and upright (Fig. 11 D–F). Some of infected plants became progressively restricted in growth, contrasting with healthy ones (Fig. 11G). Moreover, tubers of affected potato plants were smaller and/or more elongated than those in healthy plants (Fig. 12). Tuber eyes appeared to be more numerous and had characteristic indentation with ‘heavy brows’ (Fig. 12C).

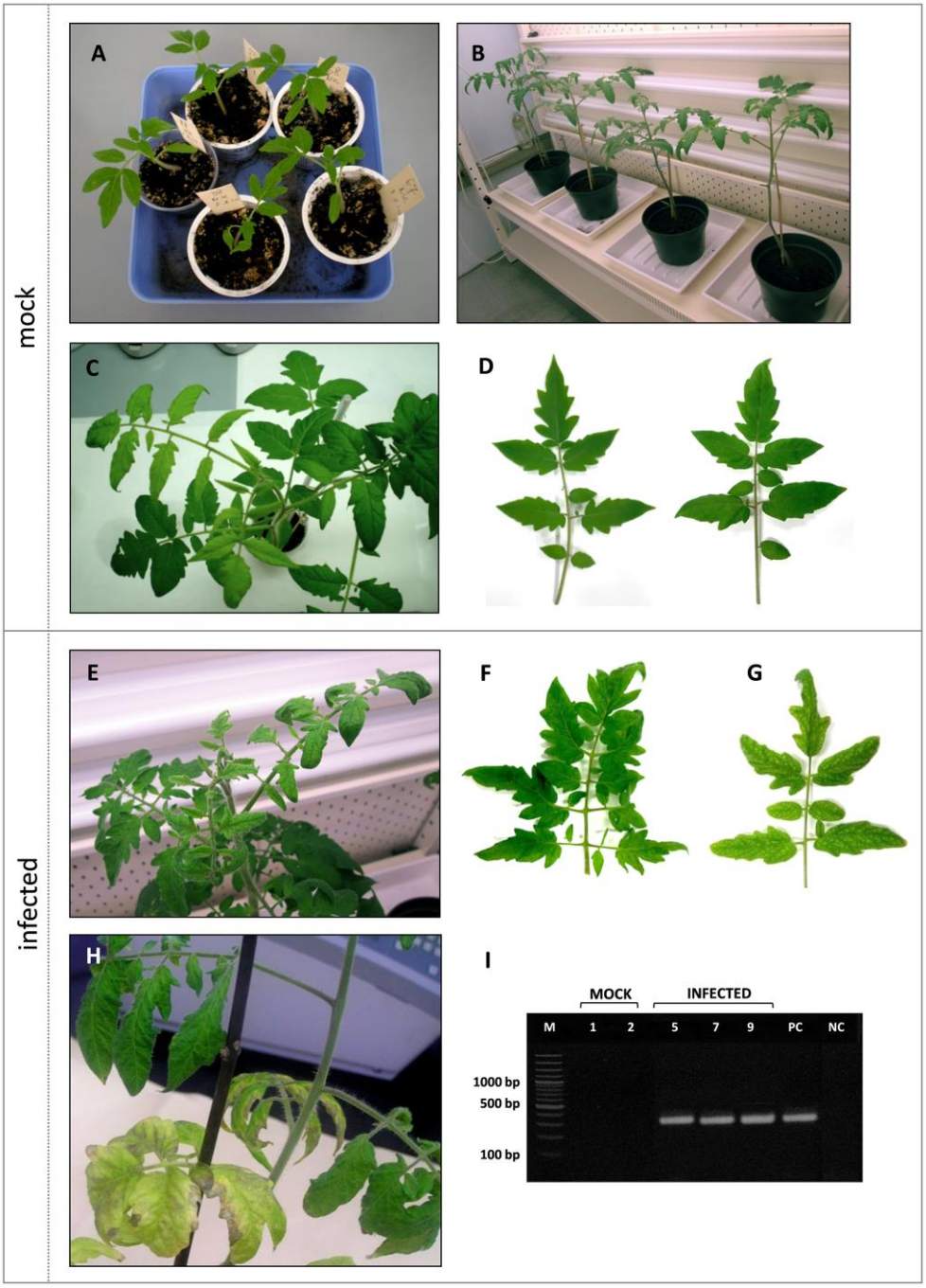

Figure 10. Experimental setup of *Solanum lycopersicum* cv. Rutgers. Mock, control plants: (A) young tomato seedlings, (B) one–month–old plants in a growth chamber, (C) mock–inoculated plant (5 wpi) and (D) healthy tomato leaves. Details of a leaf infected with PSTVd showing: (E) reduced **size** of **young leaves** at the top of the plant, (F–G) overlapping of leaflets and light vein clearing (about 5 wpi). (H) Severe symptoms of PSTVd in older tomato plants (about 9 wpi). (I) RT–PCR analysis of tomato plants (5 wpi) with individual sample number. PC, positive control PV–0064 (360 bp); NC, negative control (nuclease–free water); M, molecular weight marker (100 bp DNA ladder).

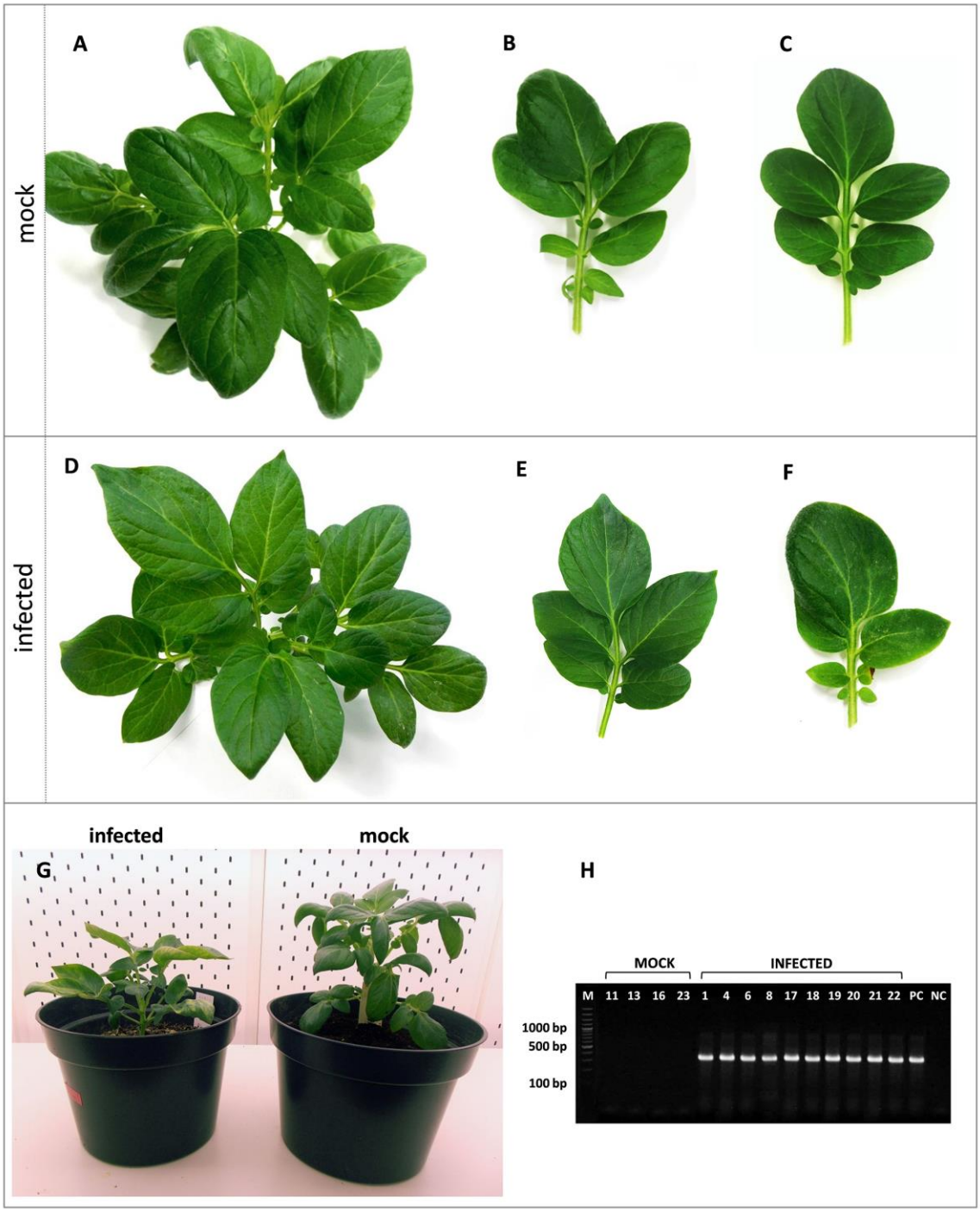

Figure 11. Experimental setup of *Solanum tuberosum* cv. Désirée. (A) Mock plant (8 wpi) and (B–C) healthy potato leaves. (D–F) Foliar symptoms of PSTVd infection (8 wpi), the leaflets of infected plants are smaller in size, deformed, pointed and upright. (G) Restricted growth in infected potato plants, contrasting with healthy ones. (H) RT–PCR analysis of potato plants (8 wpi) with individual sample number. PC, positive control PV–0064 (360 bp); NC, negative control (nuclease–free water); M, molecular weight marker (100 bp DNA ladder).

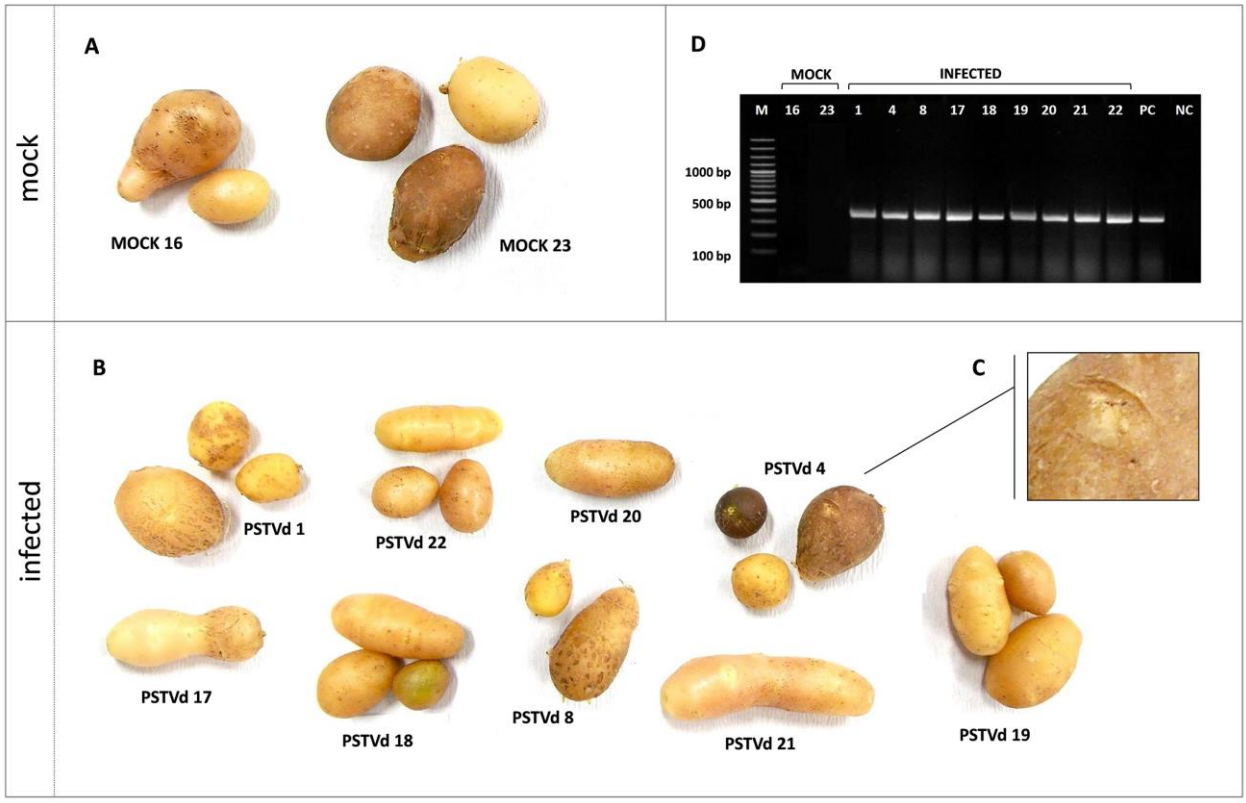

Figure 12. Experimental setup of *Solanum tuberosum* cv. Désirée: (A) healthy tubers and (B) PSTVd–infected tubers (8 wpi), (C) characteristic indentation of eyes with 'heavy brows' of infected tubers and (D) RT–PCR analysis of potato tubers (8 wpi) with individual sample number. PC, positive control PV–0064 (360 bp); NC, negative control (nuclease–free water); M, molecular weight marker (100 bp DNA ladder).

4.2.1.3. Absence of symptoms in ornamentals

Infected ornamentals did not display any visible symptoms of potato spindle tuber viroid disease until the end of the experiments, although the systemic spread of PSTVd was proven by RT–PCR. There were no differences in leaf structural features and coloration of systemically infected leaves of *P. hybrida* in which the presence of the viroid RNA was detected by RT–PCR 5 wpi (Fig. 13). In *S. laxum* plants, it took longer for a systemic viroid infection to develop, and positive RT–PCR results were obtained only after two successive inoculations (18 weeks after the first or 10 weeks after the second inoculation), as shown in Fig. 14C. A similar procedure was applied to *L. rantonnetii* plants where positive RT–PCR results (Fig. 15C) were obtained after three consecutive inoculations (22 weeks after the first or 10 weeks after the second or 4 weeks

after the third inoculation). *S. laxum* is an evergreen vine, larger than the other species tested in this study, and a slow spread of viroid infection in this species was reported by Verhoeven et al. (2010a). Similar to *S. laxum*, *L. rantonnetii* is an evergreen shrub and due to a low transmission rate of viroid within woody plants, repeated inoculations were necessary.

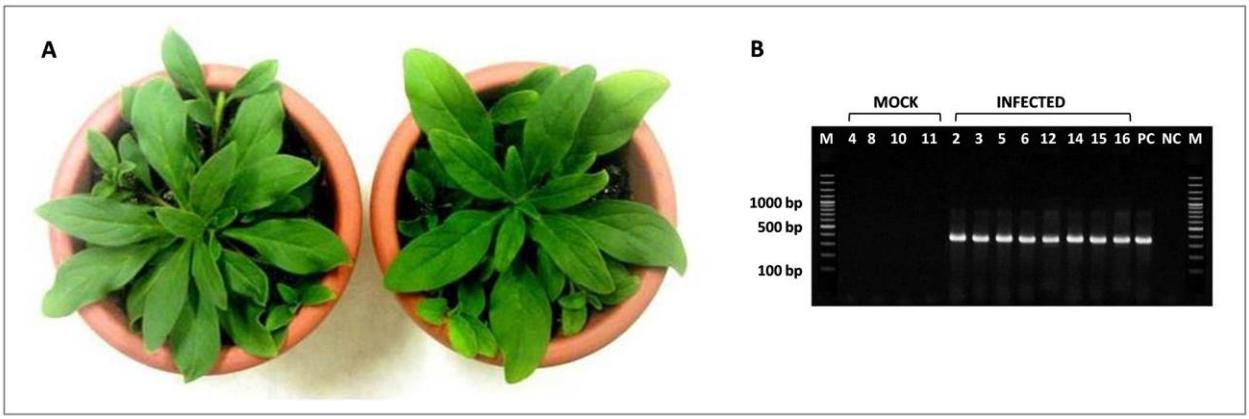

Figure 13. Experimental setup of *Petunia hybrida* without exhibiting any visible symptoms of potato spindle tuber viroid disease (5 wpi): (A) mock–inoculated (left) and PSTVd–inoculated leaves (right). (B) RT–PCR analysis of inoculated plants (5 wpi), with individual sample number. PC, positive control PV–0064 (360 bp); NC, negative control (nuclease–free water); M, molecular weight marker (100 bp DNA ladder).

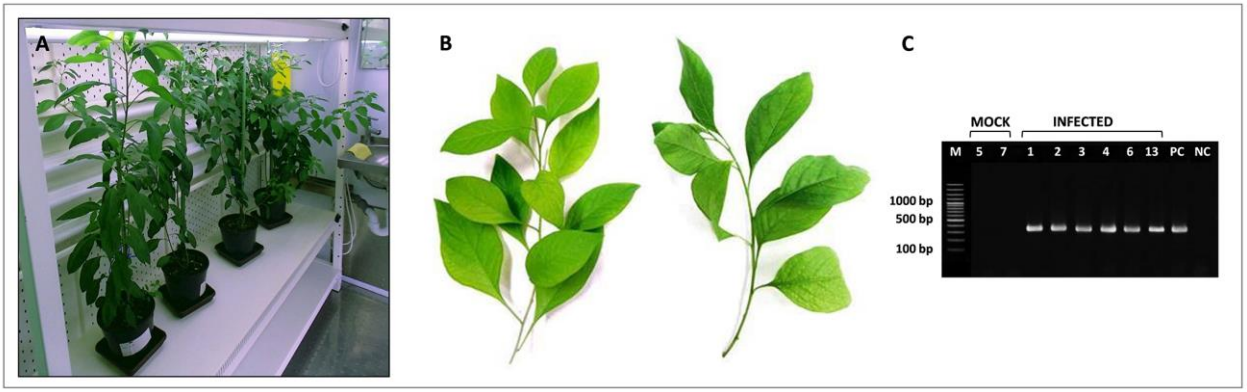

Figure 14. Experimental setup of *Solanum laxum* without exhibiting any visible symptoms of potato spindle tuber disease (18 wpi): (A) nine–month–old plants in a growth chamber, (B) mock–inoculated (left) and PSTVd–inoculated leaves (right). (C) RT–PCR analysis of inoculated plants (18 wpi), with individual sample number. PC, positive control PV–0064 (360 bp); NC, negative control (nuclease–free water); M, molecular weight marker (100 bp DNA ladder).

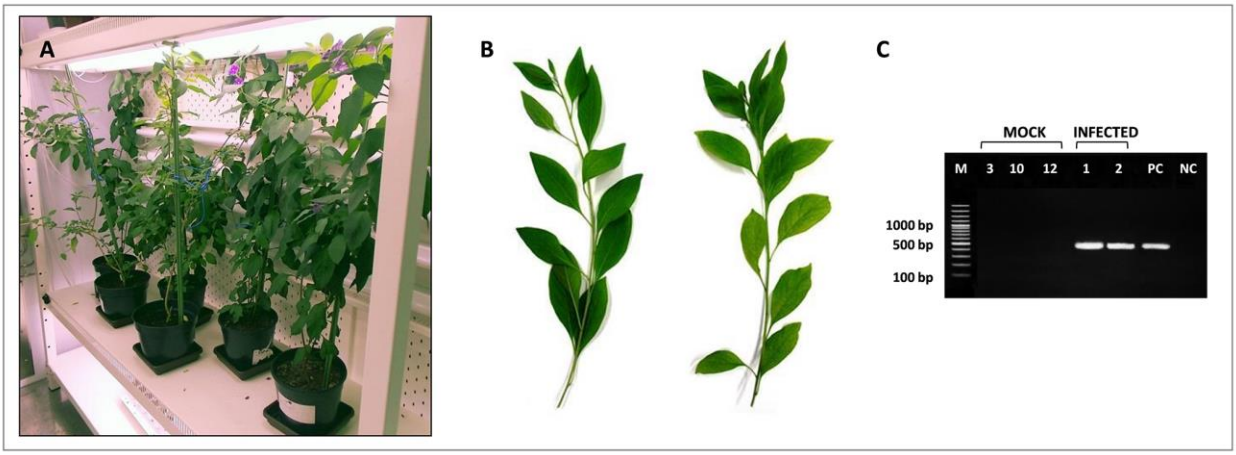

Figure 15. Experimental setup of *Lycianthes rantonnetii* without exhibiting any visible symptoms of potato spindle tuber disease (22 wpi): (A) nine–month–old plants in a growth chamber, (B) mock–inoculated (left) and PSTVd–inoculated leaves (right). (C) RT–PCR analysis of inoculated plants (22 wpi), with individual sample number. PC, positive control (360 bp); NC, negative control (nuclease–free water); M, molecular weight marker (100 bp DNA ladder).

4. 2.2. Changes in total chlorophyll and carotenoid content associated with PSTVd infection

In some plant species tested, PSTVd infection caused obvious changes in the leaf pigmentation, but in some species did not. In order to better detect potentially poorly visible differences in pigmentation, we examined the content of photosynthetic pigments (chlorophyll *a*, chlorophyll *b* and carotenoids). Total chlorophyll content (Chl *a* + *b*) showed significant reduction upon PSTVd infection in tomatoes and somewhat weaker in potatoes, while carotenoid content did not change significantly (Table 6). Ornamental plants that did not show any visible symptoms had no significant changes in the pigment content. Tomato plants were also noted for a decrease in the total chlorophyll/carotenoid ratio. Variations in the chlorophyll/carotenoid ratio are often used as an indicator of physiological state of plants i.e. senescence, stress or damage of the photosynthetic apparatus, and other changes that affect the normal course of plant biological processes (Filimon et al., 2016). It has been much less widely used diagnostically, although this ratio is said to be a sensitive marker distinguishing natural full–term senescence and senescence due to environmental stresses (Netto et al., 2005).

Table 6. Comparison of the chlorophyll *a* (Chl *a*), chlorophyll *b* (Chl *b*), total chlorophyll (Chl *a*+*b*) and carotenoid (Car) content (mg g^{-1} dry weight), and chlorophyll/carotenoid ratio (Chl *a*+*b*/Car) in leaves of of mock– and PSTVd– inoculated plants. Presented data are means ± SE of two to three experiments per species. Each experiment had at least two mock–inoculated and five PSTVd–infected plants. Statistical significance assessed by Student's t–test (*$P \leq 0.05$) between the values for mock– and PSTVd–inoculated plants of the same species.

Species	Treatment	Chl *a*	Chl *b*	Chl *a*+*b*	Car	Chl *a*+*b*/Car
S. lycopersicum	Mock	0.026 ± 0.002	0.008 ± 0.000	0.034 ± 0.002*	0.010 ± 0.001	2.749 ± 0.015
	Infected	0.016 ± 0.001	0.005 ± 0.001	0.019 ± 0.002	0.012 ± 0.001	2.187 ± 0.108
S. tuberosum	Mock	0.022 ± 0.002	0.008 ± 0.001	0.030 ± 0.002	0.011 ± 0.001	2.733 ± 0.047
	Infected	0.020 ± 0.002	0.006 ± 0.001	0.027 ± 0.002	0.010 ± 0.001	2.604 ± 0.043
S. laxum	Mock	0.012 ±0.001	0.005 ±0.000	0.017 ± 0.001	0.006 ± 0.000	2.829 ± 0.029
	Infected	0.010 ± 0.001	0.004 ± 0.000	0.015 ± 0.001	0.005 ± 0.000	2.964 ± 0.149
L. rantonnetii	Mock	0.008 ± 0.000	0.003 ± 0.000	0.011 ± 0.001	0.004 ± 0.000	2.858 ± 0.012
	Infected	0.008 ± 0.000	0.003 ± 0.000	0.011 ± 0.000	0.004 ± 0.000	2.927 ± 0.027
P. hybrida	Mock	0.008 ± 0.001	0.003 ± 0.001	0.012 ± 0.001	0.004 ± 0.000	2.851 ± 0.105
	Infected	0.010 ± 0.001	0.004 ± 0.001	0.013 ± 0.001	0.005 ± 0.000	2.809 ± 0.148

4.2.3. Effects of PSTVd infection on endogenous PGRs in solanaceous species

4.2.3.1. Changes in endogenous PGRs content in leaves of ornamental vs. crop solanaceous plants upon PSTVd infection

The endogenous content of PGRs was analyzed in 4–5 upper intact leaves of PSTVd–infected plants (top leaves were omitted) and compared with PGR content in mock–inoculated plants. Leaf samples were collected 5 to 22 weeks post–inoculation (wpi), depending on the plant species. For each plant species, samples were collected as soon as RT–PCR with PSTVd specific primers gave positive results. In addition, PGRs were analyzed in tubers of mock and infected potato plants 8 wpi, which corresponds to the early (developing) tuber stage (Katsarou et al., 2016). Changes in endogenous concentrations of PGRs are compared in Fig. 16–21 and Table 7.

Upon PSTVd infection, the endogenous CS content increased in leaves of *S. laxum*, *S. tuberosum* and *S. lycopersicum* by 117.5%, 43.7% and 14.7%, respectively (Fig. 16, Table 7). In contrast, the CS content in infected samples of *L. rantonnetii* and *P. hybrida* decreased compared to healthy plants (by 42% and 16.6%, respectively). Although several internal standards for different BRs were used during the analysis, it was possible to reliably monitor only changes in the endogenous CS content.

The endogenous concentration of SA significantly increased in PSTVd–infected plants of *S. lycopersicum* (by 164%) compared to healthy controls (Fig. 17, Table 7). A slight increase in concentration of SA (by 11.7%) was also observed in leaves of infected *S. laxum* plants. In contrast, the SA content in infected leaves of *L. rantonnetii* and *S. tuberosum* slightly decreased (by 20.2% and 16.21%, respectively) compared to healthy controls. No changes in endogenous SA content were observed between the healthy and infected petunia plants. Compared to other examined plant species, a high basal level of SA was measured in *S. lycopersicum* cv. Rutgers and *L. rantonnetii*.

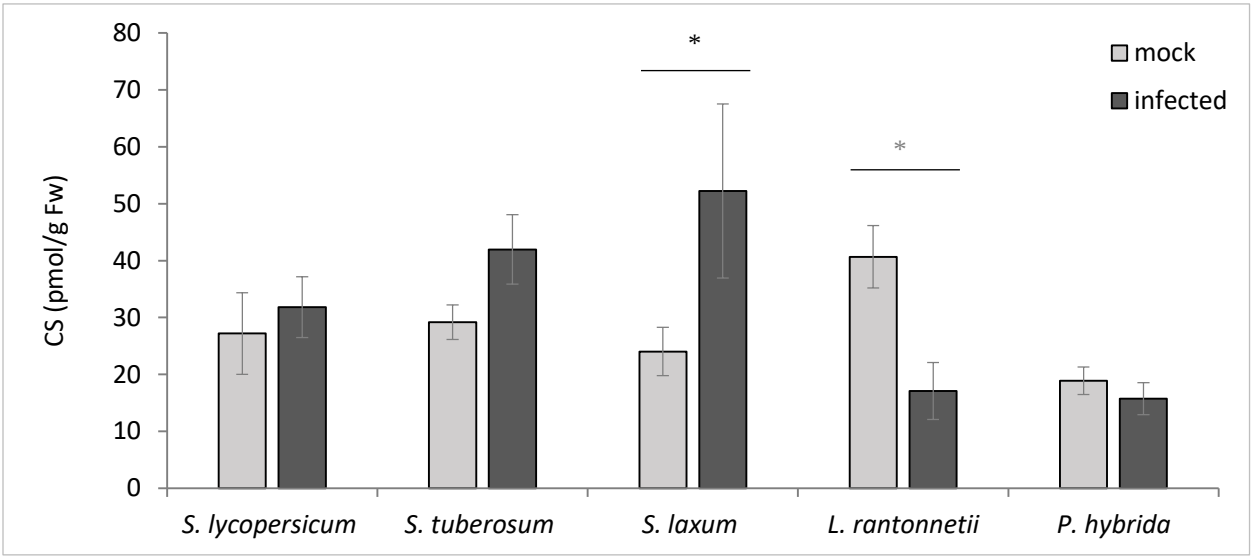

Figure 16. Changes in endogenous concentrations of castasterone (CS) in leaves of different solanaceous species, both mock– and PSTVd–inoculated plants. The data represent means ± SE of two to three experiments, at least two mock–inoculated and five PSTVd–infected plants per experiment. Student's t–test revealed differences between mock–inoculated and PSTVd–inoculated plants of the same species (*$P \leq 0.05$).

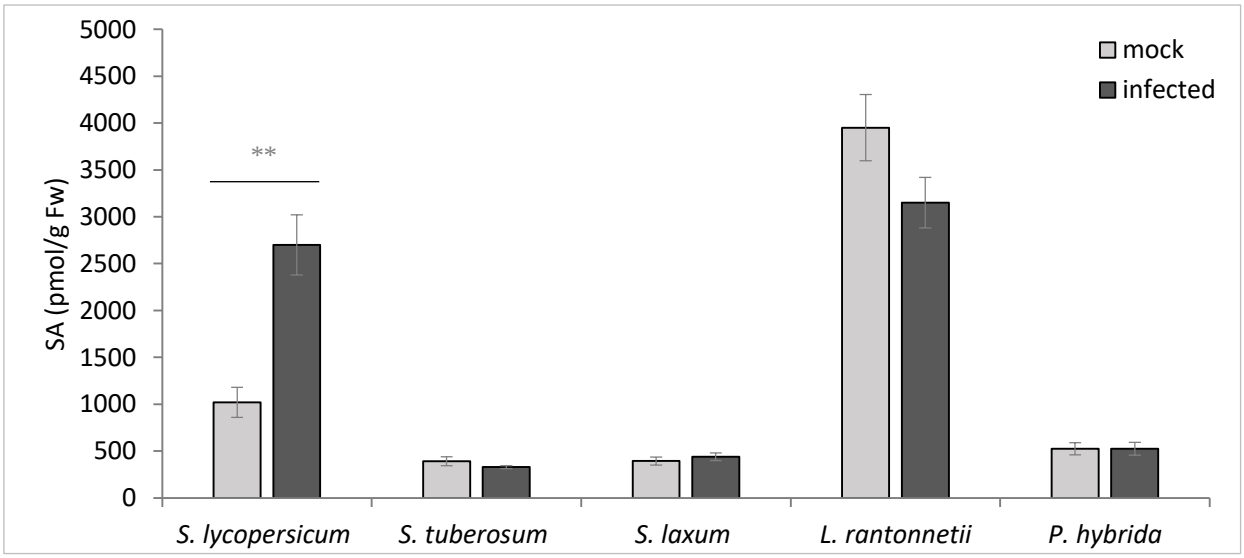

Figure 17. Changes in endogenous concentrations of salicylic acid (SA) in leaves of different solanaceous species, both mock– and PSTVd–inoculated plants. The data represent means ± SE of two to three experiments, at least two mock–inoculated and five PSTVd–infected plants per experiment. Student's t–test revealed differences between mock– and PSTVd–inoculated plants of the same species (**$P \leq 0.01$).

As shown in Fig. 18, JA significantly increased in leaves of systemically infected *S. laxum* plants 18 wpi (by 271.1%) and *S. lycopersicum* plants 5 wpi (by 136.1%), compared to healthy controls. The most significant increase in endogenous JA content was observed in infected *S. tuberosum* leaf samples 8 wpi by 388.2% compared to mock control plants. However, the concentration of endogenous JA decreased in PSTVd–infected plants of *L. rantonnetii* and *P. hybrida* compared to the healthy controls (by 63.7% and 6.2%, respectively). It seems that activations of the JA–mediated response during PSTVd infection occur in three studied members of the genus *Solanum* (tomato, potato and *S. laxum*).

A similar but less prominent trend was observed for *cis*–OPDA (the precursor of JA) in infected *S. tuberosum*, *S. laxum* and *L. rantonnetii* plants compared to healthy controls, showing an increase of 135%, 24.2% and 4.9%, respectively (Fig. 19, Table 7). No changes in *cis*–OPDA content were observed in systemically infected leaves of *S. lycopersicum* and petunia plants.

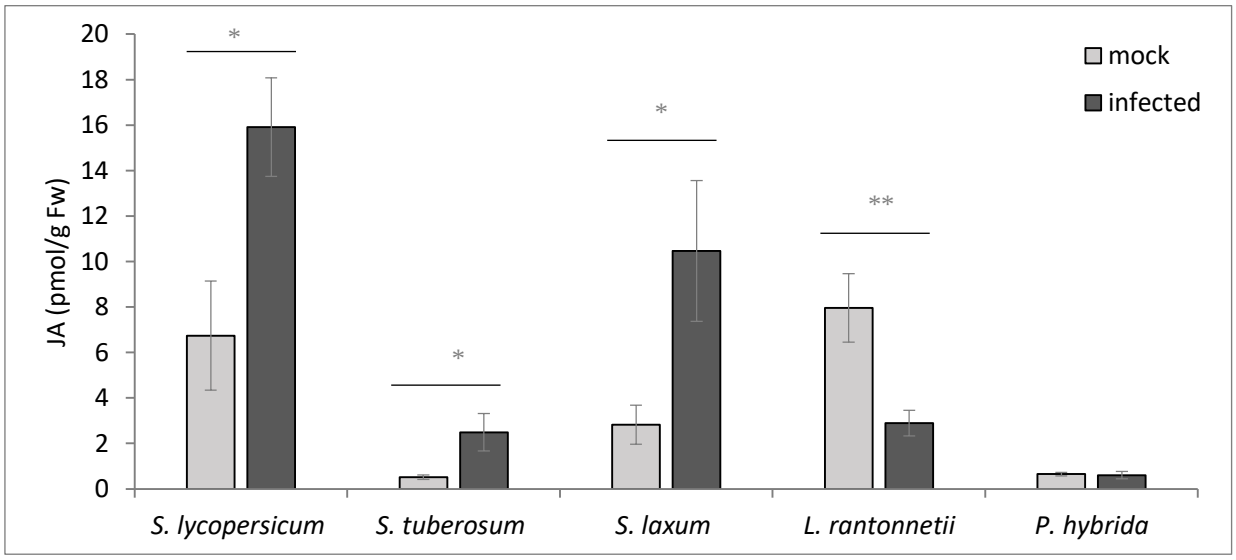

Figure 18. Changes in endogenous concentrations of jasmonic acid (JA) in leaves of different solanaceous species, both mock– and PSTVd–inoculated plants. The data represent means ± SE of two to three experiments, at least two mock–inoculated and five PSTVd–infected plants per experiment. Student's t–test revealed differences between mock–inoculated and PSTVd–inoculated plants of the same species (*$P \leq 0.05$, **$P \leq 0.01$).

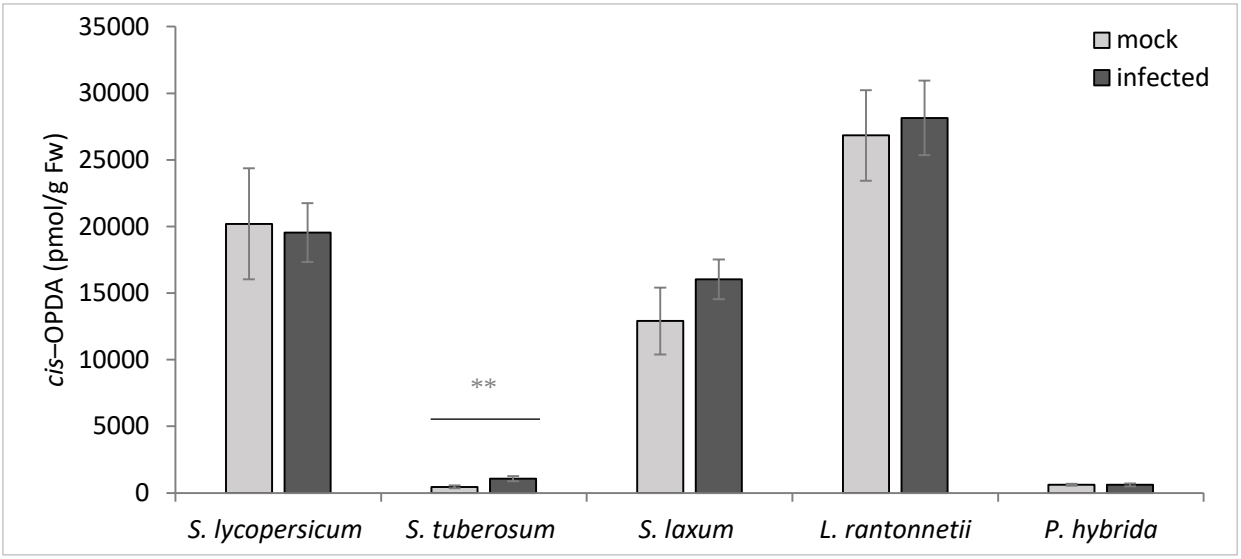

Figure 19. Changes in endogenous concentrations of *cis*–OPDA in leaves of different solanaceous species, both mock– and PSTVd–inoculated plants. The data represent means ± SE of two to three experiments, at least two mock–inoculated and five PSTVd–infected plants per experiment. Student's t–test revealed differences between mock– and PSTVd–inoculated plants of the same species (**$P \leq 0.01$).

A small increase in the endogenous ABA content was observed in PSTVd–infected leaves of *L. rantonnetii* (by 62.1%) and *S. tuberosum* (by 25.9%), compared to healthy plants (Fig. 20, Table 7). Endogenous ABA content significantly decreased only in leaves of infected *S. laxum* plants (by 35.2%), whereas no changes in ABA content was observed in systemically infected leaves of *S. lycopersicum* and *P. hybrida*. In *S. lycopersicum* cv. Rutgers, a high basal level of ABA was measured compared to other examined plant species.

As shown in Fig. 21, a significant increase in the endogenous IAA content was observed in infected leaves of *L. rantonnetii* and *P. hybrida* compared to healthy plants (by 68.7% and 24.5%, respectively). In addition, endogenous IAA moderately increased in infected leaves of *S. lycopersicum* (by 59.1%). No changes in endogenous IAA were observed in infected leaves of *S. tuberosum* and *S. laxum* (Fig. 21, Table 7).

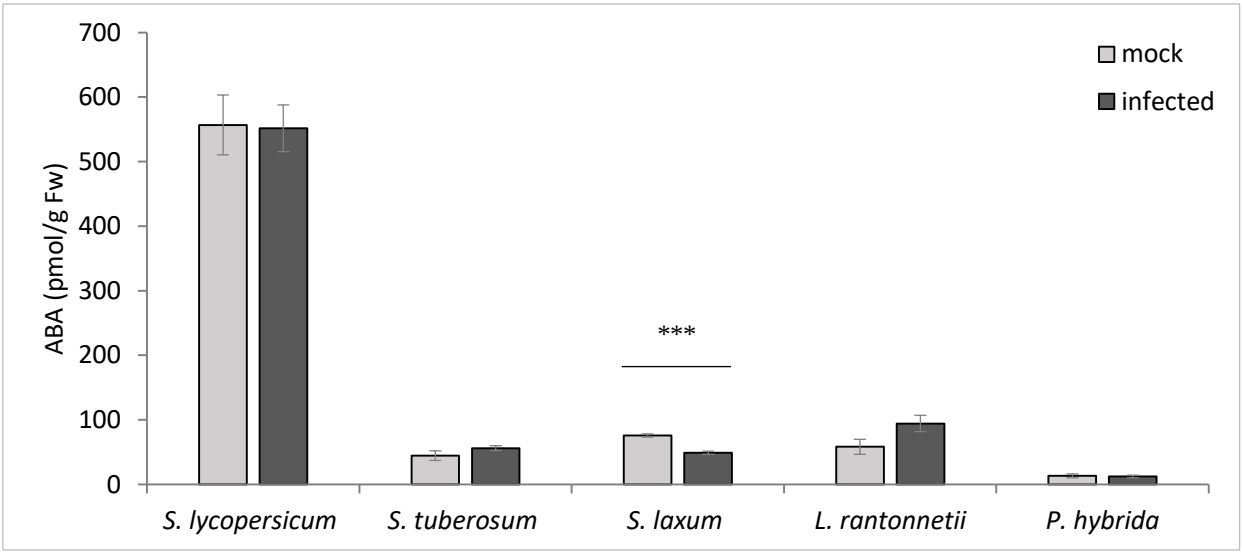

Figure 20. Changes in endogenous concentrations of abscisic acid (ABA) in leaves of different solanaceous species, both mock– and PSTVd–inoculated plants. The data represent means ± SE of two to three experiments, at least two mock–inoculated and five PSTVd–infected plants per experiment. Student's t–test revealed differences between mock–inoculated and PSTVd–inoculated plants of the same species (***$P \leq 0.001$).

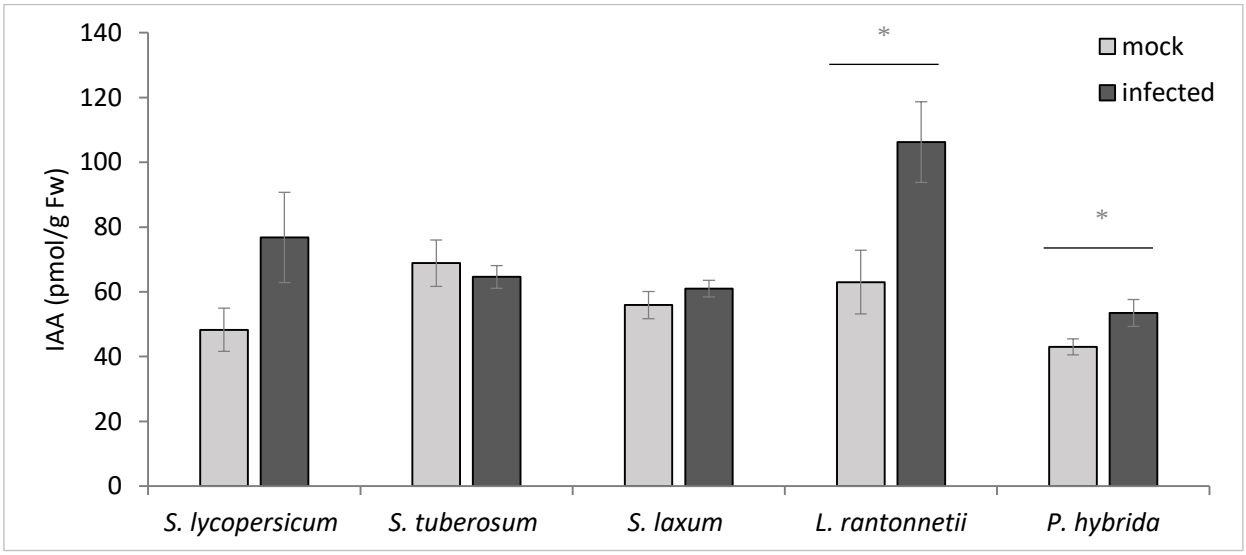

Figure 21. Changes in endogenous concentrations of IAA in leaves of different solanaceous species, both mock– and PSTVd–inoculated plants The data represent means ± SE of two to three experiments, at least two mock–inoculated and five PSTVd–infected plants per experiment. Student's t–test revealed differences between mock–inoculated and PSTVd–inoculated plants of the same species (*$P \leq 0.05$).

4.2.3.2. Organ–specific changes in potato upon PSTVd infection

Differences in response to PSTVd infection were also observed at the plant organ level (Table 7). In potato plants, symptoms were more pronounced in tubers than in leaves. Therefore endogenous PGR content was measured in both tuber and leaf tissues, in order to estimate possible effects of changes in endogenous PGRs on organ morphology.

As shown in Fig. 22, endogenous level of JA increased in both leaves and tubers of infected potato plants, but the relative increase of JA was higher in leaves. Similarly, the increase in endogenous CS was observed in both leaves and tubers of infected potato plants, but the relative increase of CS was higher in tubers. Comparing two tissue types, a slightly higher increase of endogenous IAA and ABA was also observed in tubers than in leaves of infected potato plants. Upon PSTVd infection, endogenous SA did not change either in tubers or in potato leaves, but the high basal level of endogenous SA was measured in potato tubers.

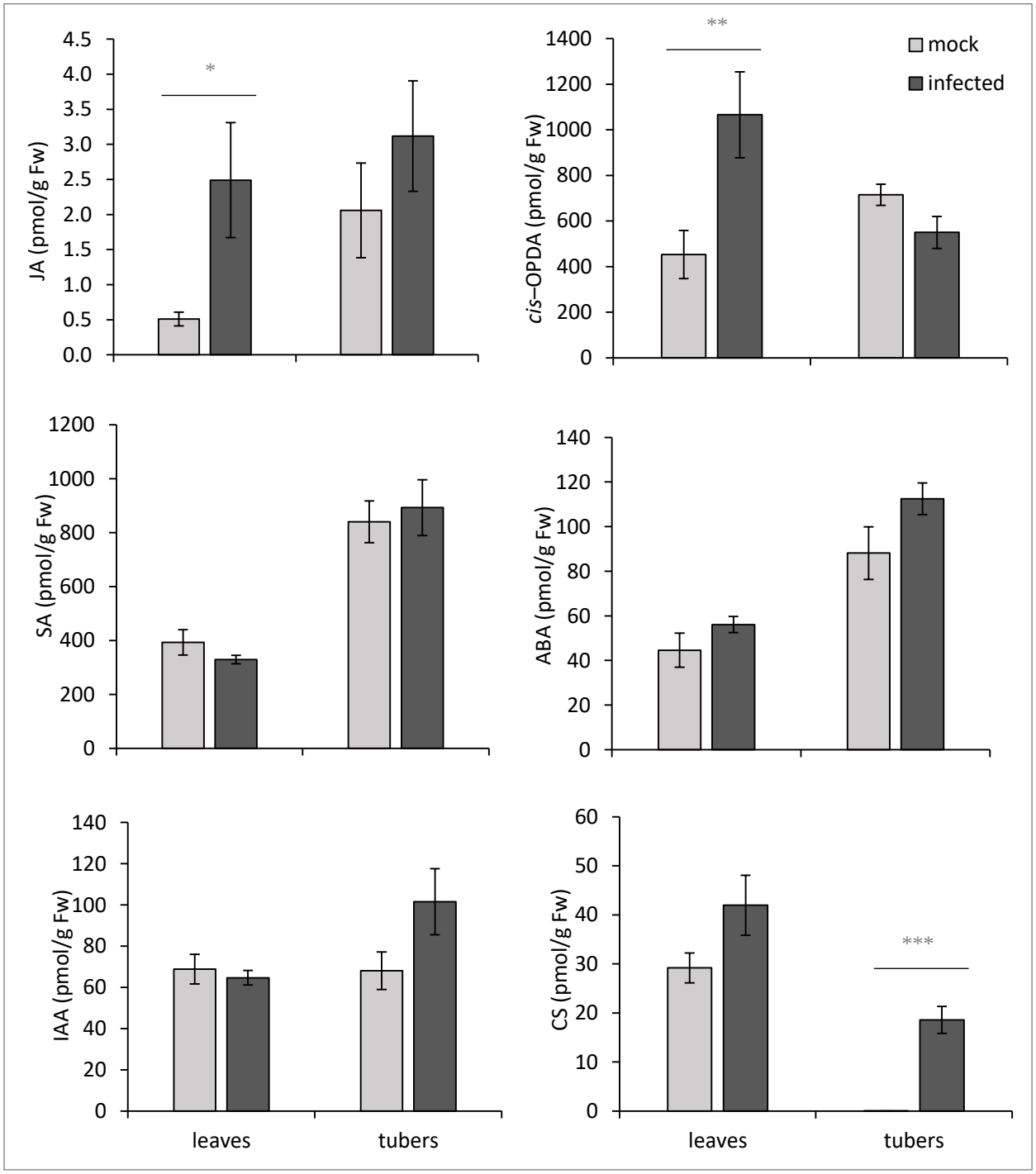

Figure 22. Changes in endogenous concentrations of jasmonic acid (JA), *cis*–OPDA, salicylic acid (SA), abscisic acid (ABA), IAA and castasterone (CS) in leaf and tuber samples, collected from mock–inoculated and PSTVd–infected potato plants 8 weeks post–inoculation. The following data represent means ± SE of two to three experiments. Each experiment had at least two mock–inoculated and five PSTVd–infected plants. Student's t–test revealed differences between mock– and PSTVd–inoculated plants of the same species (*$P \leq 0.05$, **$P \leq 0.01$, ***$P \leq 0.001$).

Table 7. PGRs content (pmol/g FW) in plant tissue (L, leaves; T, tubers) of different solanaceous species upon inoculation with PSTVd. Presented data are means ± SE of two to three experiments per species. Each experiment had at least two mock–inoculated and five PSTVd–infected plants. Student's t–test revealed differences between mock– and PSTVd–inoculated plants of the same species (*$P \leq 0.05$, **$P \leq 0.01$, ***$P \leq 0.001$).

Species	Treatment	IAA	ABA	SA	*cis*–OPDA	JA	CS
S. lycopersicum	mock L	48.27 ± 6.65	556.85 ± 46.41	1020.81 ± 161.28	20198.58 ± 4170.00	6.74 ± 2.40	27.18 ± 7.16
	infected L	76.80 ± 13.96	551.56 ± 36.09	2699.87 ± 320.59**	19539.63 ± 2220.27	15.91 ± 2.16*	31.81 ± 5.34
S. tuberosum	mock L	68.86 ± 7.16	44.57 ± 7.64	392.96 ± 47.40	453.58 ± 105.46	0.51 ± 0.10	29.19 ± 3.05
	infected L	64.62 ± 3.52	56.10 ± 3.61	329.24 ± 20.91	1065.88 ± 188.84**	2.49 ± 0.82*	41.96 ± 6.12
	mock T	68.07 ± 9.08	88.15 ± 21.73	840.08 ± 77.09	715.07 ± 45.99	2.06 ± 0.67	nd
	infected T	101.51 ± 16.03	112.46 ± 7.11	893.02 ± 103.46	550.20 ± 70.21	3.12 ± 0.79	18.58 ± 2.73***
S. laxum	mock L	55.93 ± 4.20	75.72 ± 2.50***	393.92 ± 41.87	12901.88 ± 2502.37	2.82 ± 0.86	24.02 ± 4.24
	infected L	60.99 ± 2.58	49.08 ± 2.64	440.19 ± 41.02	16022.64 ± 1488.95	10.47 ± 3.10*	52.24 ± 15.31*
L. rantonnetii	mock L	63.00 ± 9.83	58.17 ± 11.62	3950.28 ± 354.08	26830.72 ± 3390.50	7.96 ± 1.57**	40.67 ± 5.50*
	infected L	106.26 ± 12.46*	94.30 ± 12.50	3151.49 ± 269.67	28144.77 ± 2795.81	2.89 ± 0.56	17.07 ± 5.00
P. hybrida	mock L	42.97 ± 2.48	13.47 ± 2.90	524.23 ± 65.09	617.77 ± 65.80	0.65 ± 0.07	18.88 ± 2.44
	infected L	53.48 ± 4.15*	12.39 ± 2.08	525.09 ± 68.87	603.27 ± 100.56	0.61 ± 0.16	15.74 ± 2.81

nd – not detected

4.2.4. Effects of potato spindle tuber viroid infection on antioxidant enzyme activity in solanaceous species

4.2.4.1. Total soluble protein content

The protein concentration in leaf and tuber samples was determined by the Bradford method (1976) using bovine serum albumin as the standard. The protein concentration of the experimental samples was calculated using the standard curve equation and the experimental results were expressed as µg of proteins per gram of fresh weight (µg/g Fw). PSTVd–infected plants of almost all examined solanaceous species (with the exception of *L. rantonnetii*) accumulated more proteins compared to healthy controls, as shown in Fig. 23 and 24.

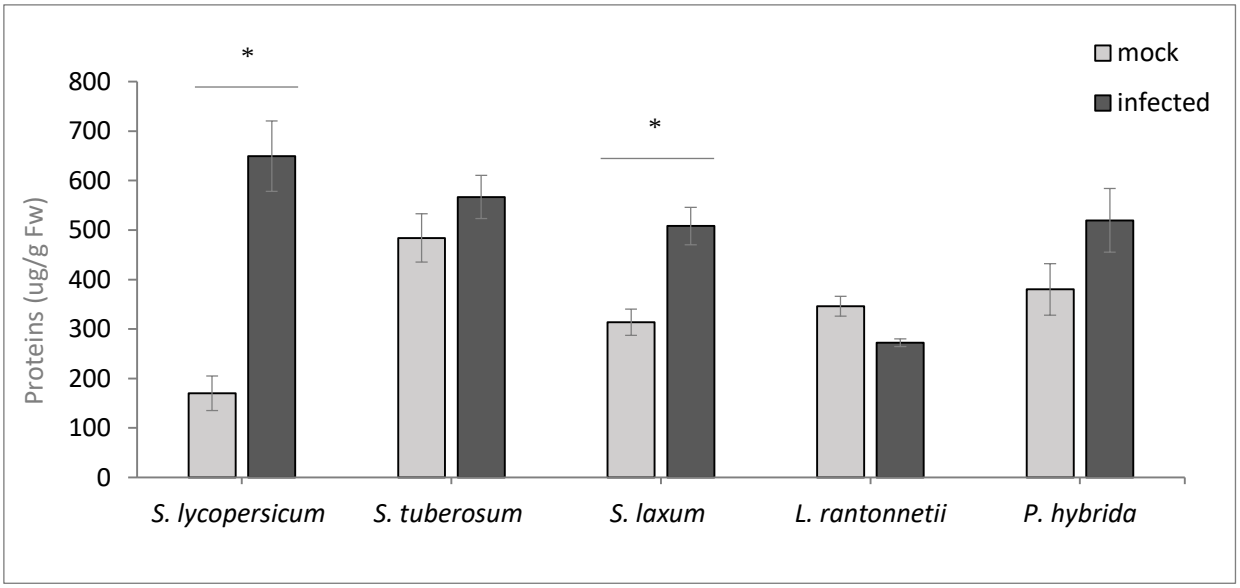

Figure 23. Total soluble protein content (µg prot/g Fw) in leaves of different solanaceous species, both mock– and PSTVd–inoculated plants. The following data represent means ± SE of two to three experiments. Each experiment had at least two mock–inoculated and five PSTVd–infected plants. Student's t–test revealed differences between mock–inoculated and PSTVd–inoculated plants of the same species (*$P \leq 0.05$).

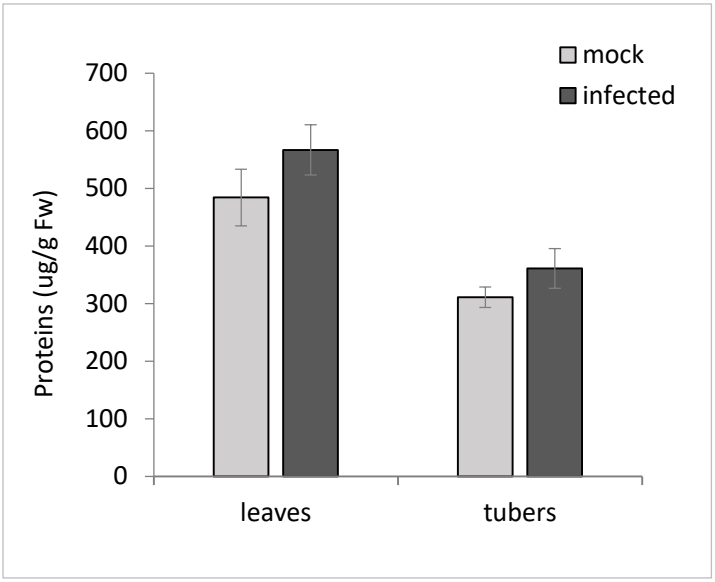

Figure 24. Total soluble protein content (µg prot/g Fw) in potato leaves and tubers, both mock– and PSTVd–inoculated samples. The following data represent means ± SE of two to three experiments. Each experiment had at least two mock–inoculated and five PSTVd–infected plants.

4.2.4.2. Analysis of guaiacol peroxidase activity

The most significant increase in GPX activity was detected in leaves of PSTVd–infected plants of *S. lycopersicum*, *S. tuberosum* and *P. hybrida* compared to healthy controls (185.5%, 53.2% and 50.1%, respectively), as shown in Fig. 25 and Table 8. A similar but less prominent trend was observed for GPX activity in leaves of infected *S. laxum* plants, increasing by 27%. In contrast, GPX activity in infected leaves of *L. rantonnetii* decreased by 31% compared to healthy controls. In *L. rantonnetii* and *S. laxum*, a higher basal level of GPX activity was observed compared to other examined plant species.

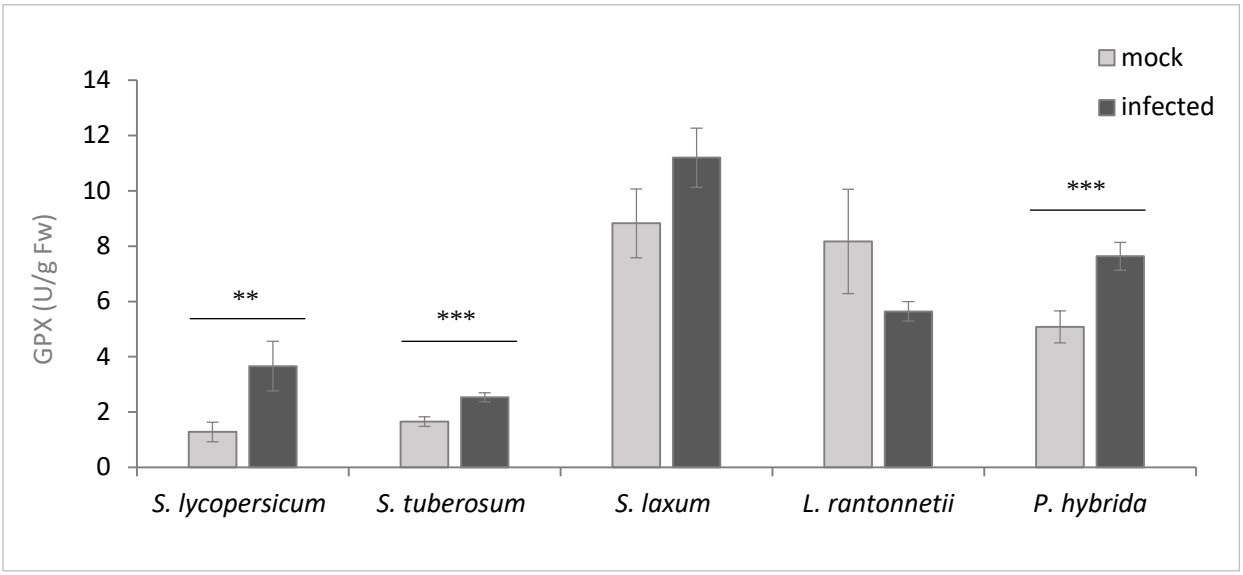

Figure 25. Changes in the activity (U/g Fw) of guaiacol peroxidase (GPX) in leaves of different solanaceous species, both mock– and PSTVd–inoculated plants. The following data represent means ± SE of two to three experiments. Each experiment had at least two mock–inoculated and five PSTVd–infected plants. Student's t–test revealed differences between mock– and PSTVd–inoculated plants of the same species (**$P \leq 0.01$, ***$P \leq 0.001$).

4.2.4.3. Analysis of ascorbate peroxidase activity

Compared to healthy plants, the most significant increase in APX activity of 903.3% was detected in PSTVd–infected plants of *S. lycopersicum*, as shown in Fig. 26 and Table 8. A similar but less prominent trend was observed for APX activity in infected *S. laxum* plants reaching a significant increase of 116.4%, compared to healthy controls. A moderate increase in APX activity was also observed in PSTVd–infected leaves of *L. rantonnetii* (an increase of 40.5%). In contrast, APX activity in infected leaves of *S. tuberosum* decreased by 4.6% compared to healthy controls. A decrease of 7.7% was also detected in infected leaves of *P. hybrida*.

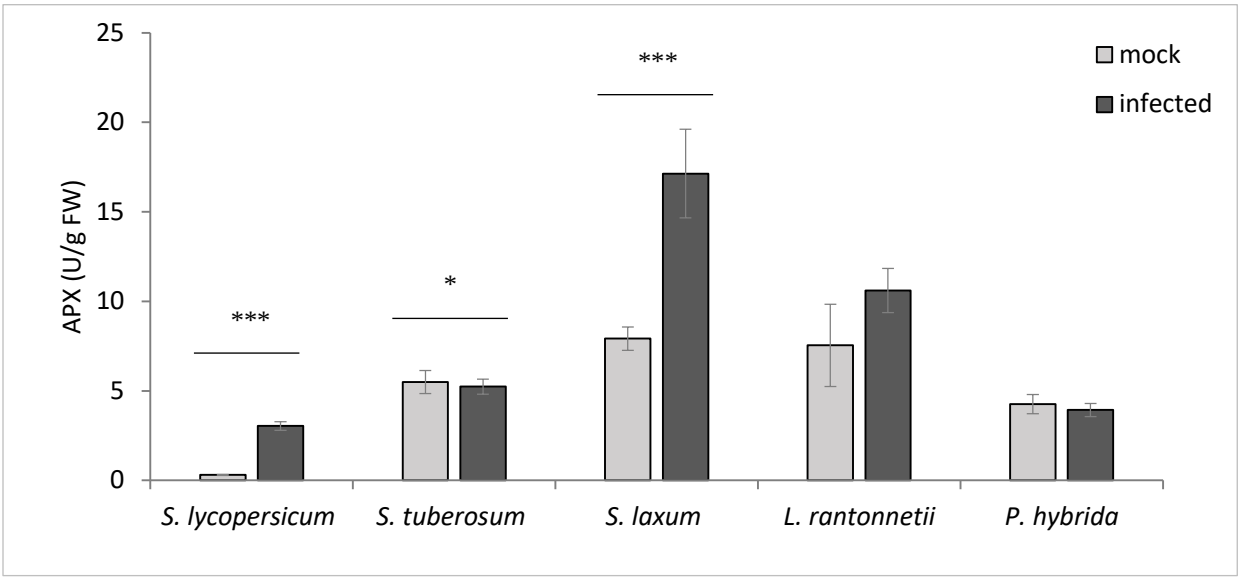

Figure 26. Changes in the activity (U/g Fw) of ascorbate peroxidase (APX) in leaves of different solanaceous species, both mock– and PSTVd–inoculated plants. The following data represent means ± SE of two to three experiments. Each experiment had at least two mock–inoculated and five PSTVd–infected plants. Student's t–test revealed differences between mock– and PSTVd–inoculated plants of the same species (*$P \leq 0.05$, ***$P \leq 0.001$).

4.2.4.4. Analysis of catalase activity

The analysis showed that CAT activity most significantly increased in PSTVd–infected plants of *S. lycopersicum* (by 578.1%), compared to healthy controls. A similar trend was observed for CAT activity in infected *L. rantonnetii* plants, increasing by 245.1% compared to healthy plants. However, a significant decrease in GPX activity was observed in infected leaves of *P. hybrida* and *S. tuberosum* (28.7% and 17.3%, respectively). It should be noted that *P. hybrida* and *S. tuberosum* showed a higher basal level of CAT activity than other plant species examined (Fig. 27, Table 8).

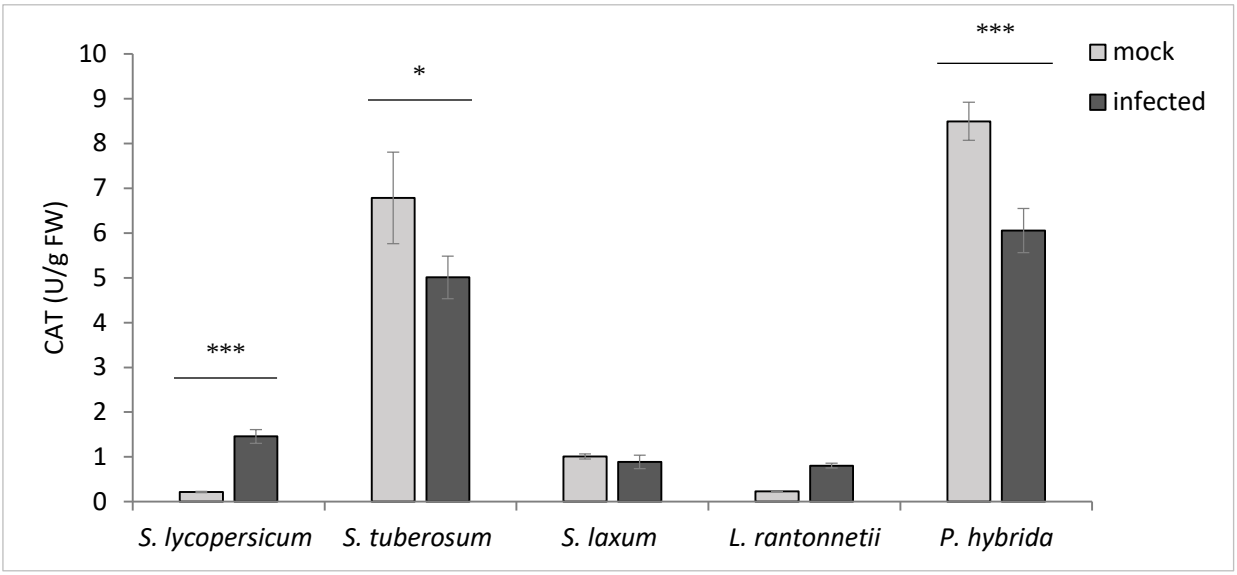

Figure 27. Changes in the activity (U/g Fw) of catalase (CAT) in leaves of different solanaceous species. The following data represent means ± SE of two to three experiments. Each experiment had at least two mock–inoculated and five PSTVd–infected plants. Student's t–test revealed differences between mock– and PSTVd–inoculated plants of the same species (*$P \leq 0.05$, ***$P \leq 0.001$).

4.2.5.5. Analysis of superoxide dismutase activity

A minor increase in SOD activity was detected in the PSTVd–infected plants *S. laxum* and *S. lycopersicum* of 52.6% and 31.3%, respectively, compared to healthy controls. However, the activity of SOD in infected leaves of *L. rantonnetii* and *P. hybrida* slightly decreased by 15.9% and 6.8%, respectively, compared to healthy plants. As shown in Fig. 28 and Table 8, there were no major changes in SOD activity between the healthy and infected plants of *S. tuberosum* (by 3.6%).

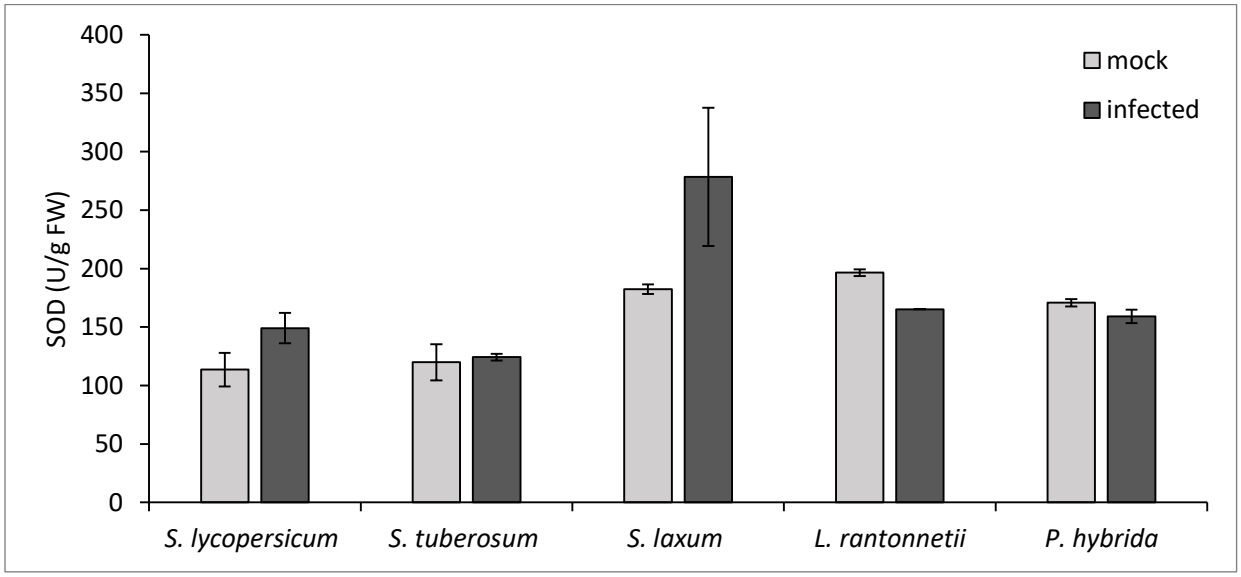

Figure 28. Changes in the activity (U/g Fw) of superoxide dismutase (SOD) in leaves of different solanaceous species. The following data represent means ± SE of two to three experiments. Each experiment had at least two mock–inoculated and five PSTVd–infected plants. According to Student's t–test, there was no statistical difference between the values.

4.2.5.6. Antioxidant enzyme activity in leaves vs. tubers of potato upon PSTVd infection

As already mentioned, the most obvious visible symptoms of PSTVd infection in potato plants manifest in tubers, therefore the activity of antioxidant enzymes was measured in order to determine differences in antioxidant response between tuber and leaf tissues. As shown in Fig. 29 and Table 8, the activity of GPX increased more in leaves than in tubers of infected plants. On the contrary, the activity of APX increased more in tubers than in leaves of infected potato plants. Furthermore, CAT activity decreased more in leaves than in tubers of infected plants, while SOD activity did not change significantly either in tubers or in potato leaves.

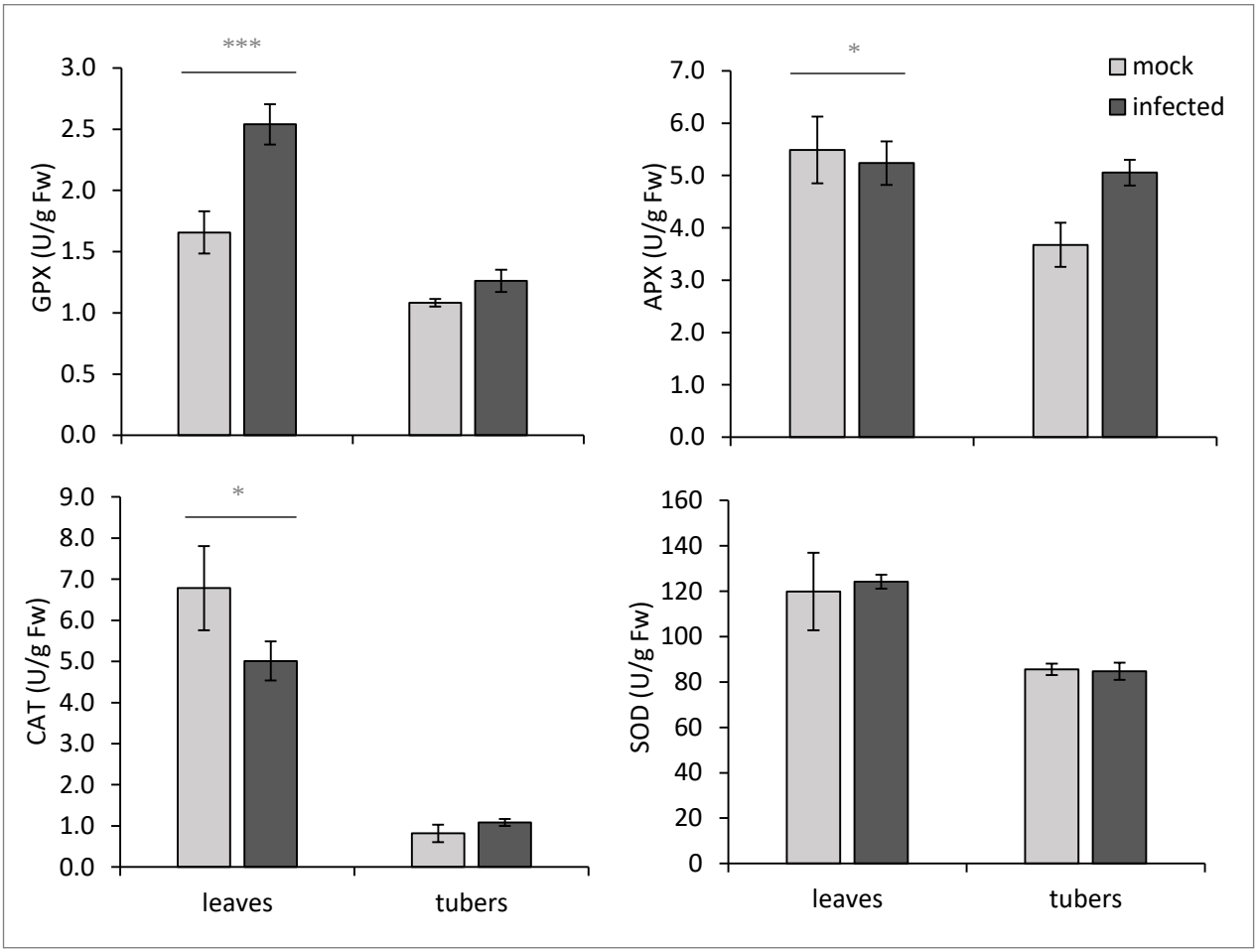

Figure 29. Changes in GPX, APX, CAT and SOD activity (U/g Fw) of leaf and tuber samples, collected from mock– and PSTVd– inoculated potato plants 8 weeks post–inoculation. The following data represent means ± SE of two to three experiments. Each experiment had at least two mock–inoculated and five PSTVd–infected plants. Student's t–test revealed differences between mock–and PSTVd–inoculated plants of the same species (*$P \leq 0.05$, ***$P \leq 0.001$).

Table 8. Antioxidative enzyme activity (U/g Fw) in plant tissue (L, leaves; T, tubers) of different solanaceous species upon inoculation. Presented data are means ± SE of two to three experiments per species. Each experiment had at least two mock–inoculated and five PSTVd–infected plants. Student's t–test revealed differences between mock–inoculated and PSTVd–inoculated plants of the same species (*$P \leq 0.05$, **$P \leq 0.01$, ***$P \leq 0.001$).

Species	Treatment	SOD	CAT	GPX	APX	Proteins (µg/g Fw)
S. lycopersicum	mock L	113.57 ± 20.24	0.215 ± 0.01	1.283 ± 0.35	0.303 ± 0.03	170.230 ± 34.97
	infected L	149.13 ± 16.03	1.458 ± 0.16***	3.663 ± 0.90**	3.040 ± 0.24***	649.344 ± 71.08*
S. tuberosum	mock L	119.88 ± 17.05	6.056 ± 1.02*	1.657 ± 0.17	5.489 ± 0.64	484.073 ± 49.04
	infected L	124.25 ± 3.06	5.011 ± 0.48	2.539 ± 0.16***	5.238 ± 0.42	566.746 ± 43.63
	mock T	85.62 ± 3.53	0.821 ± 0.21	1.083 ± 0.03	3.675 ± 0.42	310.760 ± 17.78
	infected T	84.73 ± 3.98	1.085 ± 0.08	1.261 ± 0.09	5.055 ± 0.24*	360.815 ± 34.49
S. laxum	mock L	182.52 ± 4.10	1.009 ± 0.06	8.828 ± 1.24	7.917 ± 0.66	313.645 ± 26.81
	infected L	278.50 ± 59.08	0.888 ± 0.15	11.197 ± 1.07	17.131 ± 2.47***	508.112 ± 37.70*
L. rantonnetii	mock L	196.60 ± 2.87	0.233 ± 0.01	8.172 ± 1.89	7.548 ± 2.30	284.471 ± 51.94
	infected L	165.18 ± 0.14	0.804 ± 0.05***	5.641 ± 0.35	10.604 ± 1.74	272.431 ± 7.77
P. hybrida	mock L	170.90 ± 3.64	8.497 ± 0.43***	5.084 ± 0.58	4.264 ± 0.53	380.132 ± 52.18
	infected L	159.20 ± 6.21	6.056 ± 0.49	7.633 ± 0.51***	3.934 ± 0.37	519.628 ± 64.37

5.1. SURVEY OF *POTATO SPINDLE TUBER VIROID* IN CROATIA

Viroids have a worldwide distribution and are the etiologic agents of diverse diseases affecting important crops and ornamental plants (Gómez et al., 2009). To suppress the spread of viroid infection via ornamental species, the European and Mediterranean Plant Protection Organization (EPPO) has included *Potato spindle tuber viroid* on the list of quarantine pathogens in the EU. The production area of ornamental plants in Croatia is about 300 ha, which is only 0.1% of the total agricultural area utilized in the country (Croatian Bureau of Statistics, 2016). However, even a low incidence of latent infected ornamentals could pose a serious threat as a source of viroid infections for susceptible economically important crops and vegetables, such as tomato and potato. In 2015, the annual production of potatoes was about 170 000 tonnes, while the production of tomatoes was about 39 000 tonnes (Croatian Bureau of Statistics, 2016), ranking them among the four most important crops in the country. Therefore, phytosanitary protection of potato and tomato crops is of great importance for the sustainable development of Croatian agriculture. In the survey on the status of PSTVd in various solanaceous ornamentals and crops, which was conducted in Croatia from 2009 to 2014, two ornamental solanaceous species, *Solanum laxum* and *Lycianthes rantonnetii*, were found to be PSTVd positive (Table 4). This is the first ever recorded molecular evidence of the presence of PSTVd in Croatia. Fortunately, during the survey, no example of viroid infections in tomato or potato plantation was found. Molecular characterization of the isolates from imported ornamental consignments showed close resemblance of the Croatian isolates to the isolates previously reported in the Netherlands, Italy, Belgium, Greece and Slovenia. The case of repeated infection found in Varaždin in 2012 (KF418768) was from newly imported stock, although the sequence alignment showed a 100% identity match to sequences isolated in 2009 (KF418772 and KF418773). This suggests a possibility of the same origin of importation. Molecular techniques examined in this study have proven to be effective for detection of PSTVd. However, considering a latest report of the possibility of mixed pospiviroid infections (Luigi et al., 2011), extending the survey to a larger number of different pospiviroids as well as plant host species would be desirable.

5.2. PSTVd–INDUCED CHANGES IN ENDOGENOUS PGRs CONTENT

Brassinosteroids (BRs) are a class of polyhydroxysteroids that are involved in cell and stem elongation, leaf and petiole bending, ethylene production and a plant's defense against pathogens (Clouse and Feldmann, 1999). Given their strong biological activities, castasterone and brassinolide (BL) are considered to be the most important BRs in the plant kingdom (Klahre et al., 1998). In our study, endogenous CS content increased significantly in leaves of PSTVd–infected *S. laxum*, while similar but less pronounced trend was observed in leaves of infected tomato and potato. A significant increase of endogenous CS was also detected in potato tubers harvested eight weeks after inoculation, which was a time point somewhat comparable to 'the early stage of tuber infection' (i.e. 14 wpi) described by Katsarou et al. (2016). According to Katsarou et al. (2016), the early stage of tuber and leaf infection was characterized by a strong reduction in the expression of the *DWF1* (a sterol biosynthesis gene). Also, Owens et al. (2012) showed that changes in either BR biosynthesis, signaling, or both might contribute to symptom development in viroid–infected tomato plants. According to the authors, transcripts of *DWF5* (a sterol biosynthesis gene) were upregulated, while transcripts of *DWF7* and *DWF4* (a sterol biosynthesis and a BR–specific biosynthesis gene, respectively) were downregulated in tomato cv. Rutgers 5 weeks after inoculation with PSTVd. As shown by Tanaka et al. (2005), BR homeostasis is finely modulated by the feedback expressions of multiple (at least nine) BR metabolic genes, each of which is involved not only in BR–specific biosynthesis and inactivation, but also in sterol biosynthesis. It has been shown that the activity of all BR–specific biosynthesis gene increases with the decrease of endogenous BR contents, including the gene for ROT3 which is involved in the conversion step of typhasterol (TY) to castasterone. Further research is needed to examine to what extend the PSTVd–induced increase in endogenous CS observed in this study, affects changes in the expression of genes involved in biosynthesis and signaling of BRs.

One of the most noticeable characteristics of symptomatic tomato cv. Rutgers was an exceptionally high basal level of SA and ABA in intact leaves of mock–inoculated tomato plants. The endogenous level of SA in tomato leaves increased after the PSTVd infection, while ABA remained steady. It seems that the increase in endogenous SA did not enhance the resistance of tomato cv. Rutgers against PSTVd. The role of SA in the defense response of plants against viruses varies, depending on the host species (Alazem and Lin, 2015). For example, potato plants are known

to contain a higher basal level of SA than several others plants (Jones and Dangl, 2006), but several studies have shown that the high basal level of SA in potato is not related to resistance to *Potato virus Y* (Krečič–Stres et al., 2005: Kovač et al., 2009). The high basal levels of SA raise questions about how functional SA–mediated signaling is in potato, and it has been suggested that potato might be poorly responsive to SA (Yu et al., 1997). According to our results, it would be similar to tomato cv. Rutgers.

This study shows that endogenous JA increased in systemically infected leaves of tomato, potato and *S. laxum*, regardless of the intensity of disease symptoms. The same was observed for *cis*–OPDA, only the differences were less pronounced. The results indicate that the increase in endogenous JA in systemically infected leaves can be considered as a signal involved in the immune response of these plant species to PSTVd infection, though it does not seem to be critical for the development of visible symptoms. In tomato cv. Rutgers infected with PSTVd, Owens et al. (2012) detected extensive changes in the expression of genes involved in several hormone–signaling pathways, including JA. The changes varied depending on the host genotype, so the number of upregulated genes involved in JA biosynthesis was higher in symptomatic cv. Rutgers than those observed in tolerant cv. Moneymaker plants. Indirect evidence supporting a hypothesis about the activation of the JA signaling pathway during plant defense responses against PSTVd infection is given by a tomato metabolite–profiling study (Bagherian et al., 2016), and a microarray study of genes that contain potential binding sites for PSTVd small RNAs (Wang et al., 2011a). Also, the JA response has been important against virus infection in plants. For example, systemic PVY infection of potato resulted in the accumulation of endogenous JA (Petrovič et al., 1997), while CaMV infection in *Arabidopsis* plants modulated expression of JA–responsive genes at early stages of infection (Love et al., 2005). However, as shown in pea plants, JA do not prevent systemic spreading of viruses, but reduce their titer (Clarke et al., 2000; Kyseláková et al. 2013).

Unlike in tomato, potato and *S. laxum*, there was no change in endogenous JA in *P. hybrida* while in *L. rantonnetii* endogenous JA decreased upon PSTVd infection. Differences in hormone response in *P. hybrida* and *L. rantonnetii*, compared to the other solanaceous species examined in this study, probably arise from differences in the physiology of these slightly less related species (Fig. 30). Namely, tomato, potato and *S. laxum* are members of the genus *Solanum* (subfamily

Solanideae), *L. rantonnetii* is a member of the genus *Lycianthes* (subfamily Solanideae), while *P. hybrida* belongs to the subfamily Petunoideae.

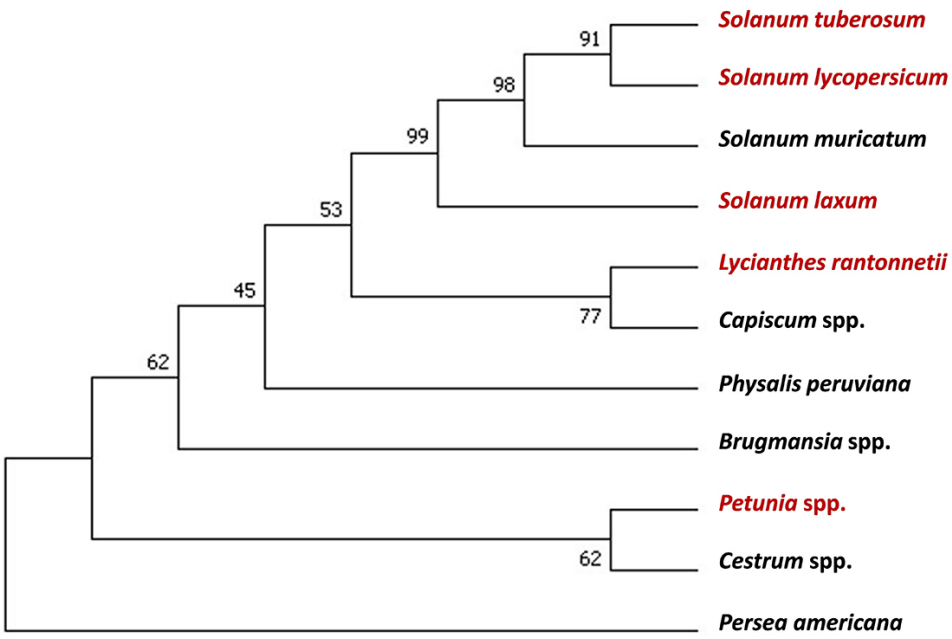

Figure 30. Phylogenetic analysis of some solanaceous species based on the similarity in the chloroplast NADH dehydrogenase subunit F (*ndhF*) gene sequences. The sequences were aligned using ClustalW algorithm and analyzed as described in chapter 3.2.3.7. Species examined in this study are indicated in red letters.

This study also showed a significant increase in endogenous IAA in leaves of infected *P. hybrida* and *L. rantonnetii* plants. At the same time, IAA was the only hormone to be accumulated in these two species upon PSTVd infection, however, the increase in IAA did not result in the onset of a visible symptom. After the infection, a moderate increase in endogenous IAA was also observed in tomato leaves and potato tubers, which may be related (at least in part) to symptom development. Auxins are known to stimulate cell and organ elongation however, IAA may also play a role in defense against viruses (Jameson and Clarke, 2002). In leaf tissues of PSTVd–infected tomato cv. Rutgers plants, the expression of three genes involved in the auxin signaling pathway were upregulated (Owens et al., 2012). Induction of auxin activity was also proposed following indole–3–acetate II pathway activation in viroid infected leaves of both Rutgers and Moneymaker tomato cultivars (Bagherian et al., 2016). On the other hand, some auxin related genes were downregulated

in infected potato tissues, suggesting that the tuber development control *via* hormones might be compromised upon PSTVd infection (Katsarou et al., 2016).

5.3. CHANGES IN THE ACTIVITIES OF ANTIOXIDANT ENZYMES IN RESPONSE TO PSTVd INFECTION

Results reported in the literature indicate that alteration in the activity of ROS–scavenging enzymes could also be a key step in the activation of phytopathogen defense (De Gara et al., 2003). Gene expression analysis in PSTVd–infected potato leaves revealed a significant enrichment of transcript categories which are connected to the response to oxidative stress and reactive oxygen species (Katsarou et al., 2016). A similar response to PSTVd infection was observed in tomato (Owens et al., 2012; Bagherian et al., 2016). These findings prompted us to analyze changes in the activity of enzymes that arise as a result of PSTVd infection and to compare differences in antioxidant response among five solanaceous species with a different sensitivity to PSTVd.

Considerable differences in antioxidant enzyme activities were noted for mock– and viroid–inoculated plants, together with some species–specific differences in the host response (Fig. 25–29). In all species examined in this study, changes in the activity of antioxidant enzymes upon PSTVd infection were found. The biggest increase in the activity of APX, CAT and GPX was observed in symptomatic tomato cv. Rutgers. The intensity of the antioxidant response upon PSTVd infection correlated with symptom appearance, which is in accordance with reports of several plant–virus interactions (Kyseláková et al., 2013). Interestingly, the increase in GPX activity was even detected in *P. hybrida* that did not show significant changes in endogenous hormone content or visible symptom upon PSTVd infection. Peroxidases, among the number of enzymes involved in the plant defense response to pathogen attack, are often the first to show changes in their activity (Milavec et al., 2001). An increase in the expression of peroxidase was also observed during the early (presymptomatic) stage of Etrog citron infected with *Citrus exocortis viroid* (CEVd), whereas the activity decreases at the postsymptomatic stage (Rizza et al., 2012).

While tomato cv. Rutgers and *L. rantonnetii* responded to PSTVd infection by increasing APX and CAT activity, in potato, *S. laxum* and *P. hybrida* APX activity increased, but CAT activity decreased (Fig. 26 and 27). Ascorbate peroxidase, together with catalase, controls the level of H_2O_2 in plant cells although the key role in decomposition of H_2O_2 belongs to APX (Sharma et al., 2012).

A decrease in CAT activity was also described in some other plant–pathogen interactions, including *Pepper mild mottle virus* (PMMoV) infection in *Nicotiana benthamiana* (Hakmaoui et al., 2012).

Depending on the plant host species, peroxidase acts as part of a different defense pathway. It is known that SA can induce production of ROS and trigger activation of antioxidant enzymes, both at local infection sites and systemic sites (De Gara et al., 2003). Also, increased activity of peroxidases has been suggested as a factor contributing to BR–induced disease resistance in cucumber plants (Xia et al., 2009). On the other hand, some studies suggest that the upregulated peroxidases, through the oxidation of IAA, might be responsible for growth reduction and malformations observed in virus–infected plants (Riedle–Bauer, 2000). In our study, the increase in GPX, APX, and CAT activity coincided with the accumulation of endogenous SA in tomato upon PSTVd infection. In symptomless *S. laxum*, increased activity of GPX, APX, and SOD coincided with the accumulation of endogenous CS, which needs to be further investigated. However, an increase in peroxidase activity in leaves of PSTVd–infected tomato and *S. laxum* plants was accompanied by an increase, not a decrease, in the endogenous IAA content. So, it can be assumed that peroxidases in these species are primarily involved in the defense response to PSTVd, while their effect on symptom development is difficult to estimate.

Also, it should be noted that after the infection with PSTVd there was a rise in protein content in all species examined in this study, apart from *L. rantonnetii*. This is consistent with gene expression studies in tomato plants upon PSTVd infection, which revealed upregulation of genes that encode proteins associated with ribosomes, cell wall and plasma membrane (Itaya et al., 2002; Owens et al. 2012). In addition, microarray analysis of RNA from potato infected with PSTVd showed enhanced expression of genes encoding heat–shock proteins and transcription factors, along with genes connected to hormone regulation and those involved in defense pathways (Katsarou et al., 2016). Usually, infected plants show a high protein content, which could be due to both the activation of the host defense mechanism and the pathogen attack mechanism (Agrios, 1997).

1. The surveillance activities described in this study revealed, for the first time, the presence of potato spindle tuber viroid disease in plants collected from different garden centres and retail nurseries in Croatia. During this survey, PSTVd was detected in two ornamental species, *Solanum laxum* and *Lycianthes rantonnetii* while no PSTVd infection was found in tomato or potato.

2. Molecular characterization of the PSTVd isolates provided the critical information on genetic relationships between PSTVd strains that occurred in Croatia and PSTVd strains that occurred in neighboring countries.

3. The data obtained in this study showed that PSTVd infection causes significant changes in endogenous PGRs content, in some symptomatic, but also in some asymptomatic species of Solanaceae. Also, the study revealed the existence of some species–specific features of the systemic hormone response of plants against PSTVd.

4. One of the most noticeable differences between symptomatic tomato and the other species with less pronounced symptoms was a high basal level of salicylic acid (SA) and abscisic acid (ABA) in leaves of mock–inoculated tomato plants.

5. A significant increase in endogenous brassinosteroide castasterone (CS) in leaves of *S. laxum* and potato tubers, suggests its possible role in the response of these species to PSTVd infection.

6. Upon PSTVd infection, jasmonic acid (JA) significantly increased in systemically infected leaves of tomato, potato and *S. laxum*, which can be considered a signal involved in the immune response of these plant species to PSTVd infection, though it does not seem to be critical for the development of visible symptoms.

7. In *P. hybrida* and *L. rantonnetii*, only endogenous level of indole–3–acetic acid (IAA) significantly accumulated upon infection with PSTVd. Differences in response of plant growth regulators in *P. hybrida* and *L. rantonnetii*, compared to the other solanaceous species examined in this study, suggest the existence of species–specific differences in their resistance response to PSTVd, most likely due to belonging to different genera.

8. In all species examined, considerable changes in enzymatic activity of guaiacol peroxidase, ascorbate peroxidase and catalase were observed upon PSTVd infection, while superoxide dismutase activity remained steady.

9. The study provides new evidences about the involvement of different plant growth regulators and antioxidant enzymes in plant defense response against PSTVd infection, and therefore can contribute to a better understanding of these processes and the development of resistance strategies.

Abouqamar S, Luo H, Laluk K, Mickelbart VM, Mengiste T (2009) Crosstalk between biotic and abiotic stress responses in tomato is mediated by *AIM1* transcription factor. The Plant Journal 58: 1–13.

Adie BA, Perez–Perez J, Perez–Perez MM, Godoy M, Sánchez–Serrano JJ, Schmelz EA, Solano R (2007) ABA is an essential signal for plant resistance to pathogens affecting JA biosynthesis and the activation of defences in *Arabidopsis*. Plant Cell 19: 1665–1681.

Adkar–Purushothama CR, Brosseau C, Giguere T, Sano T, Moffett P, Perreault JP (2015). Small RNA derived from the virulence modulating region of the potato spindle tuber viroid silences *callose synthase* genes of tomato plants. Plant Cell 27: 2178–2194.

Agrios GN (2005) Plant Pathology. 5th ed. Academic Press, San Diego.

Alazem M, Lin NS (2015) Roles of plant hormones in the regulation of host–virus interactions. Molecular Plant Pathology 16: 529–540.

Altschul SF, Madden TL, Schäffer AA, Zhang J, Zhang Z, Miller W, Lipman DJ (1997) Gapped BLAST and PSI–BLAST: a new generation of protein database search programs. Nucleic Acids Research 25: 3389–3402.

Ascencio–Ibáñez JT, Sozzani R, Lee T–J, Chu T–M, Wolfinger RD, Cella R, Hanley–Bowdoin, L (2008) Global analysis of Arabidopsis gene expression uncovers a complex array of changes impacting pathogen response and cell cycle during geminivirus infection. Plant Physiology 148: 436–454.

Avina–Padilla K, Martínez de la Vega O, Rivera–Bustamante R, Martínez–Soriano JP, Owens RA, Hammond RW, Vielle–Calzada JP (2015) In silico prediction and validation of potential gene targets for pospiviroid–derived small RNAs during tomato infection. Gene 564: 197–205.

Axtell MJ (2013) Classification and comparison of small RNAs from plants. Annual Review of Plant Biology 64: 137–159.

Baebler S, Witek K, Petek M, Stare K, Tusek–Znidaric M, Pompe–Novak M, Renaut J, Szajko K, Strzelczyk–Zyt D, Marczewski W, Morgiewicz K, Gruden K, Hennig J (2014) Salicylic acid is an indispensable component of the *Ny–1* resistance–gene–mediated response against potato virus Y infection in potato. Journal of Experimental Botany 65: 1095–1109.

Bagherian SAA, Izadpanah K, Hamzehzarghani H, Djavaheri M, Ghasemi Y (2014) Effect of infection by mild variant of potato spindle tuber viroid on metabolic profiles of tomato cultivar 'Rugers'. Iranian Journal of Plant Pathology 50: 113–118.

Bagherian SAA, Hamzehzarghani H, Izadpanah K, Djavaheri M (2016). Effects of potato spindle tuber viroid infection on tomato metabolic profile. Journal of Plant Physiology 201: 42–53.

Bajguz A (2007) Metabolism of brassinosteroids in plants. Plant Physiology and Biochemistry 45: 95–107.

Barba M, Gumpf DJ, Hadidi A (2003) Quarantine of imported germplasm. In: Hadidi A, Flores R, Randles JW, Semancik JS (Eds.) Viroids. Australia/USA, CSIRO Publishing/Science Publishers Inc., 303–311.

Bari R, Jones JDG (2009) Role of plant hormones in plant defence responses. Plant Molecular Biology 69: 473–488.

Bastas KK (2014) Importance of reactive oxygen species in plants–pathogens interactions. Selcuk Journal of Agriculture and Food Sciences 28: 11–21.

Baumberger N, Baulcombe DC (2005) *Arabidopsis* ARGONAUTE1 is an RNA slicer that selectively recruits microRNAs and short interfering RNAs. Proceedings of the National Academy of Sciences of the United States of America 102: 11928–11933.

Baumstark T, Schroder AR, Riesner D (1997) Viroid processing: switch from cleavage to ligation is driven by a change from a tetraloop to a loop E conformation. EMBO Journal 16: 599–610.

Ben Rejeb I, Pastor V, Mauch–Mani B (2014) Plant responses to simultaneous biotic and abiotic stress: molecular mechanisms. Plants: 458–475.

Bohs L, Olmstead RG (1997) Phylogenetic relationships in *Solanum* (Solanaceae) based on *ndhF* sequences. Systematic Botany 22: 5–17.

Boonham N, González Pérez L, Mendez MS, Peralta EL, Blockley A, Walsh K, Barker I, Mumford RA (2004) Development of a real–time RT-PCR assay for the detection of potato spindle tuber viroid. Journal of Virological Methods 116: 139–146.

Bradford MM (1976) A rapid and sensitive method for the quantitation of microgram quantities of protein utilizing the principle of protein–dye binding. Analytical Biochemistry 72: 248–254.

CABI/EPPO (2014) Potato spindle tuber viroid. [Distribution map]. Distribution Maps of Plant Diseases, No. April. Wallingford, UK: CABI, Map 729 (Edition 3).

Camacho Henriquez A, Sänger HL (1984) Purification and partial characterization of the major "pathogenesis–related" tomato leaf protein P14 from potato spindle tuber viroid (PSTV)–infected tomato leaves. Archives of Virology 81: 263–284.

Carbonell A, Martínez de Alba AE, Flores R, Gago S (2008) Double–stranded RNA interferes in a sequence–specific manner with infection of representative members of the two viroid families. Virology 371: 44–53.

Carr JP, Lewsey MG, Palukaitis P (2010) Signaling in induced resistance. Advances in Virus Research 76: 57–121.

Carthew RW, Sontheimer EJ (2009) Origins and mechanisms of miRNAs and siRNAs. Cell 136: 642–655.

Caverzan A, Casassola A, Brammer SP (2016) Antioxidant responses of wheat plants under stress. Genetics and Molecular Biology 39: 1–6.

Chance B, Maehly AC (1955) Assay of catalase and peroxidases. Methods in Enzymology 2: 764–775.

Clarke SF, Guy PL, Jameson PE, Schmierer D, Burritt DJ (2000) Influence of white clover mosaic potex–virus infection on the endogenous levels of jasmonic acid and related compounds in *Phaseolus vulgaris* L. seedlings. Journal of Plant Physiology 156: 433–437.

Clarke SF, Guy PL, Burritt DJ, Jameson PE (2002) Changes in the activities of antioxidant enzymes in response to virus infection and hormone treatment. Physiologia Plantarum 114: 157–164.

Clouse SD, Feldmann KA (1999) Molecular genetics of brassinosteroid action. In: Sakurai A, Yokota T, Clouse SD (eds.) Brassinosteroids: Steroidal plant hormones. Tokyo, Springer Verlag, 163–190.

Croatian Bureau of Statistics (2016) Statistical Yearbook of the Republic of Croatia 2016. Croatian Bureau of Statistics, Zagreb.

Curaba J, Singh MB, Bhalla PL (2014) miRNAs in the crosstalk between phytohormone signalling pathways. Journal of Experimental Botany 65: 1425–1438.

Das K, Roychoudhury A (2014) Reactive oxygen species (ROS) and response of antioxidants as ROS–scavengers during environmental stress in plants. Frontiers in Environmental Science 2: 53.

De Gara L, de Pinto MC, Tommasi F (2003) The antioxidant systems vis–à–vis reactive oxygen species during plant–pathogen interaction. Plant Physiology and Biochemistry 41: 863–870.

Di Serio F (2007) Identification and characterization of potato spindle tuber viroid infecting *Solanum jasminoides* and *S. rantonetti* in Italy. Journal of Plant Pathology 89: 297–300.

Di Serio F, Flores R (2008) Viroids: molecular implements for dissecting RNA trafficking in plants. RNA Biology 5: 128–131.

Di Serio F, Flores R, Verhoeven JTJ, Li S–F, Pallás V, Randles WJ, Sano T, Vidalakis G, Owens RA (2014) Current status of viroid taxonomy. Archives of Virology 159: 3467–78.

Di Serio F, Martínez de Alba AE, Navarro B, Gisel A, Flores R (2010) RNA–dependent RNA polymerase 6 delays accumulation and precludes meristem invasion of a nuclear–replicating viroid. Journal of Virology 84: 2477–2489.

Di Serio F, De Stradis A, Delgado S, Flores R, Navarro B (2013) Cytopathic effects incited by viroid RNAs and putative underlying mechanisms. Frontiers in Plant Science 3: 288.

Diener TO (1971) Potato spindle tuber "virus": IV. A replicating, low molecular weight RNA. Virology 45: 411–428.

Diener TO (1987) Potato spindle tuber. In: Diener TO (ed.) The Viroids. New York, Plenum Press, 221–233.

Diener TO, Hammond RW, Black T, Katze MG (1993) Mechanism of viroid pathogenesis: Differential activation of the interferon–induced, double–stranded RNA–activated, M(r) 68,000 protein kinase by viroid strains of varying pathogenicity. Biochimie 75: 533–538.

Diener TO (1995) Origin and evolution of viroids and viroid–like satellite RNAs. Virus Genes 11: 119–131.

Diermann N, Matoušek J, Junge M, Riesner D, Steger G (2010) Characterization of plant miRNAs and small RNAs derived from potato spindle tuber viroid (PSTVd) in infected tomato. Biological Chemistry 391: 1379–1390.

Ding B, Kwon MO, Hammond R, Owens RA (1997) Cell–to–cell movement of potato spindle tuber viroid. The Plant Journal 12: 931–936.

Ding B, (2009) The biology of viroid–host interactions. Annual Review of Phytopathology 47: 105–131.

Dingley AJ, Steger G, Esters B, Riesner D, Grzesiek S (2003) Structural characterization of the 69 nucleotide potato spindle tuber viroid left–terminal domain by NMR and thermodynamic analysis. Journal of Molecular Biology 334: 751–767.

Eamens AL, Smith NA, Dennis ES, Wassenegger M, Wang MB (2014) In *Nicotiana* species, an artificial microRNA corresponding to the virulence modulating region of potato spindle tuber viroid directs RNA silencing of a *soluble inorganic pyrophosphatase* gene and the development of abnormal phenotypes. Virology, 450–451: 266–277.

EFSA (2011) Scientific opinion on the assessment of the risk of solanaceous pospiviroids for the EU territory and the identification and evaluation of risk management options. EFSA Journal 9: 2330.

Eigen M (1993) Viral quasispecies. Scientific American 269: 42–49.

Faggioli F, Ferretti L, Albanese G, Sciarroni R, Pasquini G, Lumia V, Barba M (2005) Distribution of olive tree viruses in Italy as revealed by one–step rt–pcr. Journal of Plant Pathology 87: 49–55.

Farag MA, Huhman DV, Dixon RA, Sumner LW (2009) Metabolomics reveals novel pathways and differential mechanistic and elicitor–specific responses in phenylpropanoid and isoflavonoid biosynthesis in *Medicago truncatula* cell cultures. Plant Physiology 146: 387–402.

Filimon RV, Rotaru L, Filimon RM (2016) Quantitative investigation of leaf photosynthetic pigments during annual biological cycle of *Vitis vinifera* L. table grape cultivars. South African Journal of Enology and Viticulture 37: 1–14.

Fleet CM, Sun T–P (2005) A DELLAcate balance: the role of gibberellin in plant morphogenesis. Current Opinion in Plant Biology 8: 77–85.

Floková K, Tarkowska D, Miersch O, Strnad M, Wasternack C, Novak O (2014) UHPLC–MS/MS based target profiling of stress–induced phytohormones. Phytochemistry 105: 147–157.

Flores R, Di Serio F, Navarro B, Duran–Vila N, Owens R (2011) Viroids and viroid diseases of plants. In: Hurst CJ (ed.) Studies in Viral Ecology: Microbial and Botanical Host Systems Vol. 1. Hoboken, New Jersey, Wiley– Blackwell, 307–341.

Flores R, Hernández C, Martínez de Alba AE, Daròs JA, Di Serio F (2005) Viroids and viroid–host interactions. Annual Review of Phytopathology 43:117–139.

Flores R, Gas M–E, Molina–Serrano D, Nohales MÁ, Carbonell A, Gago S, De la Peña M, Daròs, JA (2009) Viroid replication: rolling–circles, enzymes and ribozymes. Viruses 1(2): 317-334.

Flores R, Owens RA, Taylor J (2016) Pathogenesis by subviral agents: viroids and hepatitis delta virus. Current Opinion in Virology 17: 87–94.

Flores R, Serra P, Minoia S, Di Serio F, Navarro B (2012) Viroids: from genotype to phenotype just relying on RNA sequence and structure motifs. Frontiers in Microbiology 3: 217.

Fodor J, Gullner G, Adam AL, Barna B, Komives T, Kiraly Z (1997) Local and systemic responses of antioxidants to tobacco mosaic virus infection and to salicylic acid in tobacco. Plant Physiology 114: 1443–1451.

Fraser RSS, Whenham RJ (1989) Abscisic acid metabolism in tomato plants infected with tobacco mosaic virus: relationships with growth, symptoms and the *Tm–1* gene for TMV resistance. Physiological and Molecular Plant Pathology 34: 215–226.

Fujita M, Fijita Y, Noutoshi Y, Takahashi F, Narusaka Y, Yamaguchi–Shinozaki K, Shinozaki K (2006) Crosstalk between abiotic and biotic stress responses: A current view from the points of convergence in the stress signaling networks. Current Opinion in Plant Biology 9: 436–442.

Gadea, J, Mayda ME, Conejero V, Vera P (1996) Characterization of defense–related genes ectopically expressed in viroid–infected tomato plants. Molecular Plant–Microbe Interactions 9: 409–415.

Gaffney T, Friedrich L, Vernooij B, Negrotto D, Nye G, Uknes S, Ward E, Kessmann H, Ryals J (1993) Requirement of salicylic acid for the induction of systemic acquired resistance. Science 261: 754-756.

Garcia–Marcos A, Pacheco R, Manzano A, Aguilar E, Tenllado F (2013) Oxylipin biosynthesis genes positively regulate programmed cell death during compatible infections with the synergistic pair potato virus X–potato virus Y and tomato spotted wilt virus. Journal of Virology 87: 5769–5783.

Gas ME, Hernandez C, Flores R, Daros JA (2007) Processing of nuclear viroids *in vivo*: an interplay between RNA conformations. PLOS Pathogens 3: 1813–1826.

Gast FU, Kempe D, Spieker RL, Sänger HL (1996) Secondary structure probing of potato spindle tuber viroid (PSTVd) and sequence comparison with other small pathogenic RNA replicons provides evidence for central non–canonical base–pairs, large A–rich loops, and a terminal branch. Journal of Molecular Biology 262: 652–670.

Giannopolitis CN, Reis SK (1977) Superoxide dismutases: I. Occurrence in higher plants. Plant Physiology 59: 309–314.

Gómez G, Martinez G, Pallás V (2009) Interplay between viroid–induced pathogenesis and RNA silencing pathways. Trends in Plant Science 14: 264–269.

Góra–Sochacka A, Kierzek A, Candresse T, Zagórski W (1997) The genetic stability of potato spindle tuber viroid (PSTVd) molecular variants. RNA 3: 68–74.

Gos RW (1926) Transmission of potato spindle tuber disease by cutting knives and seed piece contact. Phytopathology 16: 299–304.

Gozmanova M., Denti MA, Minkov IN, Tsagris M, Tabler M (2003) Characterization of the RNA motif responsible for the specific interaction of potato spindle tuber viroid RNA (PSTVd) and the tomato protein Virp1. Nucleic Acids Research 31: 5534–5543.

Grant MR, Jones JDG (2009) Hormone (dis)harmony moulds plant health and disease. Science 324: 750–752.

Gross HJ, Domdey H, Lossow C, Jank P, Raba M, Alberty H, Sänger HL (1978) Nucleotide sequence and secondary structure of potato spindle tuber viroid. Nature 273: 203–208.

Hadidi A, Flores R, Randles JW, Semancik JS (2003) Viroids. CSIRO Publishing, Collingwood, Australia.

Hadwan MH, Abed HN (2016) Data supporting the spectrophotometric method for the estimation of catalase activity. Data in Brief 6: 194–199.

Hakmaoui A, Pérez–Bueno ML, García–Fontana B, Camejo D, Jiménez A, Sevilla F, Barón M (2012) Analysis of the antioxidant response of *Nicotiana benthamiana* to infection with two strains of pepper mild mottle virus. Journal of Experimental Botany 63: 5487–5496.

Hammann C, Steger G (2012) Viroid–specific small RNA in plant disease. RNA Biology 9: 809–819.

Hammond RW, Zhao Y (2000) Characterization of a tomato protein kinase gene induced by infection by potato spindle tuber viroid. Molecular Plant–Microbe Interactions 13: 903–910.

Hammond RW, Zhao Y (2009) Modification of tobacco plant development by sense and antisense expression of the tomato viroid–induced AGC VIIIa protein kinase PKV suggests involvement in gibberellin signaling. BMC Plant Biology 9: 108.

Hari V (1980) Ultrastructure of potato spindle tuber viroid–infected tomato leaf tissue. Phytopathology 70: 385–387.

Heath MC (2000) Hypersensitive response–related death. Plant Molecular Biology 44: 321–334.

Hernández JA, Diaz–Vivancos P, Rubio M, Olmos E, Ros–Barceló A, Martínez–Gómez P (2006) Long–term PPV infection produces an oxidative stress in a susceptible apricot cultivar but not in a resistant cultivar. Physiologia Plantarum 126: 140–152.

Herranz MC, Niehl A, Rosales M, Fiore N, Zamorano A, Granell A, Pallas V (2013) A remarkable synergistic effect at the transcriptomic level in peach fruits doubly infected by prunus necrotic ringspot virus and peach latent mosaic viroid. Virology Journal 10: 164.

Hiddinga HJ, Crum CJ, Hu J, Roth DA (1988) Viroid–induced phosphorylation of a host protein related to a dsRNA–dependent protein kinase. Science 241: 451–453.

Huang J, Yang M, Lu L, Zhang X (2016) Diverse functions of small RNAs in different plant–pathogen communications. Frontiers in Microbiology 7: 1552.

Itaya A, Folimonov A, Matsuda Y, Nelson RS, Ding B (2001) potato spindle tuber viroid as inducer of RNA silencing in infected tomato. Molecular Plant–Microbe Interactions 14: 1332–1334.

Itaya A, Matsuda Y, Gonzales RA, Nelson RS, Ding B (2002) potato spindle tuber viroid strains of different pathogenicity induces and suppresses expression of common and unique genes in infected tomato. Molecular Plant–Microbe Interactions 10: 990–999.

Itaya A, Zhong X, Bundschuh R, Qi Y, Wang Y, Takeda R, Harris AR, Molina C, Nelson RS, Ding B (2007) A structured viroid RNA is substrate for Dicer–like cleavage to produce biologically active small RNAs but is resistant to RISC–mediated degradation. Journal of Virology 81: 2980–2994.

Ivanova D, Milev I, Vachev T, Baev V, Yahubyan G, Minkov G, Gozmanova M (2014) Small RNA analysis of potato spindle tuber viroid infected *Phelipanche ramosa*. Plant Physiology and Biochemistry 74: 276–292.

Jameson PE, Clarke SF (2002) Hormone–virus interactions in plants. Critical Reviews in Plant Sciences 21: 205–228.

Jones JD, Dangl JL (2006) The plant immune system. Nature 444: 323–329.

Jovel J, Walker M, Sanfacon H (2011) Salicylic acid–dependent restriction of tomato ringspot virus spread in tobacco is accompanied by a hypersensitive response, local RNA silencing, and moderate systemic resistance. Molecular Plant–Microbe Interactions 24: 706–718.

Kapoor D, Sharma R, Handa N, Kaur H, Rattan A, Yadav P, Gautam V, Kaur R, Bhardwaj R (2015) Redox homeostasis in plants under abiotic stress: role of electron carriers, energy metabolism mediators and proteinaceous thiols. Frontiers in Environmental Science 3:13.

Katoh K, Standley DM (2013) MAFFT Multiple sequence alignment software version 7: improvements in performance and usability. Molecular Biology and Evolution 30: 772–780.

Katsarou K, Wu Y, Zhang R, Bonar N, Morris J, Hedley PE, Bryan GJ, Kalantidis K, Hornyik C (2016) Insight on genes affecting tuber development in potato upon potato spindle tuber viroid (PSTVd) infection. PLoS ONE 11: e0150711.

Kazan K, Manners JM (2009) Linking development to defense: auxin in plant–pathogen interactions. Trends in Plant Science 14: 373–382.

Keese P, Symons RH (1985) Domains in viroids: evidence of intermolecular RNA rearrangement and their contribution to viroid evolution. Proceedings of the National Academy of Sciences of the United States of America 82: 4582–4586.

Khripach V, Zhabinskii V, De Groot A (2000) Twenty years of brassinosteroids: Steroidal plant hormones warrant better crops for the XXI century. Annals of Botany 86: 441–447.

Kim HJ, Baek KH, Lee BW, Choi D, Hur CG (2011) In silico identification and characterization of microRNAs and their putative target genes in Solanaceae plants. Genome 54: 91–98.

Kissoudis C, Sunarti S, van de Wiel C, Visser RGF, van der Linden CG, Bai Y (2016) Responses to combined abiotic and biotic stress in tomato are governed by stress intensity and resistance mechanism. Journal of Experimental Botany 67: 5119–5132.

Klahre U, Noguchi T, Fujioka S, Takatsuto S, Yokota T, Nomura T, Yoshida S, Chua NH (1998) The Arabidopsis DIMINUTO/DWARF1 gene encodes a protein involved in steroid synthesis. Plant Cell 10: 1677–1690.

Klessig DF, Malamy J (1994) The salicylic acid signal in plants. Plant Molecular Biology Reporter 26: 1439–1458.

Kloek AP, Verbsky ML, Sharma SB, Schoelz JE, Vogel J, Klessig DF, Kunkel BN (2001) Resistance to *Pseudomonas syringae* conferred by an *Arabidopsis thaliana* coronatine–insensitive (*coi1*) mutation occurs through two distinct mechanisms. The Plant Journal 26: 509–522.

Kolonko N, Bannach O, Aschermann K, Hu KH, Moors M, Schmitz M, Steger G, Riesner D (2006) Transcription of potato spindle tuber viroid by RNA polymerase II starts in the left terminal loop. Virology 347: 392–404.

Kovač M, Müller A, Milovanovič Jarh D, Milavec M, Düchting P, Ravnikar M (2009) Multiple hormone analysis indicates involvement of jasmonate signalling in the early defence of potato to potato virus Y^{NTN}. Biologia Plantarum 53: 195–199.

Kovalskaya N, Hammond RW (2014) Molecular biology of viroid–host interactions and disease control strategies. Plant Science 228: 48–60.

Krečič–Stres H, Vučak C, Ravnikar M, Kovač M (2005) Systemic potato virus Y^{NTN} infection and levels of salicylic and gentisic acids in different potato genotypes. Plant Pathology 54: 441–447.

Kumar S, Stecher G, Tamura K (2016) MEGA7: Molecular evolutionary genetics analysis version 7.0 for bigger datasets. Molecular Biology and Evolution 33: 1870–1874.

Kyseláková H, Sedlářová M, Kubala M, Nožková V, Piterková J, Luhová L, Novák O, Ilík P (2013) Reactive oxygen and nitrogen species and hormone signalling in systemic infection of pea by Pea enation mosaic virus. Plant Protection Science 49: 105–119.

Lamb C, Dixon RA (1997) The oxidative burst in plant disease resistance. Annual Review of Plant Physiology and Plant Molecular Biology 48: 251–275.

Lebas BSM, Clover GRG, Ochoa–Corona FM, Elliott DR, Tang Z, Alexander BJR (2005) Distribution of potato spindle tuber viroid in New Zealand glasshouse crops of capsicum and tomato. Australian Plant Pathology 34: 129–133.

Lee WS, Fu SF, Verchot–Lubicz J, Carr JP (2011) Genetic modification of alternative respiration in *Nicotiana benthamiana* affects basal and salicylic acidinduced resistance to potato virus X. BMC Plant Biology 11: 41.

Lenarcic R, Morisset D, Mehle N, Ravnikar M (2012) Fast real–time detection of potato spindle tuber viroid by RT–LAMP. Plant Pathology 62: 1147–56.

León J, Rojo E, Sánchez–Serrano JJ (2001) Wound signalling in plants. Journal of Experimental Botany 52: 1–9.

Li F, Pignatta D, Bendix C, Brunkard JO, Cohn MM, Tung J, Sun H, Kumar P, Baker B (2012) MicroRNA regulation of plant innate immune receptors. Proceedings of the National Academy of Sciences of the United States of America 109: 1790–1795.

Li Y, Zhang Q, Zhang J, Wu L, Qi Y, Zhou JM (2010) Identification of microRNAs involved in pathogen–associated molecular pattern–triggered plant innate immunity. Plant Physiology 152: 2222–2231.

Lichtenthaler HK (1987) Chlorophylls and carotenoids: pigments of photosynthetic biomembranes. In: Colowick SP, Kaplan NO (eds.) Methods in Enzymology. New York, Academic Press Inc., 350–382.

Llave C, Xie Z, Kasschau KD, Carrington JC (2002) Cleavage of *Scarecrow–like* mRNA targets directed by a class of *Arabidopsis* miRNA. Science 297: 2053–2056.

Love AJ, Yun BW, Laval V, Loake GJ, Milner JJ (2005) Cauliflower mosaic virus, a compatible pathogen of *Arabidopsis*, engages three distinct defense–signaling pathways and activates rapid systemic generation of reactive oxygen species. Plant Physiology 139: 935–948.

Ludwig–Müller J (2014) Auxin and the interaction between plants and microorganisms. In: Zazimalova E, Petrasek J, Benkova E (eds.) Auxin and its Role in Plant Development. Vienna, Springer, 413–434.

Luhova L, Lebeda A, Hedererová D, Peč P (2003) Activities of amino peroxidase, peroxidase and catalase in seedlings of *Pisum sativum* L. under different light conditions. Plant Soil and Environment 49: 151–157.

Luigi M, Luison D, Tomassoli L, Faggioli F (2011). Natural spread and molecular analysis of pospiviroids infecting ornamentals in Italy. Journal of Plant Pathology 93: 1–5.

Malandraki I, Papachristopoulou M, Vassilakos N (2010) First report of potato spindle tuber viroid (PSTVd) in ornamental plants in Greece. New Disease Reports 21: 9.

Mallory A, Vaucheret H (2010) Form, function, and regulation of ARGONAUTE proteins. Plant Cell 22: 3879–3889.

Mandadi KK, Scholthof K–BG (2013) Plant immune responses against viruses: how does a virus cause disease? Plant Cell 25: 1489–1505.

Mang H–G, QianW, Zhu Y, Qian J, Kang H–G, Klessig DF, Hua J (2012) Abscisic acid deficiency antagonizes high–temperature inhibition of disease resistance through enhancing nuclear accumulation of resistance proteins SNC1 and RPS4 in *Arabidopsis*. Plant Cell 24: 1271–1284.

Maniataki E, Tabler M, Tsagris M (2003) Viroid RNA systemic spread may depend on the interaction of a 71–nucleotide bulged hairpin with the host protein VIRP1. RNA 9: 346–354.

Martin WH (1922) "Spindle tuber", a new potato trouble. Hints to Potato Growers, New Jersey State Potato Association 3: 8.

Martin A, Adam H, Diaz–Mendoza M, Zurczak M, Gonzalez–Schain ND, Suarez–Lopez P (2009) Graft–transmissible induction of potato tuberization by the microRNA miR172. Development 136: 2873–2881.

Martínez–Soriano JP, Galindo–Alonso J, Maroon CJM, Yucel I, Smith DR, Diener TO (1996) Mexican papita viroid: putative ancestor of crop viroids. Proceedings of the National Academy of Science of the United States of America 93: 9397–9401.

Martínez de Alba AE, Flores R, Hernández C (2002) Two chloroplastic viroids induce the accumulation of the small RNAs associated with posttranscriptional gene silencing. Journal of Virology 76: 13094–13096.

Martínez de Alba AE, Sägesser R, Tabler M, Tsagris M (2003) A bromodomain–containing protein from tomato specifically binds potato spindle tuber viroid RNA *in vitro* and *in vivo*. Journal of Virology 77: 9685–94.

Matoušek J, Orctová L, Steger G, Škopek J, Moors M, Dědič P, Riesner D (2004) Analysis of thermal stress–mediated PSTVd variation and biolistic inoculation of progeny of viroid "thermomutants" to tomato and *Brassica* species. Virology 323: 9–23.

Matoušek J, Piernikarczyk RJJ, Týcová A, Duraisamy GS, Kocábek T, Steger G (2015) Expression of SANT/HTH Myb mRNA, a plant morphogenesis–regulating transcription factor, changes due to viroid infection. Journal of Plant Physiology 183: 85–94.

Matoušek J, Stehlik J, Procházková J, Orctová L, Wullenweber J, Füssy Z, Kováčik J, Duraisamy GS, Ziegler A, Schubert J, Steger G (2012) Biological and molecular analysis of the pathogenic variant C3 of potato spindle tuber viroid (PSTVd) evolved during adaptation to chamomile (*Matricaria chamomilla*). Biological Chemistry 393: 605–615.

McConn M, Creelman RA, Bell E, Mullet JE, Browse J (1997) Jasmonate is essential for insect defense in *Arabidopsis*. Proceedings of the National Academy of Sciences the United States of America 94: 5473–5477.

Mehle N, Gutiérrez–Aguirre I, Prezelj N, Delic D, Vidic U, Ravnikar M (2014) Survival and transmission of potato virus Y, pepino mosaic virus and potato spindle tuber viroid in water. Applied and Environmental Microbiology 80: 1455–1462.

Mertelik J, Kloudova K, Cervena G, Necekalova J, Mikulkova H, Levkanicova Z, Dedic P, Ptacek J (2010) First report of potato spindle tuber viroid PSTVd) in *Brugmansia* spp., *Solanum jasminoides*, *Solanum muricatum* and *Petunia* spp. in the Czech Republic. Plant Pathology 59: 392.

Mickelbart MV, Hasegawa PM, Bailey–Serres J (2015) Genetic mechanisms of abiotic stress tolerance that translate to crop yield stability. Nature Reviews Genetics 16: 237–251.

Milanović J, Kajić V, Mihaljević S (2014) Occurrence and molecular variability of potato spindle tuber viroid and tomato apical stunt viroid in ornamental plants in Croatia. The European Journal of Plant Pathology 139: 785–788.

Milavec M, Ravnikar M, Kovač M (2001) Peroxidases and photosynthetic pigments in susceptible potato infected with potato virus Y^{NTN}. Plant Physiology and Biochemistry 3: 891–898.

Minoia S, Carbonell A, Di Serio F, Gisel A, Carrington JC, Navarro B, Flores R (2014) Specific ARGONAUTES bind selectively small RNAs derived from potato spindle tuber viroid and attenuate viroid accumulation *in vivo*. Journal of Virology 88: 11933–11945.

Mittler R, Vanderauwera S, Gollery M, Van Breusegem F (2004) Reactive oxygen gene network of plants. Trends in Plant Science 9: 490–498.

Montalbini P, Buonaurio R, Kumar NNU (1995) Peroxidase activity and isoperoxidase pattern in tobacco leaves infected with tobacco necrosis virus and other viruses inducing necrotic and non–necrotic alterations. Journal of Phytopathology 143: 295–301.

Nakano Y, Asada K (1981) Hydrogen peroxide is scavenged by ascorbate specific peroxidase in spinach chloroplasts. Plant and Cell Physiology 22: 867–880.

Nakashita H, Yasuda M, Nitta T, Asami T, Fujioka S, Arai Y, Sekima ta K, Takatsuto S, Yamaguchi I, Yoshida S (2003) Brassinosteroid functions in a broad range of disease resistance in tobacco and rice. The Plant Journal 33: 887–898.

Nambara E, Marion–Poll A (2005) Abscisic acid biosynthesis and catabolism. Annual Review of Plant Biology 56: 165–185.

Navarro B, Gisel A, Rodio ME, Delgado S, Flores R, Di Serio F (2012) Small RNAs containing the pathogenic determinant of a chloroplast–replicating viroid guide the degradation of a host mRNA as predicted by RNA silencing. The Plant Journal 70: 991–1003.

Navarro B, Silletti MR, Trisciuzzi VN, Di Serio F (2009) Identification and characterization of potato spindle tuber viroid infecting tomato in Italy. Journal of Plant Pathology 91: 723–726.

Netto AT, Campostrini E, Gonc J, de Oliveira JG, Bressan–Smith RE (2005) Photosynthetic pigments, nitrogen, chlorophyll *a* fluorescence and SPAD–502 readings in coffee leaves. Scientia Horticulturae 104: 199–209.

Neuenschwander U, Verooij L, Friedich S, Uknes H, Kessmann Ryals J (1995) Is hydrogen peroxide a second messenger of salicylic acid in systemic acquired resistance. Plant Journal 8: 227–233.

Nielsen SL, Enkegaard A, Nicolaisen M, Kryger P, Marn MV, Pleško IM, Kahrer A, Gottsberger RA (2012) No transmission of potato spindle tuber viroid shown in experiments with thrips (*Frankliniella occidentalis*, *Thrips tabaci*), honey bees (*Apis mellifera*) and bumblebees (*Bombus terrestris*). European Journal of Plant Pathology 133: 505–509.

Nohales MA, Flores R, Daros JA (2012) Viroid RNA redirects host DNA ligase 1 to act as an RNA ligase. Proceedings of the National Academy of Sciences of the United States of America 109: 13805–13810.

Oklestkova J, Tarkowská D, Eyer L, Elbert T, Marek A, Smrzova Z, Novák O, Fránek M, Zhabinskii VN, Strnad M (2017) Immunoaffinity chromatography combined with tandem mass spectrometry: A new tool for the selective capture and analysis of brassinosteroid plant hormones. Talanta 170: 432–440.

Owens RA (2007) Potato spindle tuber viroid: the simplicity paradox resolved? Molecular Plant Pathology 8: 549–60.

Owens RA, Hammond R (2009) Viroid pathogenicity: one process, many faces. Viruses 1: 298–316.

Owens RA, Steger G, Hu Y, Fels A, Hammond RW, Riesner D (1996) RNA structural features responsible for potato spindle tuber viroid pathogenicity. Virology 222: 144–158.

Owens RA, Tech KB, Shao JY, Sano T, Baker CJ (2012) Global analysis of tomato gene expression during potato spindle tuber viroid infection reveals a complex array of changes affecting hormone signaling. Molecular Plant–Microbe Interactions 25: 582–598.

Owens RA, Thompson SM (2005) Mutational analysis does not support the existence of a putative tertiary structural element in the left terminal domain of potato spindle tuber viroid. Journal of General Virology 86: 1835–1839.

Pacheco R, Garcia–Marcos A, Manzano A, de Lacoba MG, Camanes G, Garcia–Agustin P, Diaz–Ruiz JR, Tenllado F (2012) Comparative analysis of transcriptomic and hormonal responses to compatible and incompatible plant–virus interactions that lead to cell death. Molecular Plant–Microbe Interactions 25: 709–723.

Palukaitis P (1987) Potato spindle tuber viroid: Investigation of the long–distance, intra–plant transport route. Virology 158: 239–241.

Palukaitis P (2014) What has been happening with viroids? Virus Genes 49: 175–184.

Palukaitis P, Carr JP (2008) Plant resistance responses to viruses. Journal of Plant Pathology 90: 153–171.

Papaefthimiou I, Hamilton AJ, Denti MA, Baulcombe DC, Tsagris M, Tabler M (2001) Replicating potato spindle tuber viroid RNA is accompanied by short RNA fragments that are characteristic of post–transcriptional gene silencing. Nucleic Acids Research 29: 2395–2400.

Petrovič N, Miersch O, Ravnikar M, Kovač M (1997) Potato virus Y^{NTN} alters the distribution and concentration of endogenous jasmonic acid in potato plants grown *in vitro*. Physiological and Molecular Plant Pathology 50: 237–244.

Puchta H, Herold T, Verhoeven K, Roenhorst A, Ramm K, Schmidt–Puchta W, Sanger HL (1990) A new strain of potato spindle tuber viroid (PSTVd–N) exhibits major sequence differences as compared to all other strains sequenced so far. Plant Molecular Biology 15: 509–511.

Qi Y, Denli AM, Hanon GJ (2005) Biochemical specialization within *Arabidopsis* RNA silencing pathways. Molecular Cell 19: 421–428.

Qi Y, Ding B (2003) Inhibition of cell growth and shoot development by a specific nucleotide sequence in a noncoding viroid RNA. Plant Cell 15: 1360–1374.

Querci M, Owens RA, Bartolini I, Lazarte V, Salazar LF (1997) Evidence for heterologous encapsidation of potato spindle tuber viroid in particles of potato leafroll virus. Journal of General Virology 78: 1207–1211.

Querci M, Owens RA, Vargas C, Salazar LF (1995) Detection of potato spindle tuber viroid in avocado growing in Peru. Plant Disease 79: 196–202.

Rajagopalan R, Vaucheret H, Trejo J, Bartel DP (2006) A diverse and evolutionarily fluid set of microRNAs in *Arabidopsis thaliana*. Genes and Development 20: 3407–3425.

Rao MV, Lee H, Creelman RA, Mullet JE, Davis KR (2000) Jasmonic acid signaling modulates ozone–induced hypersensitive cell death. Plant Cell 12: 1633–1646.

Raskin I (1992) Role of salicylic acid in plants. Annual Review of Plant Physiology and Molecular Biology 43: 439–463.

Riedle–Bauer M (2000) Role of reactive oxygen species and antioxidant enzymes in systemic virus infections of plants. Journal of Phytopathology 148: 297–302.

Riesner D, Henco K, Rokohl U, Klotz G, Kleinschmidt AK, Domdey H, Jank P, Gross HJ, Sänger HL (1979) Structure and structure formation of viroids. Journal of Molecular Biology 133: 85–115.

Rizza S, Conesa A, Juarez J, Catara A, Navarro L, Duran–Vila N, Ancillo G (2012) Microarray analysis of Etrog citron (*Citrus medica* L.) reveals changes in chloroplast, cell wall, peroxidase and symporter activities in response to viroid infection. Molecular Plant Pathology 13: 852–64.

Rodriguez JL, Garcia–Martinez JL, Flores R (1978) The relationship between plant growth substances content and infection of *Gynura aurantiaca* DC by citrus exocortis viroid. Physiological Plant Pathology 13: 355–363.

Ruiz–Ferrer V, Voinnet O (2009) Roles of plant small RNAs in biotic stress responses. Annual Review of Plant Biology 60: 485–510.

Sänger HL, Klotz G, Riesner D, Gross HJ, Kleinschmidt AK (1976) Viroids are single–stranded covalently closed circular RNA molecules existing as highly base–paired rod–like structures. Proceedings of the National Academy of Sciences of the United States of America 73: 3852–3856.

Schindler I, Muhlbach HP (1992) Involvement of nuclear DNA–dependent RNA polymerases in potato spindle tuber viroid replication: a reevaluation. Plant Science 84: 221–229.

Schlagnhaufer CD, Arteca RN (1985) Brassinosteroid–induced epinasty in tomato plants. Plant Physiology 78: 300–303.

Schultz ES, Folsom D (1923) Transmission, variation, and control of certain degeneration diseases of Irish potatoes. Journal of Agricultural Research 25: 43.

Schwind N, Zwiebel M, Itaya A, Ding B, Wang MB, Krczal G, Wassenegger M (2009) RNAi–mediated resistance to potato spindle tuber viroid in transgenic tomato expressing a viroid hairpin RNA construct. Molecular Plant Pathology 10: 459–469.

Semancik JS, Conejero–Tomas V (1987) Viroid pathogenesis and expression of biological activity. In: Semancik JS (ed.) Viroids and Viroid–like Pathogens, CRC Press, Boca Raton, 71 – 126.

Sharma P, Jha AB, Dubey RS, Pessarakli M (2012) Reactive oxygen species, oxidative damage, and antioxidative defense mechanism in plants under stressful conditions. Journal of Botany 37: 1–26.

Singh RP (1973) Experimental host range of the potato spindle tuber 'virus'. American Potato Journal 50: 111–123.

Singh RP, Boucher A, Somerville TH (1989) Evaluation of chemicals for disinfection of laboratory equipment exposed to potato spindle tuber viroid. American Journal of Potato Research 66: 239–246.

Singh RP, Boucher A, Somerville TH (1992) Detection of potato spindle tuber viroid in the pollen and various parts of potato plant pollinated with viroid–infected pollen. Plant Disease 76: 951–953.

Sugano S, Kaminaka H, Rybka Z, Catala R, Salinas J, Matsui K, Ohme–Takagi M, Takatsuji H (2003) Stress–responsive zinc finger gene *ZPT2–3* plays a role in drought tolerance in petunia. The Plant Journal 36: 830–841.

Sun TP, Gubler F (2004) Molecular mechanisms of gibberrellin signaling in plants. Annual Review of Plant Biology 55: 197–223.

Szalai G, Tari I, Janda T, Pestenacz A, Paldi E (2000) Effects of cold acclimation and salicylic acid on changes in ACC and MACC contents in maize during chilling. Biologia Plantarum 43: 637–640.

Takeda R, Ding B (2009) Viroid intercellular trafficking, RNA motifs, cellular factors and broad impacts. Viruses 1: 210–221.

Tanaka K, Asami T, Yoshida S, Nakamura Y, Matsuo T, Okamoto S (2005) Brassinosteroid homeostasis in *Arabidopsis* is ensured by feedback expressions of multiple genes involved in its metabolism. Plant Physiology 138: 1117–1125.

Tedder P, Zubko E, Westhead DR, Meyer P (2009) Small RNA analysis in *Petunia hybrida* identifies unusual tissue–specific expression patterns of conserved miRNAs and of a 24mer RNA. RNA 15: 1012–1020.

Tessitori M, Maria G, Capasso C, Catara G, Rizza S, De Luca V, Catara A, Capasso A, Carginale V (2007) Differential display analysis of gene expression in Etrog citron leaves infected by *Citrus viroid III*. Biochimica et Biophysica Acta 1769: 228–235.

The Tomato Genome Consortium (2012) The tomato genome sequence provides insights into fleshy fruit evolution. Nature 485: 635–641.

Ton J, Flors V, Mauch–Mani B (2009) The multifaceted role of ABA in disease resistance. Trends in Plant Science 14: 310–317.

Torres MA, Jones JDG, Dangl JL (2006) Reactive oxygen species signaling in response to pathogens. Plant Physiology 141: 373–378.

Tripathy BC, Oelmüller R (2012) Reactive oxygen species generation and signaling in plants. Plant Signaling and Behavior 7: 1621–1633.

Tuteja N, Gill SS, Trivedi PK, Asif MH, Nath P (2010) Plant growth regulators and their role in stress tolerance. In: Anjum NA (ed.) Plant Nutrition and Abiotic Stress Tolerance I. Plant Stress 4 (Special Issue 1), Global Science Book, Japan, 1-18.

Unterholzner SJ, Rozhon W, Papacek M, Ciomas J, Lange T, Kugler KG, Mayer KF, Sieberer T, Poppenberger B (2015) Brassinosteroids are master regulators of gibberellin biosynthesis in Arabidopsis. Plant Cell 27: 2261–2272.

Vazquez F, Blevins T, Ailhas J, Boller T, Meins F (2008) Evolution of *Arabidopsis MIR* genes generates novel microRNA classes. Nucleic Acids Research 36: 6429–6438.

Vera P, Tornero P, Conejero V (1993) Cloning and expression analysis of a viroid–induced peroxidase from tomato plants. Molecular Plant–Microbe Interactions 6: 790–794.

Verhoeven JThJ, Botermans M, Roenhorst JW, Westerhof J, Meekes ETM (2009) First report of potato spindle tuber viroid in Cape gooseberry (*Physalis peruviana*) from Turkey and Germany. Plant Disease 93: 316.

Verhoeven JThJ, Hüner L, Virscek Marn M, Mavric Plesko I, Roenhorst JW (2010a) Mechanical transmission of Potato spindle tuber viroid between plants of *Brugmansia suaveoles, Solanum jasminoides* and potatoes and tomatoes. European Journal of Plant Pathology 128: 417–421.

Verhoeven JThJ, Jansen CCC, Roenhorst JW (2008a) First report of pospiviroids infecting ornamentals in the Netherlands: citrus exocortis viroid in *Verbena* sp., potato spindle tuber viroid in *Brugmansia suaveolens* and *Solanum jasminoides*, and tomato apical stunt viroid in *Cestrum* sp. Plant Pathology 57: 399.

Verhoeven JThJ, Jansen CCC, Botermans M, Roenhorst JW (2010b) Epidemiological evidence that vegetatively propagated, solanaceous plant species act as sources of potato spindle tuber viroid inoculum for tomato. Plant Pathology: 59, 3–12.

Verhoeven JThJ, Jansen CCC, Roenhorst JW (2008b) *Streptosolen jamesonii* 'Yellow', a new host plant of potato spindle tuber viroid. Plant Pathology 57: 399.

Verhoeven JThJ, Jansen CCC, Willemen TM, Kox LFF, Owens RA, Roenhorst JW (2004) Natural infections of tomato by citrus exocortis viroid, columnea latent viroid, potato spindle tuber viroid and tomato chlorotic dwarf viroid. European Journal of Plant Pathology 110: 823–831.

Verhoeven JThJ, Roenhorst JW (2010) High stability of original predominant pospiviroid genotypes upon mechanical inoculation from ornamentals to potato and tomato. Archives of Virology 155: 269–274.

Verhoeven JThJ, Roenhorst JW, Owens RA (2011) Mexican papita viroid and tomato planta macho viroid belong to a single species in the genus *Pospiviroid*. Archives of Virology 156: 1433–1437.

Virščeк Marn M, Mavrič Pleško I, Gerič Stare B (2013) Variability of potato spindle tuber viroid isolates from ornamental hosts in Slovenia. Journal of Plant Pathology 95: 411–415.

Visser M, Bester R, Burger JT, Maree HJ (2016) Next–generation sequencing for virus detection: covering all the bases. Virology Journal 13:85.

Vlot AC, Dempsey DA, Klessig DF (2009) Salicylic acid, a multifaceted hormone to combat disease. Annual Review of Phytopathology 47: 177–206.

Vriet C, Russinova E, Reuzeau C (2012) Boosting crop yields with plant steroids. Plant Cell 24: 842–857.

Wang MB, Bian XY, Wu LM, Liu LX, Smith NA, Isenegger D, Wu RM, Masuta C, Vance VB, Watson JM, Rezaian A, Dennis ES, Waterhouse PM (2004) On the role of RNA silencing in the pathogenicity and evolution of viroids and viral satellites. Proceedings of the National Academy of Sciences of the United States of America 101: 3275–3280.

Wang SM, Hou XL, Ying L, Cao XW, Zhang S, Wang F (2011a) Effects of turnip mosaic virus (TuMV) on endogenous hormones and transcriptional level of related genes in infected non–heading Chinese cabbage. Journal of Nanjing Agricultural University 5: 13–19.

Wang Y, Ding B (2010) Viroids: small probes for exploring the vast universe of RNA trafficking in plants. Journal of Integrative Plant Biology 52: 28–39.

Wang Y, Shibuya M, Taneda A, Kurauchi T, Senda M, Owens RA, Sano T (2011b) Accumulation of potato spindle tuber viroid–specific small RNAs is accompanied by specific changes in gene expression in two tomato cultivars. Virology 413: 72–83.

Wasilewskaa A, Vlad F, Sirichandra C, Redko Y, Jammes F, Valon C, Frey NF, Leung J (2008) An update on abscisic acid signaling in plants and more. Molecular Plant 1: 198–217.

Wassenegger M, Spieker RL, Thalmeir S, Gast FU, Riedel L (1996) A single nucleotide substitution converts potato spindle tuber viroid (PSTVd) from a noninfectious to an infectious RNA for *Nicotiana tabacum*. Virology 226: 191–197.

Wasternack C (2007). Jasmonates: An update on biosynthesis, signal transduction and action in plant stress response, growth and development. Annals of Botany 100: 681–697.

Whenham RJ, Fraser RSS, Brown LP, Payne JA (1986) Tobacco mosaic virus induced increase in abscisic–acid concentration in tobacco leaves: intracellular location in light and dark–green areas, and relationship to symptom development. Planta 168: 592–598.

Wiesyk A, Candresse T, Zagorski W, Gora–Sochacka A (2011) Use of randomly mutagenized genomic cDNA banks of potato spindle tuber viroid to screen for viable versions of the viroid genome. Journal of General Virology 92: 457–466.

Xia XJ, Wang YJ, Zhou YH, Tao Y, Mao WH, Shi K, Asami T, Chen ZX, Yu JQ (2009) Reactive oxygen species are involved in brassinosteroid–induced stress tolerance in cucumber. Plant Physiology 150: 801–814.

Xie F, Frazier TP, Zhang B (2010) Identification, characterization and expression analysis of microRNAs and their targets in the potato (*Solanum tuberosum*). Gene 473: 8–22.

Xie Z, Allen E, Fahlgren N, Calamar A, Givan SA, Carrington JC (2005) Expression of Arabidopsis *MIRNA* genes. Plant Physiology 138: 2145–2154.

Yalpani N, Enyedi AJ, Leon J, Raskin I (1994) Ultraviolet light and ozone stimulate accumulation of salicylic acid, pathogen–related proteins and virus resistance in tobacco. Planta 193: 373–376.

Yalpani N, Shulaev V, Raskin I (1993) Endogenous salicylic acid levels correlate with accumulation of pathogenesis–related proteins and virus resistance in tobacco. Phytopathology 83: 702–708.

Yang W, Liu X, Zhang J, Feng J, Li C, Chen J (2010) Prediction and validation of conservative microRNAs of *Solanum tuberosum* L. Molecular Biology Reports 37: 3081–3087.

Yu D, Liu Y, Fan B, Klessig DF, Chen Z (1997) Is the high basal level of salicylic acid important for disease resistance in potato? Plant Physiology 115: 343–349.

Zenk MHM, Müller G (1964) Biosynthesis von p–hydroxyben–Zoesaure und anderer Benzoesauren in hoheren Pflanzen. Zeitschrift für Naturforschung 19: 398–405.

Zhang W, Luo Y, Gong X, Zeng W, Li S (2009) Computational identification of 48 potato microRNAs and their targets. Computational Biology and Chemistry 33: 84–93.

Zhang Y, Yin J, Jiang D, Xin Y, Ding F, Deng Z, Wang G, Ma X, Li F, Li G, Li M, Li S, Zhu S (2013) A universal oligonucleotide array with a minimal number of probes for the detection and identification of viroids at the genus level. PLOS ONE 8: e64474.

Zheng Y, Wang Y, Ding B, Fei Z (2017) Comprehensive transcriptome analyses reveal that potato spindle tuber viroid triggers genome–wide changes in alternative splicing, inducible trans-acting activity of phasiRNAs and immune responses. Journal of Virology 91: e00247–17.

Zhong X, Archual AJ, Amin AA, Ding B (2008) A genomic map of viroid RNA motifs critical for replication and systemic trafficking. Plant Cell 20: 35–47.

Zhu Y, Green L, Woo YM, Owens R, Ding B (2001) Cellular basis of potato spindle tuber viroid systemic movement. Virology 279: 69–77.

Zhu, Y, Qi Y, Xun Y, Owens R, Ding B (2002) Movement of potato spindle tuber viroid reveals regulatory points of phloem–mediated RNA traffic. Plant Physiology 130: 138–146.

Zhuang BC, Xu B, Liao L (1993) Change of superoxide dismutase, peroxidase and storage protein in soyabean leaves after infection with soyabean mosaic virus. Acta Phytopathol Sinica 23: 261–265.

ABA	absicic acid
APX	ascorbate peroxidase
bp	base pair
BR	brassinosteroid
C	Celsius degree
CaLCuV	*Cabbage leaf curl virus*
CaMV	*Cauliflower mosaic virus*
CAT	catalase
cDNA	complementary DNA
CDVd	*Citrus dwarfing viroid*
CEVd	*Citrus exocortis viroid*
cis–OPDA	*cis*–12–oxophytodienoic acid
CK	cytokinin
CS	castasterone
DNA	deoxyribonucleic acid
dNTPs	deoxynucleotide triphosphates
dsRNA	double–stranded RNA
ET	ethylene
GA	gibberellic acid
GPX	guaiacol peroxidase
GR	glutathione reductase
GSH	glutathione
ha	hectare
HR	hypersensitive response
IAA	indole–3–acetic acid
JA	jasmonic acid
kDa	kilodalton
MAPK	mitogen–activated protein kinase
miRNA	microRNA
mRNA	messenger RNA
MW	molecular weight

PCR	polymerase chain reaction
PGR	plant growth regulator
PKR	double–stranded RNA–dependent protein kinase
PKV	protein kinase viroid–induced
PLMVd	*Peach latent mosaic viroid*
RNA	ribonucleic acid
RNase	ribonuclease
PGRs	plant growth regulators
PSTVd	potato spindle tuber viroid
PTGS	post–transcriptional gene silencing
PVX	*Potato virus X*
PVY	*Potato virus Y*
RISC	RNA–induced silencing complex
ROS	reactive oxygen species
RT	reverse transcription
RT–PCR	reverse transcription–polymerase chain reaction
SA	salicylic acid
SAM	shoot apical meristem
SAR	systemic acquired resistance
siRNAs	small interfering RNA
SOD	superoxide dismutase
sRNA	small RNA
ssRNA	single–stranded RNA
TGS	transcriptional gene silencing
TMV	*Tobacco mosaic virus*
UHPLC–MS/MS	ultra–high performance liquid chromatography–tandem mass spectrometry
UV	ultraviolet
vd–sRNA	viroid–derived small RNA
wpi	weeks post–inoculation

8. CURRICULUM VITAE

Jasna Milanović was born on November 13th 1980 in Zagreb where she completed her primary and secondary education. She received a Bachelor of Science degree in biology from the Faculty of Science, University of Zagreb in 2008 under the guidance of prof. Mladen Krajačić on the topic "*Chromatography of viral and satellite double stranded RNAs on monolithic columns"*. She is also the recipient of the University of Zagreb Rector's award for the best student scientific work in the academic year 2002/2003. Since 2009 she has been working as a virologist at the Institute for Plant Protection in Zagreb. She is currently head of the Laboratory for virology at the same Institute and is involved in a national monitoring and surveillance program as a project coordinator for several plant quarantine viruses. Over the years, she has reviewed several manuscripts for Plant Pathology and Journal of Integrative Agriculture. She is a member of the Croatian Society of Biochemistry and Molecular Biology, and the European Society for Virology.

List of Publications:

Journal articles in CC journals:

Milanović J, Kajić V & Mihaljević S (2014) Occurrence and molecular variability of potato spindle tuber viroid and tomato apical stunt viroid in ornamental plants in Croatia. The European Journal of Plant Pathology 139: 785–788.

Abstracts in Book of abstracts:

Milanović J, Kajić V, Mihaljević S (2014) Molecular variability of PSTVd in ornamental plants in Croatia. Book of Abstracts of the Symposium on DNA Habitats and its RNA Inhabitants, Salzburg, Austria, 57. (poster, international peer–review, abstract, scientific)

Novak A, Milanović J, Kajić V (2011) First PepMV finding in Croatia. Book of Abstracts of the 5th Balkan Symposium on Vegetables and Potatoes, Tirana, Albania, 45. (poster, international peer–review, abstract, scientific)

Novak A, Milanović J, Kajić V (2010) Current status of PepMV in Croatia. Book of Abstracts of the III International Symposium on Tomato Diseases, Ischia, Naples–Italy, 61. (lecture, international peer–review, abstract, scientific)

Scientific papers in other journals:

Milanović J, Kajić V, Novak A (2011) Prvi nalaz pepino mosaic virusa (PepMV) u Hrvatskoj. Glasilo biljne zaštite 5: 353–356.

Nonscientific papers in other journals:

Novak A, Milanović J, Kajić V (2010) Current status of PepMV in Croatia. Acta Horticulturae 914: 193–196.